Effect of Topography, Stiffness and Biochemicals on Neuronal Differentiation

by

Fan Feng

A thesis
presented to the University of Waterloo
in fulfillment of the
thesis requirement for the degree of
Master of Applied Science
in
Chemical Engineering

Waterloo, Ontario, Canada, 2022

Author's Declaration

I hereby declare that I am the sole author of this thesis. This is a true copy of the thesis, including any required final revisions, as accepted by my examiners.

I understand that my thesis may be made electronically available to the public.

Abstract

The mechanical and biochemical modifications of the hydrogel substrates play an essential role in tissue engineering research and neurodegenerative therapies. Topography, stiffness, and biochemicals are known to have important influences on neural cells, such as cell adhesion, proliferation, migration, and differentiation. These factors not only affect cells independently but also have a combined effect. The purpose of this thesis is to investigate these impacts on neural cells. We first hypothesized that topography and stiffness would affect neuronal differentiation and maturation. Polyacrylamide hydrogels were used to provide promising scaffolds for human neural progenitor cells (hNPCs) attachment. Both healthy hNPCs and Rett-syndrome disease hNPCs were used to examine the cell behaviors on different combinations of topographies and stiffnesses. Then healthy hNPCs were cultured for 21 days to assess the effects on neuronal differentiation and maturation.

Next, we hypothesized that topography and biochemicals would impact cell adhesion and differentiation. With biocompatibility and biodegradability properties, polyvinyl alcohol (PVA) hydrogels are considered a great resource for regenerative medicine. However, the plain PVA surface rarely supports cell attachment. The biochemical modifications are necessary for further cell studies. PC12 cell lines were used to study the cell adhesion, proliferation, and viability on various biochemical conjugation. Then PC12 cell lines were seeded on the PVA substrates with different topographies and biochemicals to study the combined effect on cell differentiation and the neurite length.

Overall, the findings of this research work show the specific combinations of mechanical and biochemical modifications would promote cell adhesion and differentiation.

Acknowledgements

I would like to express my sincerest gratitude to my supervisor, Associate Professor. Evelyn Yim for her enormous support and patient guidance. Prof. Yim always provided suggestions when I meet difficulties and give her expert insights on the challenges during the research. I am extremely grateful for the opportunity that I could join the Yim Lab and work on these projects.

I would like to thank the thesis committee members, Professor Ting Tsui and Assistant Professor Tiz Mekonnen for their willingness to be my examiner and indispensable suggestions which help to improve the contents of this thesis.

I would like to thank all lab members of the Yim lab: Dr. Yuan Yao, Ms. Sabrina Mattiassi, Ms. YeJin Jeong, Ms. Linan Cui, Mr. Wesley Luu, and Mr. Joshua Kunihiro for their help and guidance. Special thanks to Dr. Yuan Yao and Ms. Sabrina Mattiassi for their mentor and suggestions. I am very grateful for your help and friendship, which have supported me to overcome the difficulties.

Lastly, I would like to thank my parents, who have given me the most support and encouragement. I really appreciate the opportunity and freedom they offered. I would like to thank my wonderful friends for their help and support.

Table of Contents

List of Figures

List of Tables

Chapter 1 Introduction

1.1 Background

Neurodegenerative diseases occur when nerve cells in the brain lose function or are damaged. The diseases, such as Alzheimer's disease, spinal muscular atrophy, Rett syndrome, may lead to a movement disorder, cognitive impairment and even death[1]. Recent studies have shown that cell therapy based on neural stem cell (NSC) transplantation is a promising therapeutic strategy for neurodegenerative diseases, due to the ability of human NSCs to self-renew and differentiate into multiple cell types[2, 3]. In addition, the non-stem cell progeny of NSCs is known as neural progenitor cells (NPCs)[4]. Human NPCs (hNPCs) are the progenitor cells of the central nervous system, which are also able to proliferate and differentiate into different cell types, such as neurons, oligodendrocytes, and astrocytes. The characterization of the NPCs can be determined by their location in the brain, morphology and function. hNPCs can be derived from induced pluripotent stem cells, which can be obtained directly from patients[5]. Therefore, hNPCs are an excellent candidate to develop a stem cell-based model for clinical therapies and regenerative medicine[6].

In order to provide a compatible and low toxic environment for stem cell transplantation and long-term survival of stem cells[7], hydrogels can be considered as a reliable resource. Due to biocompatibility and biodegradability, hydrogels have been widely used in tissue engineering and drug screening[8]. Polyacrylamide and polyvinyl alcohol hydrogels can be two great scaffolds for cell studies. Hydrogels with various surface modifications, such as topography, stiffness, and biochemicals would benefit cellular response.

The topography is an important factor to regulate the cell behaviors, such as cell adhesion, proliferation, and differentiation[9]. Also, different topographies have been found

to influence cell morphology and migration depending on the patterns[9, 10]. The topographic patterns in micro/nanoscale could be fabricated using various methods. Feature size, cost, and efficiency of the fabrication are all important factors to consider in both *in viv*o and *in vitr*o studies[8]. Moreover, since the native brain tissue is very soft, neural stem cells are sensitive to the scaffold stiffness[11, 12]. Cell survival, function and performance are directly related to the stiffness of the substrate[12]. Stiffness could also regulate neural cell proliferation and differentiation to target cell types. For example, Kozaniti *et al.* stated soft substrates could enhance human mesenchymal stem cells (hMSCs) migration, while stiff substrates promote differentiation into bone cells[13]. These cues provide an understanding of the optimal biomimetic materials and further benefit the clinical research[12, 13]. Biochemical cues are another key element influencing cell growth, attachment, and differentiation. However, plain hydrogels, such as PVA have been shown to have limited capacity to support cell adhesion and spreading due to their low affinity to protein[14]. Biochemicals, such as extracellular matrix protein, cell adhesion and growth factor can be necessities for modification. Also, one advantage of this approach is that it can be delivered more directly and efficiently, compared to mechanical cues[15].

1.2 Hypothesis and Objectives

Since the mechanical and biochemical cues can guide neural cell behavior, we hypothesized that topography, stiffness, and biochemicals would promote neuronal differentiation.

Based on the hypothesis, this project has been divided into two aims.

Aim 1: Evaluate the effect of topography and stiffness on neuronal differentiation and maturation.

To investigate the effect of different topographies and stiffnesses, polyacrylamide (PAA) hydrogels were fabricated with various topographies and stiffnesses. Both healthy hNPCs and Rett-syndrome disease hNPCs were cultured on the PAA hydrogels to

evaluate the cell response. Then, the healthy hNPCs were cultured on the substrates for 21 days to further evaluate the effect on neuronal differentiation and maturation by immunofluorescence staining and quantitative real-time reverse-transcription polymerase chain reaction (RT-qPCR).

Aim 2: Evaluate the effect of topography and biochemicals on neuronal cells.

The behaviours of PC12 cells were evaluated on polyvinyl alcohol (PVA) hydrogels with different topographical and biochemical cues. Different biochemicals were used to modify the PVA surface. Cell attachment, proliferation and viability on the substrate were examined. Lastly, the combined effects of topographies and biochemicals on neuronal differentiation were analyzed.

1.3 Thesis Outline

Chapter 1 gives a general background and the motivation of this thesis project and introduces the hypothesis and objectives.

Chapter 2 presents a literature review, including the introduction of neural cells, hydrogels used in tissue engineering, and the effect of topography, stiffness, and biochemicals on neuronal differentiation in previous studies.

Chapter 3 explains aim 1 and describes the effect of topography and stiffness on hNPCs differentiation and maturation.

Chapter 4 explains aim 2 and illustrates the impact of topography and biochemicals on neuronal cells.

Chapter 5 concludes with the major findings in this thesis and recommends the potential improvements and future scope.

Chapter 2 Literature Review

2.1 Introduction of Neural Cells

2.1.1 Neural Stem Cells and Neural Progenitor Cells

The central nervous system (CNS) and peripheral nervous system (PNS) are two components of the nervous system. The CNS consists of the brain and spinal cord. The PNS is mainly composed of peripheral nerves and is divided into the autonomic nervous system and somatic nervous system. The nerve fibers of the PNS link the CNS to the body. These functional neurons are known as afferent neurons, which input to the CNS; and efferent neurons, which output from the CNS[16].

Neural stem cells (NSCs) are self-renewable and proliferative, which allows them to produce progeny cells indefinitely. Also, NSCs are multipotent cells and can primarily differentiate into different cell types: neurons, astrocytes, and oligodendrocytes. Neurons and glial cells are two main cell types in the nervous system. Neurons support the signal transmission throughout the nervous system. Astrocytes and oligodendrocytes are together called glial cells in the CNS, which assist the transmission in neurons[3, 17].

Neural progenitor cells (NPCs) are able to proliferate and differentiate into various cell types. NPCs are present both in fetal and adult neural tissue[18]. In general, embryonic NPCs in the fetal brain was considered to have greater potential than adult NPCs[5]. Additionally, NPCs are an excellent resource for modelling brain development and developing future cell replacement therapies. NPCs can be derived from both embryonic stem cells (ESCs) and induced pluripotent stem cells (iPSC)[5].

2.1.2 Induced Pluripotent Stem Cells

The iPSCs are derived from adult somatic cells[19] and possess the ability of unlimited self-renewal[20]. IPSCs can differentiate into every appropriate cell type, such as neural lineages and mesenchymal lineages[20, 21].

Compared to ESCs, iPSCs have similar cell morphology, proliferation, and gene expression[22]. However, iPSCs can be obtained directly from patients, which makes them easier to acquire. The differentiation of iPSCs has been developed in both 2D and 3D dimensions and recent studies already demonstrate the potential for iPSCs to mimic brain tissue and generate organoids instead of simple cell culturing[20]. Therefore, iPSCs are promising to use in cell therapies and disease modelling[19]. However, the long-term culture and maturation of iPSC-derived neuronal cells *in vitro* remains a challenge[23].

2.1.3 Neural Stem and Progenitor Cells in Neurological Disease and Therapy

Neurological diseases could lead to movement disorders, language deteriorations, breathing problems or cognition impairment[1, 24]. Alzheimer's disease, Parkinson's disease, and acute spinal cord injury are common neurological disorders[2, 25]. Such diseases are particularly dangerous as neurons normally are not capable to replicate or replace themselves[26]. Due to the ability to self-renew and differentiate to multiple cell types, neural stem/progenitor cells (NSPCs) hold promise for the treatment of disorders of the central nervous system and neurodegenerative disease[2, 23]. The implementation of therapeutic strategies can be roughly divided into three categories: activation of endogenous NSPCs, cell transplantation and disease model mimicking using NSPCs[27].

Studies have shown that endogenous cell generation could be promoted by hormones, neurotrophic factors and growth factors, such as nerve growth factor (NGF), endothelial growth factor and epidermal growth factor, which could protect neural cells from damage[3, 27]. For example, Cole *et al.* showed that bone morphogenic protein 4 can regulate neuronal and glial cell development from endogenous NSPCs in response to CNS injuries[28].

Cell transplantation in neural regeneration is achieved by secretion of paracrine factors, rather than the ability of transplanted cells to differentiate into functional cell types. The transplantation of NSCs into a mouse model with Alzheimer's dementia reduced the effect of inflammation[27]. Mothe *et al.* also demonstrated that multipotent NSPCs transplanted into mice with spinal cord injuries could survive and further differentiate[29]. Furthermore, since NSPCs can differentiate into neurons, astrocytes, and oligodendrocytes, nervous system disorders can be treated by culture-based neurons[27].

2.1.4 Rett Syndrome and treatment

Rett syndrome (RTT) is a common neurodevelopmental disease. RTT is caused by the mutation of methyl-CpG-binding protein 2 (MECP2). MECP2 is located on the X chromosome, which causes the disorder to commonly appear in females. Females have another spare X chromosome while males have only one X and typically do not survive[30, 31]. The symptoms of RTT are mental retardation, loss of language, loss of movement control, stereotypic hand movements, etc.[32]. The abnormal mechanisms in RTT can be classified into three categories: unusual dendritic arborisation and synaptic maturation, mitochondrial dysfunction, and activity of astrocytic lineage, which could give cues for the further treatment of RTT[33, 34].

One promising result of the studies is that the defects in RTT are not permanent, and the disorder is reversible[35]. As mentioned above, due to the abilities of self-renewal and pluripotency, human ESCs are a suitable resource to model human neuronal disease *in vitro*. In addition, since human iPSCs have similar abilities with human ESCs and they have the capacity to differentiate into specific cell types, the iPSCs derived from RTT patients are promising to study in both 2D monolayers and 3D scaffolds[20, 32].

Our lab previously studied the human RTT on 3D graphene scaffolds and analyzed the effect of electrical stimulation on human NPCs derived from RTT patient iPSCs *in vitro*. The 3D graphene scaffolds were able to support the adhesion, proliferation, and

differentiation of RTT cells. Also, the electrical stimulation affected the neuronal differentiation and maturation of both wild-type and RTT-type human NPCs, demonstrating its potential as a promising therapeutic method for neurological disorders in the future[36].

2.1.5 PC12 Cell Lines

The PC12 cell lines are derived from rat pheochromocytoma and are commonly used in neurobiological and neurotoxicological research[37, 38]. Due to ease of passage and culture, PC12 cell lines are the great resource for studying cell attachment, morphology, and differentiation on various substrates[39]. The differentiation behaviors of PC12 cells can be evaluated by cell sizes, neurite number and neurite length[40]. NGF can induce neurite outgrowth of PC12 cells by activating the receptor tyrosine kinase[41, 42]. In addition to NGF, PC12 cell lines also respond to many growth factors, neurotrophins, and neurotransmitters, which is suitable for the study of neuronal differentiation *in vitro*[38, 43].

The study from Orlowaska *et al.* demonstrated that the concentration of NGF and the substrate coating materials affected the differentiation of PC12. The coatings with Poly-L-lysine (PLL)/Laminin and PLL/Fibronectin provided excellent attachment and improved the differentiation and neurites outgrowth with 100 ng/ml NGF[44]. Foley *et al*. evaluated the topographic effect on regulating the neurites of PC12 on silicon surfaces. The extension of neurites aligned with the topographic guidance[45]. Also, Wu *et al.* cultured PC12 cell lines on a GelMA substrate to study the effect of stiffness on neuronal outgrowth. With increasing stiffness, the adhesion of PC12 cell lines was reduced while the differentiation and neurite length first increased and then decreased[46]. Further explanation of the substrate effects on cells will be discussed in chapter 2.3.

2.2 Hydrogels for Tissue Engineering

2.2.1 Introduction and Application of Hydrogels

Hydrogels are three-dimensional networks of hydrophilic polymer chains that can be crosslinked either physically or chemically from liquid solutions to solid substrates[47, 48]. Hydrogels have been widely used in tissue engineering, drug screening, and biosensors, due to their properties of suitable biocompatibility and low toxicity. Hydrogels can be categorized as natural, synthetic or hybrid. Natural hydrogels are defined as the polymer having natural origins, such as gelatin and collagen, while synthetic hydrogels are integrated with synthetic polymers, such as polyamides[49]. Since natural hydrogels are fragile and difficult to handle, they have limited applications. Synthetic hydrogels are more popular because of the longer lifetime, higher tunable mechanical strength, and higher water content capacity, which could better fulfill their use in cell culture, self-healing, and medicine delivery[8, 48, 50].

Cells are sensitive to the conditions of their microenvironment, such as stiffness, roughness, and porosity[50]. Both natural and synthetic hydrogels could provide great scaffolds for cell culture since they have similar structures to the extracellular matrix (ECM) of native tissues and could be used to improve or replace organs[51]. Also, the interaction between the cells and materials should be efficient and non-cytotoxic. Therefore, the physical characteristics of the hydrogel, such as biocompatibility, biodegradability, bioactivity as well as compatibility with further surface modification are very important for cell culture[50]. Recent studies also demonstrated that hydrogels could support cell attachment and proliferation, as well as guide differentiation to various cell types[47].

For drug delivery, hydrogels provide drugs with a substrate and prevent the drug from environmental contamination due to their porous structure. The porosity can be modulated by controlling the crosslinking degree. Another important factor that needs to

be considered in drug delivery is their diffusion coefficient. In order to meet the therapeutic needs, sustained release of the drug for a long-term period is required, which is another advantage of hydrogels. The duration of drug release can be controlled by the covalent bonding with other functional groups, according to the local temperature, pH and enzymes[48, 51]. After the drug is consumed, the degradability could be an essential capacity of hydrogels to avoid leaving toxic residues[48].

Another application of hydrogels is self-healing, which is similar to that of skin and bones in the natural body. Self-healing hydrogels can be formed by covalent bonds and non-covalent interactions[52]. However, the appropriate mechanical strength, excellent biocompatibility and long-term stability are still major concerns that need to address for future therapeutic application.

2.2.2 Polyacrylamide Hydrogels

Polyacrylamide (PAA) is a synthetic polymer, which is prepared by the polymerization of acrylamide monomer and *N*, *N*′-methylenebisacrylamide (bisacrylamide) and catalyzed by ammonium persulfate and *N*, *N*, *N*′, *N*′-tetramethylethylenediamine. The method of copolymerizing with N-acryloyl-6-aminocaproic acid (ACA) could help PAA gels better couple with ECM protein[53]. PAA hydrogels are usually bound to coverslips and can be fabricated easily. In addition, PAA substrates have been shown to support cell adhesion, proliferation, and differentiation and can further conjugate with proteins. Therefore, PAA hydrogels have become a promising scaffold for cell culture *in vitro* and study the influence of substrates in tissue engineering[47, 54].

One advantage of PAA hydrogels is enabling the control of stiffness, which could mimic the matrix elasticity *in vitro* and match the soft tissue *in vivo*[54, 55]. The stiffness of PAA gel could be changed by altering the percentage of acrylamide and bisacrylamide. Wang *et al.* showed that a ratio between acrylamide and bisacrylamide of 50 to 1

supported more cell adhesion with high crosslinking density. It also increased the rate of cell proliferation[56]. Moreover, Pelham *et al*. demonstrated that normal rat kidney epithelial and 3T3 fibroblastic cells responded to different mechanical properties of the PAA substrate. Both cell adherent structures and motile behaviour varied depending on the flexibility. The cell spreading rate and stability decreased as the rigidity of the substrate decreased[57].

Furthermore, PAA hydrogels have been made with different topographies to study the effects of topographies on cells. For example, Al-Haque *et al.* stated that the topography and stiffness of polyacrylamide substrates affected cardiac fibroblast response. Also, the combinative effect of topography and stiffness directed the cell elongation and orientation on polyacrylamide substrates[54].

2.2.3 Polyvinyl Alcohol (PVA) Hydrogels

Polyvinyl alcohol (PVA) is a hydrophilic synthetic polymer, which has been widely used in various fields. In tissue engineering, due to the properties of biocompatibility and biodegradability, PVA hydrogels can be used for repair and regeneration[58]. Also, in therapeutic research, PVA hydrogels can be used to mimic tissue with suitable mechanical strength properties and tissue-like elasticity. One of the applications of PVA is in the vascular system, such as vascular cell culturing, vascular material replacement and implants, due to their low toxicity, high water content and transparency[58, 59].

PVA hydrogels are often prepared by a freeze-thaw method, which involves repeated cycles of freezing at -20 °C for 8 hours and thawing at higher than room temperature for up to 4 hours[60]. With increasing repetitions of the freeze-thaw cycle, the crystallinity is reinforced. At the same time, the stability of the structure is also improved, which would benefit biomedical applications[60]. Vrana *et al*. also demonstrated that vascular cells responded differently to various hydrogel structures. An optimal number of freeze-thaw

cycles could improve surface morphology and protein adsorption, which could further enhance the cell attachment together with the collagen coating[61].

Besides the traditional freeze-thaw crosslinking method, Chaouat *et al.* provided a novel method to prepare PVA hydrogels, which are crosslinked with sodium trimetaphosphate (STMP). STMP and PVA mixture was cast on a Petri dish for at least 24 hours until the water evaporated. The film could be easily fabricated and removed from the surface, avoiding the melting process. Moreover, one of the biggest advantages is low toxicity. STMP is food graded crosslinker and avoids toxic additives. With the suitable compatibility, elasticity, and high mechanical strength, PVA hydrogels from this crosslinking method are promising for use in the replacement of rat arterial vessels[62]. Recently, Ma *et al*. provided another mixed-solvent physical crosslinking method to prepare PVA hydrogels, using dimethyl sulfoxide and *N*, *N*-dimethylformamide. This new method could provide higher mechanical strength, water content, reswelling rate and a more stable crosslinked structure at a certain temperature range (25–65 °C), which could be appropriate in wide applications[59].

However, since unmodified PVA cannot directly support cell adhesion, surface modification is necessary. Previous studies from our lab by Yao *et al*. showed that PVA with fucoidan conjugation could support human endothelial cell attachment. Fucoidan is a long chain sulfated polysaccharide obtained from brown algae, which has anti-inflammatory and anti-cancer properties. Fucoidan modified PVA has been reported to promote endothelial cell growth and can be used in the development of vascular grafts[63].

2.3 Effect of Topography, Stiffness and Biochemicals on Neuronal Differentiation

2.3.1 Effect of Topography on Neuronal Differentiation

With the various advantages of hydrogels in tissue engineering, recent research has demonstrated that the incorporation of topographical modification could further benefit cell studies. Different cell types, such as human mesenchymal stem cells (hMSCs) and NSPCs could respond differently to the topographically patterned substrates. Moreover, different topographies would affect cell morphology, adhesion, and proliferation as well as regulate the neuronal differentiation to different cell types[9, 64, 65].

The topographic pattern could be fabricated in micro/nanoscale by various methods, such as electron beam lithography, nanoimprint lithography, and electrospinning method. Casting the crosslinking solution on the prepared templated molds is one of the popular methods. The advantage of the casting method is simple and low cost. However, the quality of the patterns would be challenging to control, and the fabrication is less efficient[8, 66, 67]. Moreover, the topographical modification of the substrates would affect the surface properties, such as hydrophobicity, protein adsorption, and mechanical properties which would further influence the cellular responses[8].

For example, Qi *et al.* demonstrated the effect of topographical patterns on adult NSCs behaviors. Three different patterns, linear micro-pattern (LMP), circular micro-pattern (CMP), and dot micro-pattern (DMP) were fabricated by the photolithography method on silicon substrates. With the coating of laminin, all three patterns could regulate the adult NSCs adhesion, morphology, and proliferation. Also, the topographical patterns could direct the preference of stem cell differentiation towards different cell types. The most neuronal differentiation was promoted on LMP substrates, compared to the unpatterned control substrates. However, the differentiation to astrocytes occurred the least on LMP substrates. Furthermore, with a smaller feature size of 2 μm width, both

LMP and CMP substrates could better upregulate the extent of differentiation when compared to the 10 μm substrate[9]. Another example from Moe *et al*. showed that topographical cues guided the cell response. Isotropic and anisotropic patterns were prepared in micro/nanometer dimensions by nano-imprinting lithography and fabricating on polydimethylsiloxane (PDMS) replicas of multi-architecture chips. Anisotropic gratings of 2 μm and 250 nm, and isotropic 1 μm pillars enhanced the differentiation of murine NPCs into neurons while isotropic gratings with 2 μm holes and 1 μm pillars promoted glial differentiation[65]. Moreover, the topography could not only direct the neurite extension in alignment with the grating axis but also influence neurite elongation. Chua *et al*. used the soft lithography method to fabricate PDMS substrates with different depths to study the differentiation of murine NPCs. With increasing grating depth, the neurite elongation and alignment of murine NPCs also increased[68].

Therefore, the topographical cues on cellular response are complicated and systematic comparisons between various topography are worth being evaluated, which could further benefit cell therapy.

2.3.2 Effect of Stiffness on Neuronal Differentiation

Stiffness is an important property in biomaterials and is usually quantified by the elastic or Young's modulus[50]. Native brain tissue is one of the softest tissues in the human body. The elastic modulus (E) of brain tissue is about 0.5 to 1 kPa[12], while that of endothelial tissue and skeletal muscle is in the range of 1 to 10 kPa[12, 69], that of cartilage is about 1 MPa, and that of bone is up to 2-4 GPa[50]. Therefore, stiffness plays an essential role in modulating stem cell survival, function, and regeneration[12, 21, 70].

Recent research demonstrates that substrate rigidity modulates adhesion, migration, proliferation, and differentiation of stem cells. Park *et al*. stated that bone marrow MSCs could adhere better to stiffer substrates[71]. Also, Zhu *et al*. presented that neural crest stem cells (NCSCs) seeded on a very rigid substrate (about 1 GPa) had a larger spreading area

and focal adhesion than those seeded on a lower stiffness substrate (15 kPa and 1 kPa)[21]. Similarly, Saha *et al.* showed that adult NSCs could spread well soon after seeding on a surface with a stiffness greater than 100 Pa. Conversely, cells could not spread well and formed clumps when seeding on a softer surface with stiffness of about 10 Pa[72]. Additionally, the stiffness of the substrate regulated the differentiated behavior of stem cells both *in vitro* and *in vivo*[12, 21, 72]. Different cell types responded differently to various rigidity. For example, neurons favoured a soft hydrogel surface with E smaller than 1 kPa[12, 73], while astrocytes favoured a moderately stiffer scaffold with E equal to 9 kPa[74].

The study by Leipzig *et al*. demonstrated that soft substrates with Young's modulus below 1kPa could enhance the neural differentiation of NSPCs, which were separated from neurogenic regions of the adult brain. Astrocyte differentiation only appeared on the substrates with stiffness $E < 1$ kPa and $E = 3.5$ kPa. Oligodendrocyte differentiation was favored on stiffer surfaces with $E > 7$ kPa, while the maturation of oligodendrocytes was optimal on scaffolds with stiffness less than 1 kPa[12]. Another example from Saha *et al.* stated that the lineage of the differentiated cell population varied with the stiffness of the substrate. After differentiating for 6 days, cells on the substrate with the stiffness of 500 Pa showed optimal neuronal differentiation. With a softer surface, the percentage of neuronal differentiation would be higher, while differentiation into glial cells would be lower. In other words, the expression of astrocytes was stronger while the expression of neuronal cells was lower on the stiffer substrate. One interesting observation was that the substrate with a stiffness greater than 100 Pa could promote both neuronal and glial differentiation. However, for softer substrates, the cells could either promote neuronal differentiation or induce neuronal lineage commitment[72]. Moreover, substrate stiffness could affect the neurite length in NSCs differentiation. Stukel *et al.* stated that hydrogels with softer surfaces (0.1 and 0.8 kPa) could improve neurite extension compared to stiffer substrates with 4.2 and 7.9 kPa[75].

Therefore, the stiffness of the substrates regulates cell response. Also, the combined effect of substrates, such as stiffness and topography are worth being further developed.

2.3.3 Effects of Biochemicals on Neural Cells

2.3.3.1 Effects of Extracellular Matrix

Since most inorganic surfaces do not support cell aggregation and adhesion, chemical modification, which is realized by changing the chemical composition of the substrate surface plays a vital role in modulating cell behaviors[9, 76, 77]. Noncovalent and covalent interactions are two main categories of the coating material attachment. Noncovalent interactions are easier to implement because they do not require chemical modification before immobilization. In contrast, the covalent modification would be more stable due to chemical bonding, which is more suitable for use in improving neuronal cell adhesion[76, 78].

ECM and cell adhesion molecules (CAM) are mainly used in promoting cell attachment, migration, and differentiation. ECM is a three-dimensional support network[15]. Three main components of ECM are glycosaminoglycans (GAGs), proteoglycans and fibrous proteins[79]. Laminin, collagen, and fibronectin are representative ECM proteins[76]. The structure of ECM is shown below in Figure 1[80].

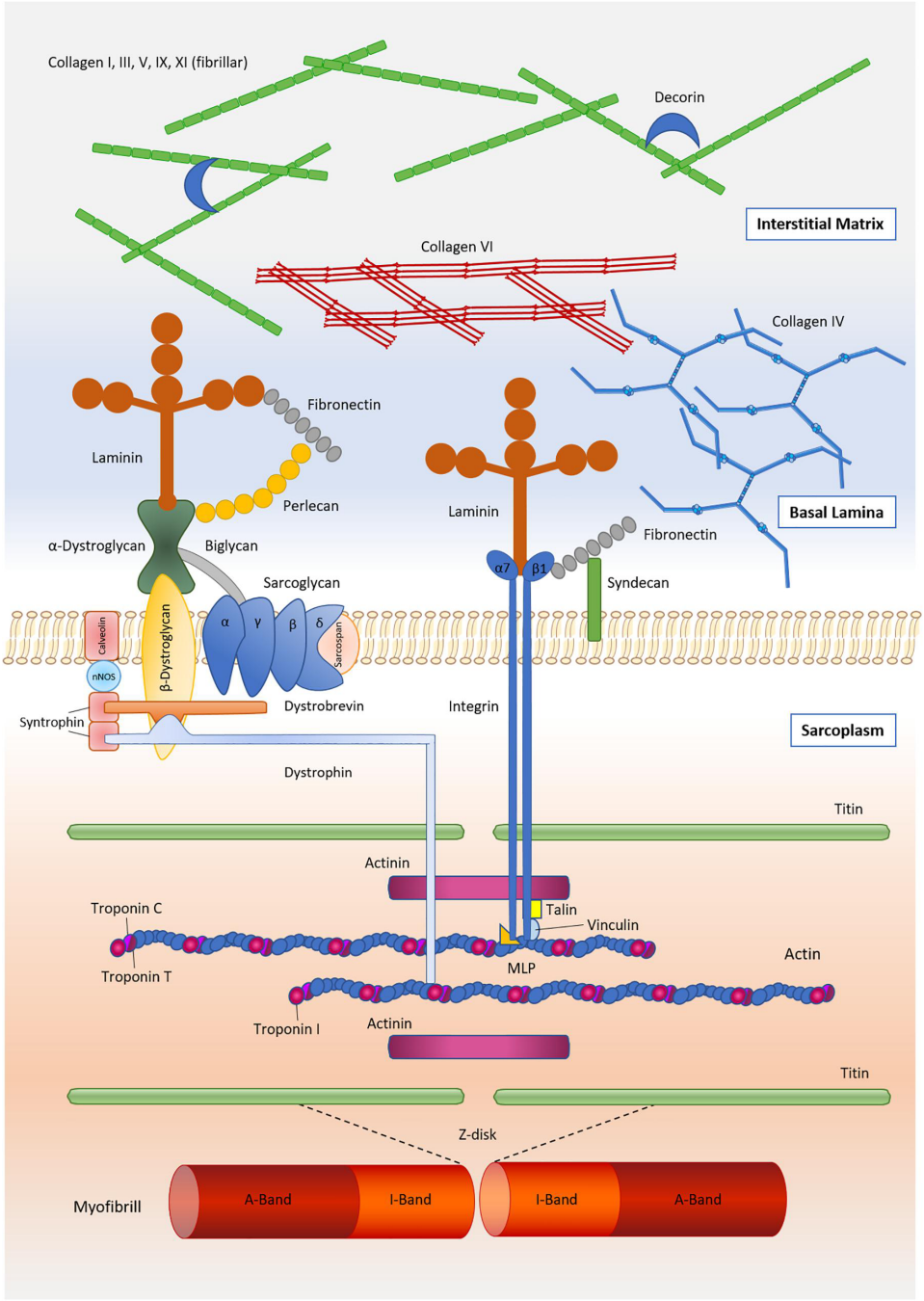

Figure 1. The components of the skeletal muscle extracellular matrix (ECM). Laminin, collagen, and fibronectin are representative ECM proteins, which could promote the formation of a high-affinity state[80]. Copyright © 2020, Frontiers Media S.A.

Laminin was first discovered in mouse Engelbreth-Holm-Swarm (EHS) sarcoma and is widely used in nervous system studies[81]. It is a type of glycoprotein and the main constituent of the basement membrane and can enhance cell response to the environment. Laminin plays a significant role in cell differentiation and supports the development of early embryos and organs[12, 15, 82, 83]. Laminin also aids in the differentiation of epithelial cells and induces neurite outgrowth[83]. Collagen is known as the most abundant ECM in most tissues and is synthesized by fibroblasts and myofibroblasts. Besides these, collagen can be produced by endothelial cells[15, 81]. Collagen is commonly used for gel scaffolds, providing tensile strength in ECM, and supporting cell adhesion and migration. In addition, it enhances the myogenic and osteogenic differentiation of stem cells[84]. Fibronectin is another kind of glycoprotein and is abundant in the blood[83]. It works as "biological glue" and benefits the adhesion and migration of cells[82] as well as wound healing[15]. Fibronectin also promotes the differentiation of hMSCs towards insulin-producing cells[85].

Besides these, PLL and poly-l-ornithine (PLO) are widely used in neuronal cell studies. The polyamino acids promote cell adhesion by the charge interaction of the substrate surface[76]. And Ge *et al.* shows PLO promotes more neuronal and oligodendrocyte differentiation of NSPCs when compared to PLL and fibronectin[86].

Cell behaviors vary on different chemically modified surfaces, and the response of cells to biomaterials also depends on the specific cell type[76]. The effect of surface chemical modification would be various. Additionally, the efficiency of the protein binding to the surface is worth further studying.

2.3.3.2 Effect of Growth Factors on Neuronal Differentiation

Growth factors, such as NGF, basic fibroblast growth factor (bFGF), epidermal growth factor (EGF), and vascular endothelial growth factor (VEGF) have been proved to have an additive effect on regulating cell behaviors.

NGF is another common growth factor for PC12 cell line use that has been mentioned above in chapter 2.1.5. In general, NGF is a member of a neurotrophin family and binds to the protein tyrosine kinase receptor[42, 87]. NGF can be generated by every peripheral tissue and organ. NGF plays a vital role in neuronal development and maintenance of phenotype and ensures the functional integrity of neurons. Furthermore, NGF is promising for clinical use in central neurodegenerative diseases, vascular diseases, and immune system defects[87]. EGF was the first growth factor to be discovered and it binds to the epidermal growth factor receptor with other EGF family members. EGF stimulates cell proliferation and differentiation and could be further used in the development of cancer therapy[88]. BFGF is a heparin-binding protein and a member of the fibroblast growth factor which can also control the proliferation and differentiation of various cell types[89]. BFGF could have further therapeutic potential in wound healing, tumor treatment, and nervous system disease[90]. For example, Liu *et al*. showed that cell culture medium with bFGF along with N2 and B27 supplements could support the self-renewal of human ESCs and maintain the cells in an undifferentiated state. Also, the human ESCs cultured medium with bFGF, N2 and B27 supplements could enhance cell viability and proliferation[91].

In addition, Choi *et al.* demonstrated that the combinations of growth factors have significant effects on NSCs proliferation and differentiation while a single growth factor produces a low rate of neural differentiation. The combination of bFGF and insulin growth factor-I promoted the most differentiation. Also, the combination of NGF and brain-derived neurotrophic factor shows an additive effect and the most differentiation towards neurons[92].

Chapter 3 Effect of Topography and Stiffness on Human Neural Progenitor Cells Differentiation and Maturation

3.1 Introduction

Cells respond differently to substrates with various mechanical properties, such as topography, stiffness, and porosity. Topographic patterns such as the pillar, groove, and grating can be fabricated in micro/nanoscale and affect cell adhesion, morphology, proliferation, and differentiation[9, 65]. For example, the spread cell morphology with a large cell area could be observed on the pillar surface, while cell elongation was observed on the groove surface [93]. The neurite extension and elongation can also be modulated by topographic patterns. Additionally, with increasing grating depth, the neurite alignment was also enhanced [68]. The stiffness also manipulates cell morphology and proliferation. For instance, the neural crest stem cells have a larger spreading area[21], and bone marrow mesenchymal stem cells proliferate better on stiffer substrates[21, 71]. Also, the surface rigidity regulates the differentiation into different cell types. Neurons would favour a soft hydrogel surface with E less than 1 kPa[12, 73], while astrocytes prefer a moderately stiffer scaffold with roughness at about 9 kPa[74].

Therefore, we hypothesized that various topographies and stiffnesses would affect neuronal differentiation and maturation.

In this chapter, we explore the effect of different topographies and stiffnesses on neural cells. Human neural progenitor cells (hNPCs) were cultured on the polyacrylamide (PAA) hydrogel, which was prepared using N-acryloyl-6-aminocaproic acid (ACA). The PAA-ACA substrates were fabricated with different topographies combined with different stiffnesses. The stiffness was modulated by changing the ratio of acrylamide and bisacrylamide and the topographies were fabricated using prepared pattered molds. Both Wild-type (WT) and Rett-syndrome type (RTT) hNPCs were seeded on the substrates with various combinations of topographies and stiffnesses to analyze the cell response.

Then WT cells were cultured for 21 days on PAA-ACA gels and further analyzed with the DAPI, TUJ1, and MAP2 markers in immunofluorescence staining. Quantitative real-time reverse-transcription polymerase chain reaction (RT-qPCR) was operated with the GAPDH as a housekeeping gene, TUJ1 to express neuronal differentiation, MAP2 to express neuronal maturation and Syn1 to detect the degree of synaptic maturation.

3.2 Method and Materials

3.2.1 hNPCs Maintenance and Differentiation

The hNPCs were used to study the effect of topography and stiffness. The primary hNPCs were obtained from Dr. Eyleen Goh's lab at the National University of Singapore. The generation protocol can be found in the study by Chin *et al.*[94] The hNPC lines and the isogenic control line without the MECP2 mutation (denoted as CTRL) were induced from iPSCs from one Rett patient with a 320 nucleotide deletion at nucleotide number 1155 (denoted as RTT). The Rett patient fibroblasts (GM11272) were obtained from Coriell Institute for Medical Research (New Jersey, USA). The neural progenitor cells used in this study were derived from induced pluripotent stem cells, which were reprogrammed from Rett patient-specific fibroblasts in Dr. Goh's lab; the induction and the preliminary characterizations were described in Chin *et al*.[94] The work is performed under the University of Waterloo Ethics Approval (41244).

The hNPCs cultured with maintenance media, which contains Dulbecco's Modified Eagle Medium/Nutrient Mixture F-12 (DMEM/F12 (1:1)) (LS11330032 Grand Island Biological Company) and Neurobasal medium (LS21103049 Grand Island Biological Company), 1% N2 supplement 100X (LS17502048 Grand Island Biological Company), 1% penicillin-streptomycin 10,000 μg/ml (PS) (LS15140122 Grand Island Biological Company), 2% B27 supplement 50X (LS17504044 Grand Island Biological Company), 1% GlutaMAX™ supplement 100X (LS35050061 Grand Island Biological Company). Beside those, bovine serum albumin (BSA) (A3294 Sigma Aldrich) in 1X Phosphate-

buffered saline (PBS) solution, which was diluted with 10X PBS (Fisher BioReagents BP399-20), Human Recombinant LIF (78055 STEMCELL Technologies Inc.) in 1X PBS, CHIR99021 (C2447 Cellagen Technology) in dimethyl sulfoxide (DMSO) (D5879 Sigma Aldrich) and SB431542 (C7243 Cellagen Technology) in DMSO were added. The specific volume for each substance is shown below in Table 1.

Table 1. Composition in a volume of 50 ml maintenance media for hNPCs.

Reagent	Maintenance Media	Final Concentration
DMEM/F-12 medium	23.5 ml	-
Neurobasal medium	23.5 ml	-
N2 supplement 100X	0.5 ml	1X
Penicillin streptomycin 10,000 µg/ml	0.5 ml	1X
B27 supplement 50X	1 ml	1X
GlutaMAX™ supplement 100X	0.5 ml	1X
Bovine serum albumin (5 mg/ml)	50 µl	5 µg/ml
Human Recombinant LIF (50 µg/ml)	10 µl	10 ng/ml
CHIR99021(0.8 mM)	187.5µl	3 µM
SB431542 (10 mM)	10 µl	2 µM

Once the cells reached 90% confluence, the supernatant maintenance media was removed, and the plate surface was rinsed with warmed 1X PBS. Then Accutase Cell detachment solution (25-058-CI Corning Incorporated) was added, and the plate was incubated at 37 °C until most of the cells were detached. The same amount of maintenance media was added. The cells were transferred into a 15 ml centrifuge tube and centrifuged for 5 min at 1000 rpm. The upper suspension was discarded, and 5 ml fresh maintenance media was added. The cell solution was gently pipetted up and down two to three times to resuspend the cell pellet. Cells were counted by hemocytometer and seeded at 50,000 cell/ cm^2 on a plate or flask coated with Matrigel® Basement Membrane Matrix (354248 Corning Incorporated).

Matrigel was first thawed at 4 °C and diluted to 1:50 with cold DMEM/F12 medium. The plate was incubated with the Matrigel solution for either 30 min at 37 °C in an incubator, 1 hour at room temperature or overnight at 4 °C.

After seeding, 0.5 µM 4-[(1R)-1-aminoethyl]-N-4-pyridinyl-trans-cyclohexanecarboxamide (ROCK inhibitor) (Y-27632 STEMCELL Technologies Inc.) was added, which was reconstituted in deionized water. The plate or flask was maintained in a 37 °C incubator with 5% CO_2, 99% humidity and 50% of the maintenance media was changed every other day.

The differentiation media was composed with DMEM/F12 (1:1) medium, Neurobasal medium, 1% N2 supplement 100X, 1% 10,000 µg/ml PS, 2% B27 supplement 50X, 1% GlutaMAX™ supplement 100X. The specific volume for each substance is shown below in Table 2.

Table 2. Composition in a volume of 50 ml differentiation media for hNPCs.

Reagent	Differentiation Media	Final Concentration
DMEM/F-12 medium	24 ml	-
Neurobasal medium	24 ml	-
N2 supplement 100X	0.5 ml	1X
Penicillin streptomycin 10,000 µg/ml	0.5 ml	1X
B27 supplement 50X	1 ml	1X
GlutaMAX™ supplement 100X	0.5 ml	1X

3.2.2 Polyacrylamide (PAA) Hydrogels Fabrication

3.2.2.1 Activate Coverslips

Polyacrylamide (PAA) hydrogel was fabricated on a 12mm diameter round coverslip (CLS-1760-012 Chemglass Life Sciences) according to the protocol developed by Yip *et al.* [95]. The coverslips were first slightly immersed in ethanol and flamed. They were then

submersed in a 0.5% (v/v) solution of (3-Aminopropyl) triethoxysilane (ATPES) (A3648 Sigma Aldrich) in deionized water for 30 min. After this, the coverslips were rinsed with deionized water six times, each time for 5 min. Kim wipes were used to soak up most of the water and the coverslips were dried at room temperature for about 1 hour. The coverslips were then incubated in 0.5% glutaraldehyde (G6257 Sigma Aldrich) in 1X PBS solution for another 30 min, and rinsed with deionized water three to six times, each time for 5 min. After the coverslips were dried at room temperature overnight, they could be stored at 4 °C with calcium chloride to prevent moisture.

3.2.2.2 Pre-polymerized Hydrogel

The N-acryloyl-6-aminocaproic acid (ACA) solution was first prepared with ACA powder (A1896 TCI America) dissolved in 0.35 M Sodium hydroxide in filtered deionized water and filtered with 0.2 μm syringe filter. The solution could be stored at 4 °C for up to one month. The polyethylene terephthalate (PET) (ES301445 Goodfellow Cambridge Limited) molds with 2 μm gratings, 5 μm gratings, and 10 μm gratings were fabricated. The 2 μm gratings refer to the topographic gratings with width of 2 μm, space of 2 μm and height of 2 μm. Similarly, the 5 μm gratings refer to the topographic gratings with width of 5 μm, space of 5 μm and height of 5 μm, and the 10 μm gratings have the gratings width of 10 μm, space of 10 μm and height of 10 μm. The PET molds were fabricated in our lab by Ms. S Mattiassi previously[96] and the fabrication method was according to the study by Yip *et al*.[97]. The molds were dried with air before use. In order to prepare 100 mM 2-(*N*-morpholino) ethanesulfonic acid (MES) buffer, one pack of MES buffered saline (Thermo Scientific™ 0028390) was dissolved in 500 ml of autoclaved water. Each pack contains 0.1M MES, 0.9% sodium chloride and the pH is 4.7. Then 5M NaOH was used to adjust the MES buffer to pH 6.1 then the solution was filtered with a 0.2 μm syringe filter.

The pre-polymerized solutions were mixed with 40% acrylamide solution (1610140 Bio-Rad), 2% bis-acrylamide solution (1610142 Bio-Rad), 500mM ACA solution and

filtered deionized water. PAA-ACA gels of different stiffnesses were fabricated and the specific volume of each substance is shown below in Table 3. The activated coverslips were then placed in the petri dish. Then ammonium persulfate (APS) (A3678 Sigma Aldrich) and *N*,*N*,*N*′,*N*′-Tetramethylethylenediamine (TEMED) (T7024 Sigma Aldrich) were added. 18 µl of the mixed solution was distributed drop by drop on the different positions of each coverslip. The prepared PET mold with different patterns was carefully placed on the top and the plate on the table was carefully knocked two to three times to make sure the solutions were spread evenly on the coverslips. Then the plates were first incubated at 37 °C for 20 min. After the polymerization was completed, MES buffer was added to each petri dish and the plates were incubated overnight at 4 °C for up to one week. The stiffness was defined as the resistance to the applied force. A previous study in our lab by Ms. S Mattiassi measured the Young's modulus of PAA-ACA gels using a compressive test with MicroTester (CellScale, Canada)[96]. The modulus was equal to the slope of the linear portion of the stress versus strain curve.

Table 3. Composition in a volume for 100 µl PAA-ACA gel pre-polymerized solution with different stiffnesses.

	Stiffness			
Reagent	6.2 kPa	14.4 kPa	31.6 kPa	110.5 kPa
40% Acrylamide (µl)	7.5	10	13.8	25
2% bis-acrylamide (µl)	6.5	8.5	11.5	21.5
500mM ACA (µl)	20	20	20	20
Filtered DI water (µl)	64	59.5	52.7	31.5
TEMED (µl)	1	1	1	1
APS (µl)	1	1	1	1

3.2.2.3 Conjugation of Extracellular Matrix

After the incubation with MES buffer, the PET molds were carefully removed from the PAA-ACA gels and gel samples were washed with MES buffer three times. Patterns

were checked by the Microscope Primovert (415510-1101-000 Carl Zeiss) to ensure that the gratings were clear, and no big bubbles were present on the gels. Then the samples were sterilized under ultraviolet light for 30 min in a biosafety cabinet.

The PAA-ACA gels were activated by 0.5M N-Hydroxysuccinimide (NHS) (130672 Sigma Aldrich) and 0.2M N-(3-Dimethylaminopropyl)-N′-ethylcarbodiimide hydrochloride) (EDC) (E7750 Sigma Aldrich) in 100 mM MES buffer. The solution was filtered with a 0.2 μm syringe filter and 750 μl was added to the gel for each well. The samples were immersed with the solution on the shaker for 30 min at room temperature and then washed with the sterilized 1X PBS three times. Then the PAA-ACA gels were coated with 0.5 mg/ml Poly-L-lysine hydrobromide (PLL) (molecular weight 30,000 – 70,000) (P2636 Sigma Aldrich) dissolved with sterilized 1X PBS for 2 hours at room temperature. Blank coverslips were also prepared as a control. Similarly, samples were coated with 0.1 mg/ml Poly-L-ornithine (PLO) (molecular weight 30,000 – 70,000) (P4957 Sigma Aldrich) diluted with sterilized 1X PBS.

After the incubation, samples were washed with sterilized 1X PBS three times and conjugated with 20 μg/ml Laminin (LAM), which is from Engelbreth-Holm-Swarm (EHS) mouse tumor (354232 Corning Incorporated) diluted with sterilized 1X PBS. Samples were placed in a 37 °C incubator for 2 hours and then washed with sterilized 1X PBS one more time for 5 min. The plate could be sealed and stored at 4 °C for up to one week or incubated with warmed DMEM/F12 medium before cell seeding to avoid the residual PBS diluting the culture media.

3.2.3 Cell Seeding

hNPCs were seeded with maintenance media and 5 μM ROCK inhibitor. Seeding density was at 20,000 cells/$cm^{2.}$ Then all the media was changed to differentiation media after 24 hours. The media composition is mentioned above in Table 2.

The plate was maintained for 21 days in a 37 °C incubator with 5% CO_2, 99% humidity and 50% of the media was changed every other day.

3.2.4 Immunofluorescence Staining

After 21 days, cells were washed three times with sterile 1X PBS, then fixed with filtered pH-adjusted 4% paraformaldehyde for 20 min at room temperature. Then they were washed with 1X PBS three times and permeabilized with 0.25% Triton™ X-100 (T8787 Sigma Aldrich) in 1X tris-buffered saline (TBS), which was diluted with 10X TBS (pH 7.4) (BP2471-500 Fisher BioReagents) in for 15 min at room temperature. Samples were washed with 1X TBS three times and blocked with 1% bovine serum albumin (BSA) and 10% goat serum in filtered 1X TBS for 1 hour at room temperature or overnight at 4 °C.

Next, the samples were immunofluorescently stained with a primary antibody solution, which consisted of 1% goat serum, beta III Tubulin (TUJ1) (1:600) (Rabbit Anti-beta III Tubulin antibody, Polyclonal, Abcam), microtubule-associated protein 2 (MAP2) (1:600) (mouse Anti-MAP2 antibody, Polyclonal, Abcam) and 1X TBS, overnight at 4 °C. Then samples were washed with 0.05% Triton™ X-100 and 1% goat serum in 1X TBS three times, each time for 5 min. Samples were incubated overnight at 4 °C with the secondary antibody solution, which contains Alexa-Fluor 488 goat anti-rabbit IgG for TUJ1 (1:750) (A11034 Invitrogen™), Alexa-Fluor 546 goat anti-mouse IgG for MAP2 (1:750) (A11003 Invitrogen™) and 1X TBS.

Samples were washed with 1X TBS three times each for 10 min, and then stained with 4',6-Diamidino-2-Phenylindole, Dihydrochloride (DAPI) solution (1:2200) (D9542 Sigma Aldrich) and Alexa Fluor 546 phalloidin (1:500,) (A22283 Invitrogen™) for 1 hour at room temperature.

After washing with 1X TBS three times, samples were mounted on 24mm * 50mm cover glasses (thickness between 0.17mm to 0.25mm) (12-543D, 24X502602811G Fisher

brand™) with Fluoromount-G™ Mounting Medium (5018788 Invitrogen™) overnight in the fridge to settle down. A Zeiss fluorescence microscope (Axio Observer Z1) was used for imaging and ImageJ was used for analysis.

3.2.5 RNA Isolation

Once the cells were cultured on PAA-ACA gel for 21 days, the isolation of RNA was performed according to the RNeasy Mini Handbook using the RNeasy Mini Kit (74104 QIAGEN).

The initial steps were similar to the first part of cell passaging. The excess media in each well was aspirated, and the plate surface was rinsed with 500 µl warmed 1X PBS for each well. Then 500 µl Accutase Cell detachment solution per well was added and incubated at 37 °C for about 5 min ensuring most of the cells were detached. The same amount of differentiation media was added and transferred into a 15 ml centrifuge tube. The cells were centrifuged for 5 min at 1,000 rpm and the supernatant was discarded.

Then 600 µl of Buffer RLT was added to each sample. The solution was pipetted up and down to make sure the cell pellet was loosed in the buffer and no cell clumps were visible. The same amount of 600 µl 70% ethanol was added and the solution was mixed well by pipetting. Then up to 700 µl of the sample was transferred to the RNeasy spin column. The spin column was placed in a 2 ml collection tube, which was directly provided in the RNeasy kit. The lid was closed gently and the whole tube was centrifuged for 15s at 10,000 rpm. The wasted flow collected in the 2 ml collection tube was discarded after each centrifugation. The volume of each sample was 1,200 µl and was transferred either in 600 µl volumes twice or in one volume of 700 µl and another of 500µl. The tube was tapped upside down on the Kim wipes several times, ensuring there was no residual flow.

700 µl of Buffer RW1 was added to the RNeasy spin column. Similarly, the lid was closed gently, and the whole tube was centrifuged for 15s at 10,000 rpm to wash the

membrane of the spin column. The flow-through was disposed and the 2 ml collection tube was tapped upside down a few times.

11 ml Buffer RPE concentrate was provided in the RNeasy kit and was prepared by adding 44 ml 100% ethanol before the first-time use. 500 µl of Buffer RPE was added to the spin column and the wasted flow was discarded after the centrifugation for 15s at 10,000 rpm. Another 500 µl of Buffer RPE was added to the spin column. The tube was centrifuged for 2 min at 10,000 with the lids closed. The long centrifugation was to dry the membrane and make sure no ethanol was left. The spin column was carefully removed to avoid contact with the flow-through. Optionally, the spin column could be placed in a new 2 ml collection tube and centrifuged for 1 min at 10,000 rpm to eliminate the remnant of Buffer RPE.

The spin column was then placed in a new 1.5 ml collection tube with a lid. 30 µl of RNAse-free water was added directly to the spin column membrane and avoiding adding to the wall of the spin column. The RNA was eluted by centrifugation for 1 min at 10,000 rpm. If the expected RNA amount was more than 30 µl, the previous step would be repeated by adding another 30 µl of RNAse-free water and centrifuging again.

3.2.6 cDNA Synthesis

Ribonucleic acid (RNA) amount of each sample was measured by a NanoDrop ND-1000 Spectrophotometer. A 1 µl RNA sample was diluted with 4 µl RNAse-free water and measured twice. RNase-free water was used as blank. The concentration and purity of RNA were the averages of the two measurements.

Then iScript™ cDNA Synthesis Kit **(**1708890 Bio-Rad) was used to convert RNA to complementary deoxyribonucleic acid (cDNA). Up to 1 µg of RNA was converted to cDNA each time to ensure optimal synthesis efficiency. For each reaction, 4 µl of 5x iScript reaction mix, 1 µl iScript reverse transcriptase, RNA sample and nuclease-free water were mixed thoroughly. The volume of each sample depended on the concentration,

which was calculated from the Nanodrop result and the rest was the nuclease-free water. The total amount for each reaction mix was 20 µl.

The reaction mix was incubated in a thermal cycler. The sample was held at 25 °C for 5 min for priming. Then held at 46 °C for 20 min for reverse transcription, followed by 1 min at 95 °C for RT inactivation. Samples could be held in 4 °C overnight before the samples would be further analyzed. Then samples could be directly used for RT-qPCR experiments or stored in a -80 °C freezer.

3.2.7 Quantitative Real-time Reverse-transcription Polymerase Chain Reaction

The RT-qPCR was operated with SsoFast™ EvaGreen® Supermix (1725201 Bio-Rad) and StepOne™ Real-Time PCR System (4379216 Applied Biosystems™).

For each primer, 10 µl of SsoFast EvaGreen Supermix solution, 1 µl of forward primer, 1 µl of reverse primer and 6 µl of RNase-free water were first mixed together. The primer sequences used for RT-qPCR is shown below in Table 4. The primer sequence of human glyceraldehyde-3-phosphate dehydrogenase (GAPDH), hTUJ1, hMAP2, and human Synapsin I (hSyn1) were according to our lab's previous publication [36] and the primer sequence of human hypoxanthine phosphoribosyl-transferase 1 (hHPRT1), and human beta (β)-actin (hACTB) were designed by PrimerQuest Tool (Integrated DNA Technologies, Inc.).

A total of 18 µl Supermix solution was added to 96-well reaction plate (LS4346906 Applied Biosystems™) and then 2 µl of cDNA sample was added. The pipette tips were changed between each well and the solution was mixed thoroughly. Then the plate was sealed with ThermalSeal RT2RR™ film (TS-RT2RR-100 EXCEL Scientific, Inc.) and centrifuged at 2400 rpm for 1 min.

The StepOne™ Software was used and the run method was set up with holding, cycling, and melt curve stage. For the cycling stage, the reaction temperature was increased to 95 °C for 15 sec and then lowered to 58 °C for 1 min. The above two steps

were repeated for 40 cycles to obtain the Ct value. The level of gene expression was calculated using ΔΔCt method and fold gene expression is equal to $2^{\wedge-(\Delta\Delta Ct)}$ [98].

Table 4. Primer Sequence for RT-qPCR.

Marker	Direction	Sequence
hGAPDH	Forward	5'-CTGACTTCAACAGCGACACC-3'
	Reverse	5'-AGGGGTCTACATGGCAACTG-3'
hTUJ1	Forward	5'-GGCCTTTGGACATCTCTTCA-3'
	Reverse	5'-ATACTCCTCACGCACCTTGC-3'
hMAP2	Forward	5'-GCATATGCGCTGATTCTTCA-3'
	Reverse	5'-CTTTCCGTTCATCTGCCATT-3'
hSyn1	Forward	5'-GA TGGGCAAGGTCAAGGTTG-3'
	Reverse	5'-ATTTGGCATCGATGAAGGGC-3'
hHPRT1	Forward	5'- GCTGACCTGCTGGATTACAT -3'
	Reverse	5'-CCCTGTTGACTGGTCATTACA-3'
hACTB	Forward	5'-GCATCCTCACCCTGAAGTA-3'
	Reverse	5'-CACGCAGCTCATTGTAGAAG-3'

3.2.8 Statistical Analysis

Statistical analysis was determined using GraphPad Prism 8 software. One-way analysis of variance (ANOVA) was used to detect the significant difference among each sample group. N.S. denotes there is no significant difference. Data were presented with mean ± standard deviation of three biological replicates.

3.3 Results

3.3.1 Characterization of Patterned PAA-ACA Hydrogels

The patterned PAA-ACA hydrogels were prepared with PET molds. Three dimensions of 2 μm gratings, 5 μm gratings, and 10 μm gratings were fabricated. The 2 μm gratings refer to the topographic gratings with width of 2 μm, space of 2 μm and height of 2 μm. Also, the 5 μm gratings refer to the topographic gratings with width of 5 μm, space of 5 μm and height of 5 μm, and the 10 μm gratings have the gratings width of 10 μm, space of 10 μm and height of 10 μm. The phase-contrast images were taken by Zeiss Primovert microscope. The surface characterization of the patterned PAA-ACA hydrogels and the cross-sectional view of the pattern are shown below in Figure 2.

According to another lab member Ms. S Mattiassi's measurement, the mechanical moduli of the PAA-ACA hydrogels were: 6.1 ± 0.6 kPa for the "6.2 kPa" gel, 12.9 ± 2.5 kPa for the "14.4 kPa" gel, 22.9 ± 3.2 kPa for the "31.6 kPa" gel and 92.6 ± 4.9 kPa for the "110.5 kPa"[96].

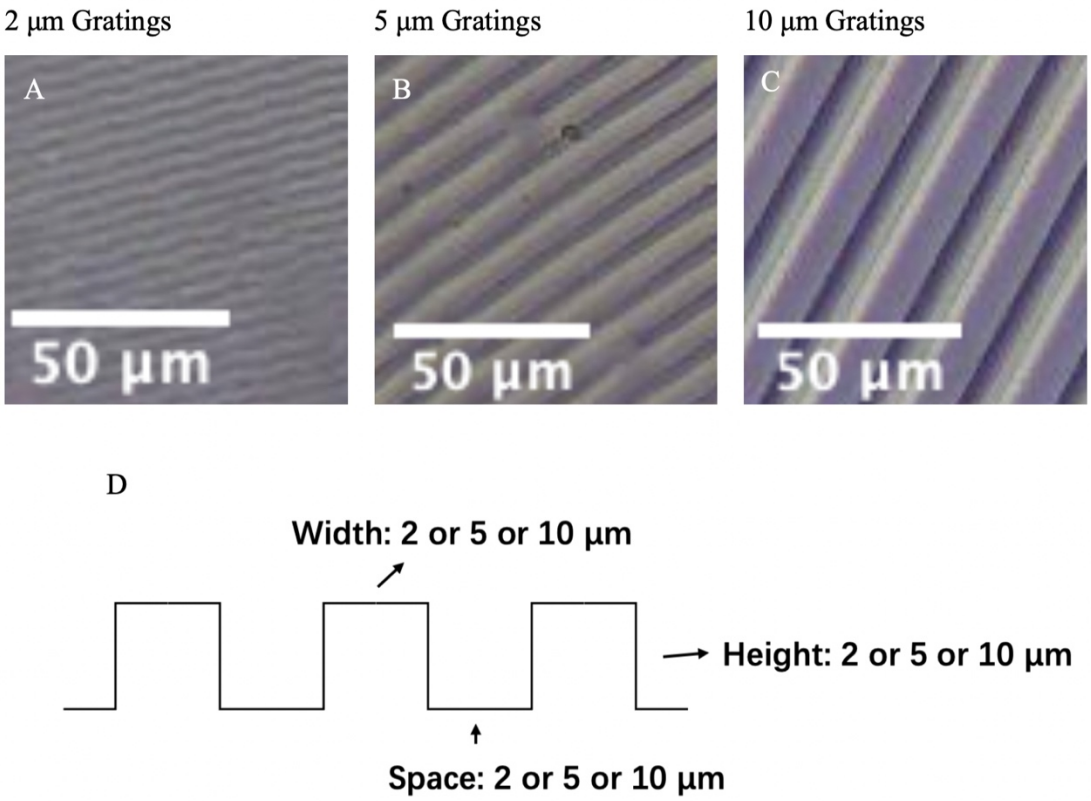

Figure 2. Surface characterization of patterned PAA-ACA hydrogels and the cross-sectional view of the pattern. The substrates were fabricated with 2 μm gratings (A), 5 μm gratings (B), and 10 μm gratings (C) and the phase-contrast images were taken by Zeiss Primovert microscope. The gratings dimensions of 2 μm gratings are width of 2 μm, space of 2 μm and height of 2 μm. The gratings dimensions of 5 μm gratings are width of 5 μm, space of 5 μm and height of 5 μm. The gratings dimensions of 10 μm gratings are width of 10 μm, space of 10 μm and height of 10 μm. Scale bars in all phase-contrast images are 50 μm. (D) Cross-sectional view of the pattern.

3.3.2 WT hNPCs Differentiation on Substrates with Different Topographies and Stiffnesses

WT hNPCs were cultured on PAA-ACA substrates with different topographies and stiffnesses. The surface was coated with PLL + LAM. Cells were seeded with maintenance media and ROCK inhibitor and all the media was replaced with differentiation after 24 hours. Cell behaviors on Day 1 after the replacement with differentiation media are shown below in Figure 3. The seeding density was 20,000 cells/cm^2 and the glass coverslips coated with PLL + LAM were used as a control to ensure cells were healthy and able to differentiate (Figure 3 I). WT hNPCs could adhere and differentiate on both unpatterned PAA-ACA gels (Figure 3 A-D) and PAA-ACA gels with 2 μm gratings (Figure 3 E-H). Cells could also respond and attach to the PAA-ACA substrates of four different stiffness, with Young's modulus of 6.2 kPa (Figure 3 A and E), 14.4 kPa (Figure 3 B and F), 31.6 kPa (Figure 3 C and G) and 110.5 kPa (Figure 3 D and H). Compared to the unpatterned substrates, higher cell densities were shown on the surface with 2 μm gratings. With more cells adhered, the topographic pattern could promote more cell attachment. Also, the cell bodies and branches on the patterned substrates were longer. The elongation and extension of the cells were aligned in the direction parallel to the grating axis, while cells spread randomly on both unpatterned PAA-ACA gels and control coverslips. Moreover, on the patterned PAA-ACA gels, the softest one (6.2 kPa) had the most cells attached and longest cell branches, which could support more cell adhesion and differentiation.

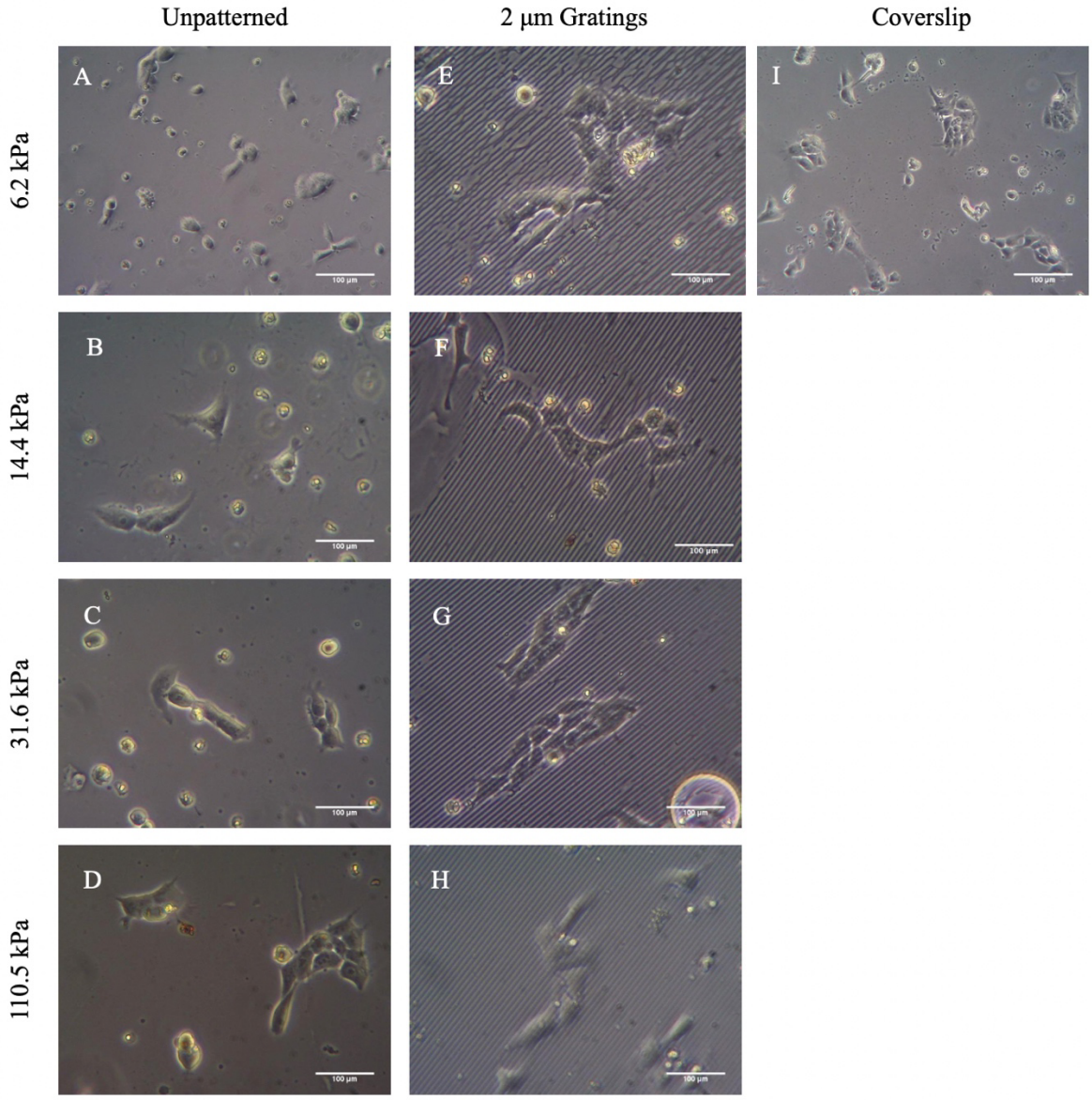

Figure 3. Representative phase-contrast images of WT hNPCs on PAA-ACA substrates with PLL+LAM coating on Day 1 after the replacement with differentiation media. WT hNPCs were cultured on the unpatterned PAA-ACA hydrogels (A-D) and PAA-ACA hydrogels with 2 µm gratings (E-H). Four different stiffness with Young's modulus of 6.2 kPa (A and E), 14.4 kPa (B and F), 31.6 kPa (C and G) and 110.5 kPa (D and H) were

fabricated with topographies. The seeding density was 20,000 cells/cm^2 and glass coverslips coated with PLL+LAM were used as control (I). Scale bars in all images are 100 μm.

3.3.3 RTT hNPCs Differentiation on Substrates with Different Topographies and Stiffnesses

Rett syndrome (RTT) is a genetic neurological disorder caused by the maturation of MECP2, which participates in the neural cells [34]. Therefore, the neuronal differentiation of RTT would be a promising solution for RTT therapy. RTT hNPCs derived from patient iPSCs were seeded on substrates with different topographies and stiffnesses to evaluate the response of the cell. The PAA-ACA surfaces were coated with PLL+LAM and the cells were seeded with maintenance media and ROCK inhibitor at the seeding density of 10,000 cells/cm^2. Similarly, all the media were changed to differentiation media and the glass coverslips coated with PLL+LAM were used as control. Cells behaviors on Day 1 and Day 9 after the replacement to differentiation media are shown below in Figure 4. RTT cells were seeded on PAA-ACA hydrogels with various combinations of topography and stiffness, which were 2 μm gratings + 6.2 kPa (Figure 4 A and F), 10 μm gratings + 14.4 kPa (Figure 4 B and G), 10 μm gratings + 31.6 kPa (Figure 4 C and H) and 2 μm gratings + 110.5 kPa (Figure 4 D and I). All these combinations could support cell adhesion and differentiation. Similar to WT hNPCs, the differentiation of RTT cells also extended following the axis of the gratings, while no preference of the directions as shown on unpatterned gels. On Day1, cell numbers were similar on the PAA-ACA substrates with different topographies and stiffnesses. On day 9, more cells were well attached and remained on the scaffold. PAA-ACA substrates with 2 μm gratings had more cells attached and larger spreading areas, compared to the 10 μm gratings pattern. However, the cells grew into clusters over time, which were difficult to observe and analyze with phase-contrast images.

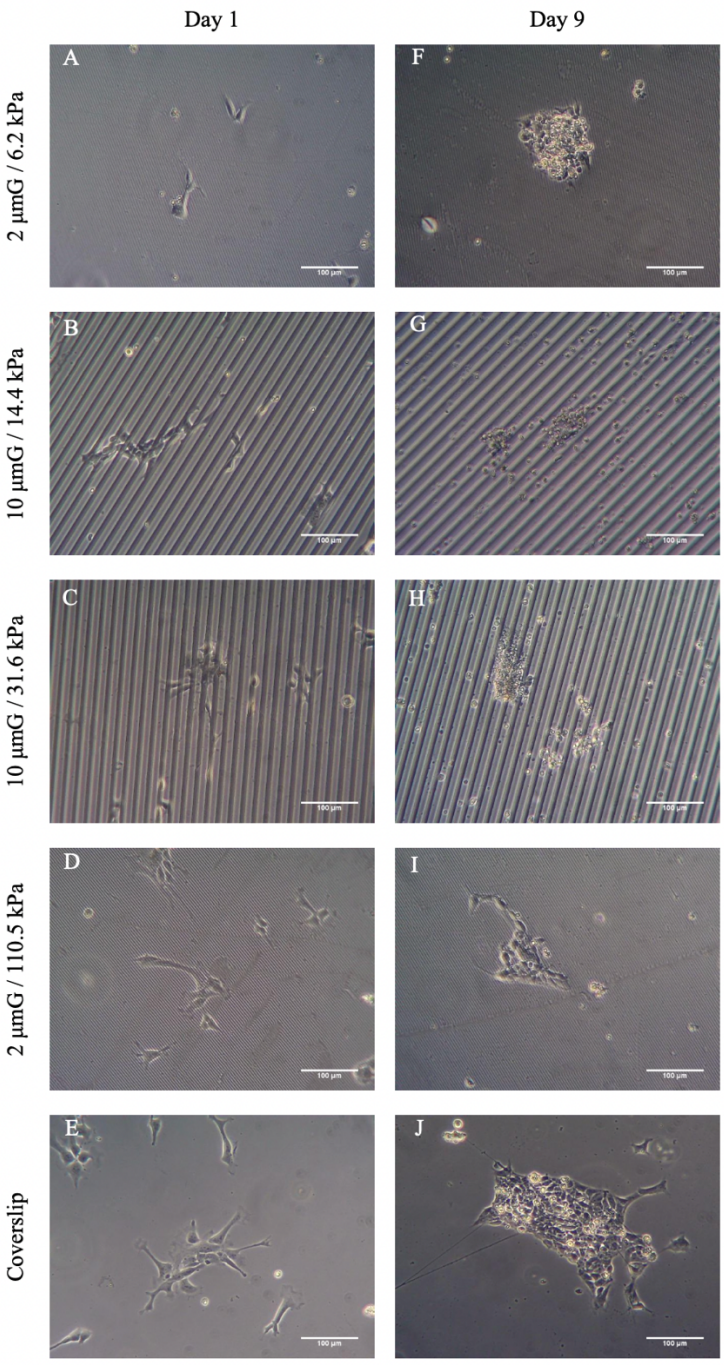

Figure 4. Representative phase-contrast images of RTT hNPCs on PAA-ACA substrates with PLL+LAM coating on Day 1 (A-E) and Day 9 (F-J) after the replacement with

differentiation media. RTT hNPCs were cultured on the hydrogels with different combinations of topography and stiffness, which were 2 μm gratings + 6.2 kPa (A and F), 10 μm gratings + 14.4 kPa (B and G), 10 μm gratings + 31.6 kPa (C and H) and 2 μm gratings + 110.5 kPa (D and I). The seeding density was 10,000 cells/cm^2 and glass coverslips coated with PLL+LAM were used as control (E and J). Scale bars in all images are 100 μm.

3.3.4 Effect of Topography and Stiffness on Neuronal Differentiation and Maturation

Next, the neuronal differentiation and maturation of hNPCs on different topographies and stiffnesses were analyzed. WT hNPCs were cultured on the PAA-ACA substrates for 21 days and analyzed by immunofluorescence staining. Representative staining images are shown below in Figure 5. PAA-ACA substrates were fabricated with unpatterned (Figure 5 A and E), 2 μm gratings (Figure 5 B and F), 5 μm gratings (Figure 5 C and G), and 10 μm gratings (Figure 5 D and H) combined with two different stiffness, with Young's modulus of 6.2 kPa (Figure 5 A-D) and 110.5 kPa (Figure 5 E-H). The surfaces of PAA-ACA gels were coated with PLL + LAM to help induce the differentiation. Also, glass coverslips coated with PLL + LAM were treated as control. After culturing for 21 days, cells were stained against DAPI for cell nuclei, TUJ1 for neuronal differentiation and MAP2 for neuronal maturation.

Shown by the expression of the TUJ1 marker in all images, hNPCs seeded on the PAA-ACA substrates with various topographies and stiffnesses were able to differentiate to neurons after 21 days. Also, cells seeded on the substrates all showed the expression of the MAP2 marker which indicated the neurons were able to remain on the scaffold and mature. The arrows with white outlines denoted the direction of the gratings' axis. Cells elongated aligned with the grating pattern. WT hNPCs seeded on the patterned surfaces had longer neurites compared to the unpatterned scaffold. The topographic cues were able to promote neurite elongation. Moreover, different topographies and stiffnesses of PAA-ACA substrates could affect neuronal differentiation and maturation. Softer substrates

showed higher expression of the TUJ1 marker. In the softer sample group, patterned substrates showed higher expression of the MAP2 marker.

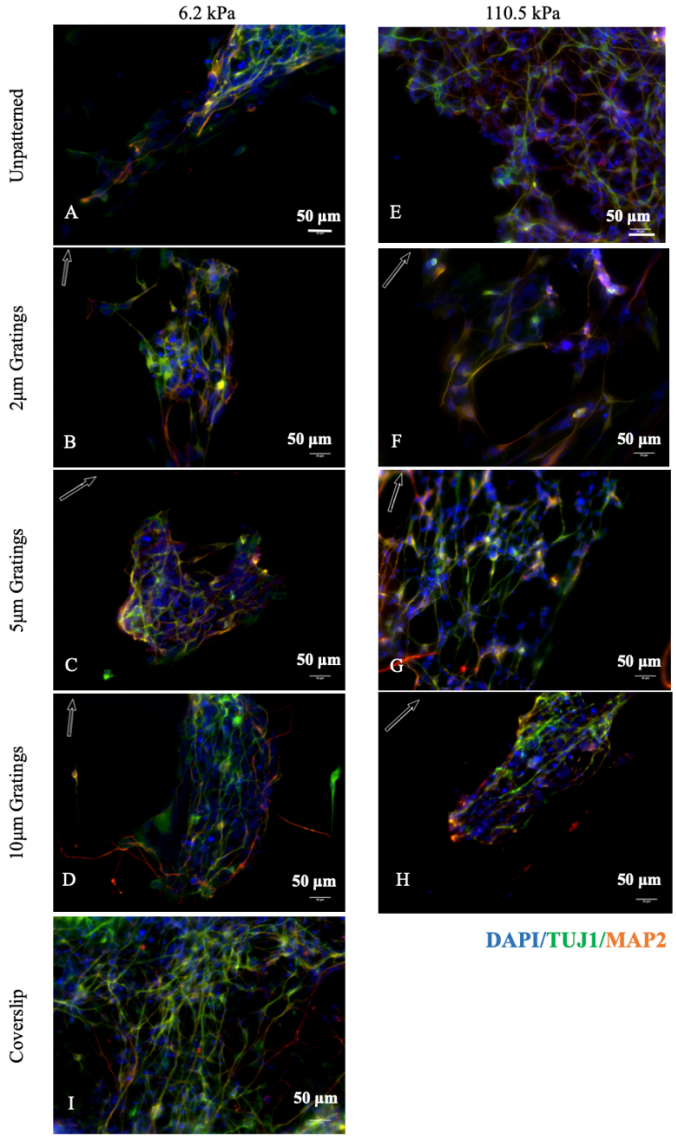

Figure 5. Representative immunofluorescence images of WT hNPCs on PAA-ACA substrates with PLL+LAM coating. WT hNPCs were seeded on the unpatterned PAA-ACA hydrogels (A and E) and PAA-ACA hydrogels with 2 μm gratings (B and F), 5 μm

gratings (C and G), and 10 μm gratings (D and H) combined with the stiffness of 6.2 kPa (A-D) and 110.5 kPa (E-H). Seeding density was 20,000 cells/cm^2 and glass coverslips coated with PLL+LAM were used as control (I). Cells were differentiated for 21 days and then stained with DAPI (blue channel) as a counterstaining, TUJ1 (green channel) and MAP2 (orange channel). White arrows indicate the direction of gratings. Scale bars in all images are 50 μm.

Representative staining images of separated channels and merged are shown below. Figure 6 showed the WT hNPCs seeded on the PAA-ACA substrates with the stiffness of 6.2 kPa and combined unpatterned (Figure 6 A-D), 2 μm gratings (Figure 6 E-H), 5 μm gratings (Figure 6 I-L), and 10 μm gratings (Figure 6 M-P). The PAA-ACA substrates with PLL + LAM coating and the seeding density was 20,000 cells/cm^2. Cells were differentiated for 21 days and then stained with DAPI for cell nuclei (exhibited blue fluorescence) (Figure 6 A, E, I, M), TUJ1 for neuronal differentiation (exhibited green fluorescence) (Figure 6 B, F, J, N) and MAP2 for neuronal maturation (exhibited orange fluorescence) (Figure 6 C, G, K, O). The merged channels (Figure 6 D, H, L, P) with white arrows indicate the direction of gratings.

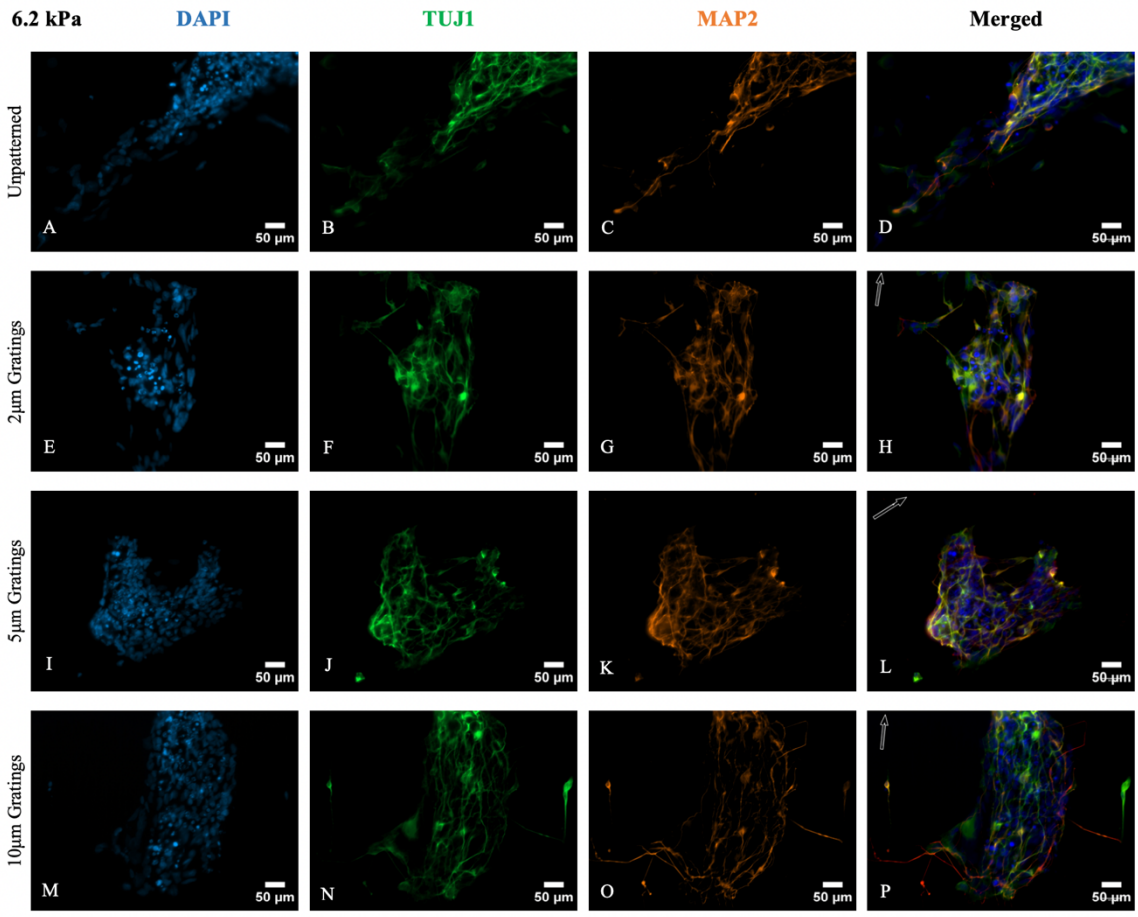

Figure 6. Representative immunofluorescence images with separated channels. WT hNPCs were seeded on the unpatterned PAA-ACA hydrogels (A-D) and PAA-ACA hydrogels with 2 μm gratings (E-H), 5 μm gratings (I-L), and 10 μm gratings (M-P) combined with the stiffness of 6.2 kPa. The PAA-ACA substrates with PLL+LAM coating and the seeding density was 20,000 cells/cm^2. Cells were differentiated for 21 days and then stained with DAPI (blue channel) as a counterstaining (A, E, I, M), TUJ1 (green channel) for neuronal differentiation (B, F, J, N) and MAP2 (orange channel) for neuronal maturation (C, G, K, O). The merged channels (D, H, L, P) with white arrows indicate the direction of gratings. Scale bars in all images are 50 μm.

Representative staining images of separated channels and merged are shown below. Figure 7 showed the WT hNPCs seeded on the PAA-ACA substrates with the stiffness of 110.5 kPa and combined unpatterned (Figure 7 A-D), 2 μm gratings (Figure 7 E-H), 5 μm gratings (Figure 7 I-L), and 10 μm gratings (Figure 7 M-P). The PAA-ACA substrates were coated with PLL+LAM and the glass coverslips also coated with PLL+LAM were used as control (Figure 7 Q-T). The seeding density was 20,000 cells/cm^2. Cells were differentiated for 21 days and then stained with DAPI for cell nuclei (exhibited blue fluorescence) (Figure 7 A, E, I, M, Q), TUJ1 for neuronal differentiation (exhibited green fluorescence) (Figure 7 B, F, J, N, R) and MAP2 for neuronal maturation (exhibited orange fluorescence) (Figure 7 C, G, K, O, S). The merged channels (Figure 7 D, H, L, P, T) with white arrows indicate the direction of gratings.

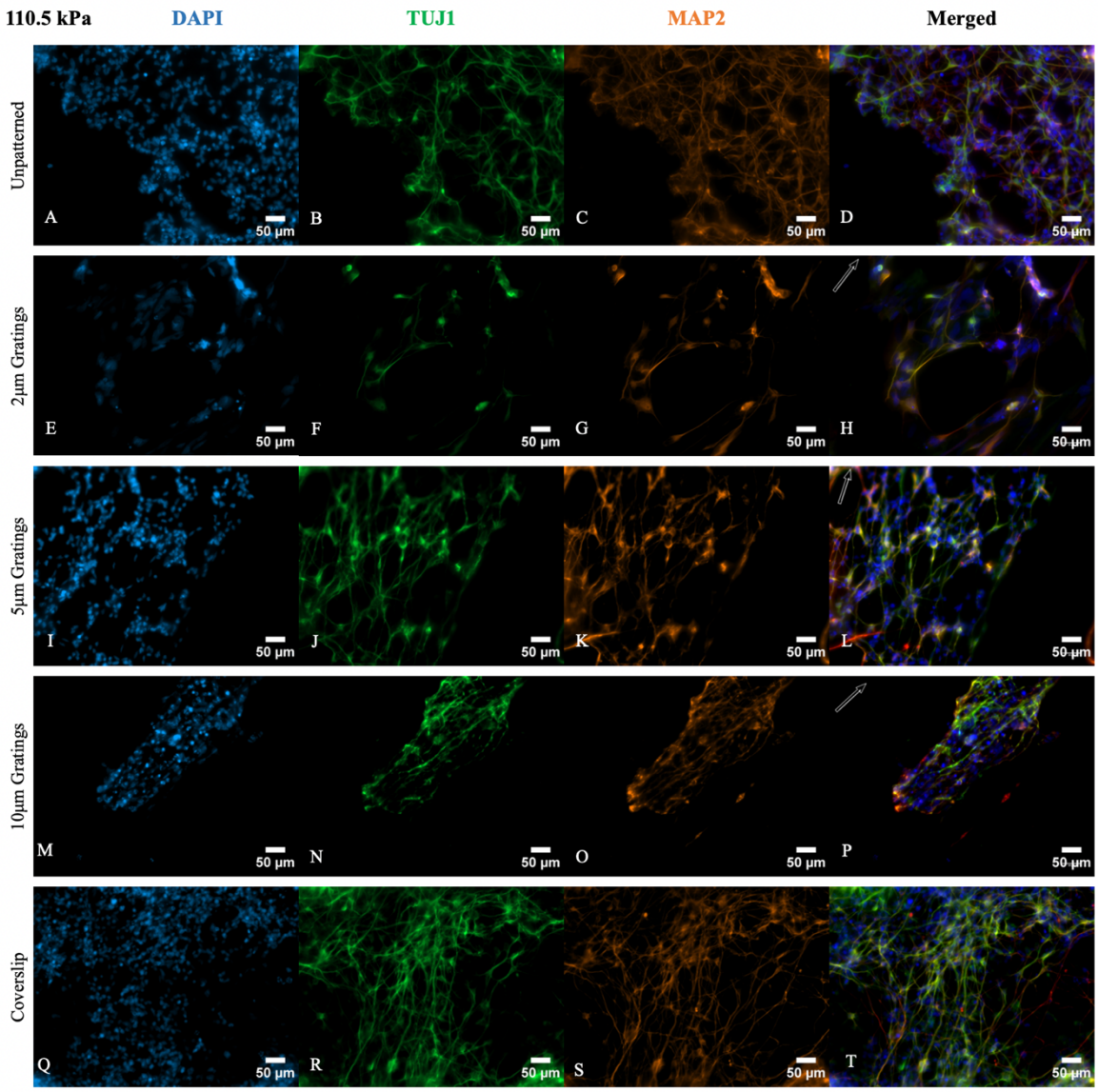

Figure 7. Representative immunofluorescence images with separated channels. WT hNPCs were seeded on the unpatterned PAA-ACA hydrogels (A-D) and PAA-ACA hydrogels with 2 μm gratings (E-H), 5 μm gratings (I-L), and 10 μm gratings (M-P) combined with the stiffness of 110.5 kPa. The PAA-ACA substrates were coated with PLL+LAM and the glass coverslips also coated with PLL+LAM were used as control (Q-T). and the seeding density was 20,000 cells/cm^2. Cells were differentiated for 21 days

and then stained with DAPI (blue channel) as a counterstaining (A, E, I, M, Q), TUJ1 (green channel) for neuronal differentiation (B, F, J, N, R) and MAP2 (orange channel) for neuronal maturation (C, G, K, O, S). The merged channels (D, H, L, P, T) with white arrows indicate the direction of gratings. Scale bars in all images are 50 μm.

In order to further determine the effect of topography and stiffness on hNPC neuronal differentiation and maturation, gene expression data were generated by RT-qPCR. Similarly to the previous procedure, hNPCs were cultured on the unpatterned, 2 μm gratings, 5 μm gratings, and 10 μm gratings combined with the stiffnesses of 6.2 kPa and 110.5 kPa for 21 days. PAA-ACA surfaces were coated with PLL+LAM and the glass coverslips also coated with PLL+LAM were used as control. RNA was first isolated and then converted to cDNA. Three technical replicates per sample per gene primer were performed. GAPDH was used as the housekeeping gene. The mean ± standard error values of gene expression from three biological replicates are shown below in Figure 8. The protein expression of TUJ1 indicated neuronal differentiation, the expression of MAP2 indicated neuronal maturation and the expression of Syn1 indicated the degree of synaptic maturation. The level of gene expression was calculated using ΔΔCt method normalized to the housekeeping gene GAPDH of each of the samples and then normalized to the control on glass coverslips. Fold gene expression was equal to $2^{\wedge-(\Delta\Delta Ct)}$.

According to the RT-qPCR data, ANOVA analysis showed no significant difference between each sample group. However, when comparing the average value of three replicates, the PAA-ACA hydrogels with the combination of softer substrates (6.2 kPa) and 2 μm gratings induced the most neuronal differentiation (Figure 8 A). The gel surfaces with the combination of softer substrates and 5 μm gratings provided the most neuronal maturation (Figure 8 B) and mature synapses (Figure 8 C).

From the expression of the TUJ1 marker, the softer substrates overall promoted more neuronal differentiation than the stiffer substrates (110.5 kPa) except for the substrates with 10 μm gratings. 2 μm gratings on softer substrates promoted the most differentiation

toward to neurons while the unpatterned surface on the stiffer substrates induced the least neuronal differentiation. When comparing the effect of topographies, with increasing grating size, the neuronal differentiation would decrease in the softer sample groups. However, in the stiffer sample group, 10 μm gratings topography provided the most neuronal differentiation when compared to 2 μm gratings and 5μm gratings topographies, which showed an inverse tendency.

For neuronal maturation, the softer substrates also performed better than the stiffer substrates, except the substrates with 10 μm gratings. The softer substrates with 5 μm gratings promoted the most neuronal maturation while 2 μm gratings on the stiffer substrates provided the least maturation. Moreover, all topographies with grating patterns support more maturation than the unpatterned surface in the softer sample group. However, only 5 μm gratings and 10 μm gratings promoted more maturation than unpatterned surface in the more rigid sample group.

Also, for the expression of the Syn1 marker, again, the softer substrates also performed better than the stiffer substrates, except the substrates with 10 μm gratings. Only the softer surface with 2 μm gratings and 5 μm gratings promoted more mature synapses than all the stiffer substrates. In the softer sample group, 5 μm gratings showed the highest degree of mature synapses and 10 μm gratings showed the lowest. In contrast, the 10 μm gratings pattern showed the highest degree of mature synapses and the unpatterned one showed the lowest.

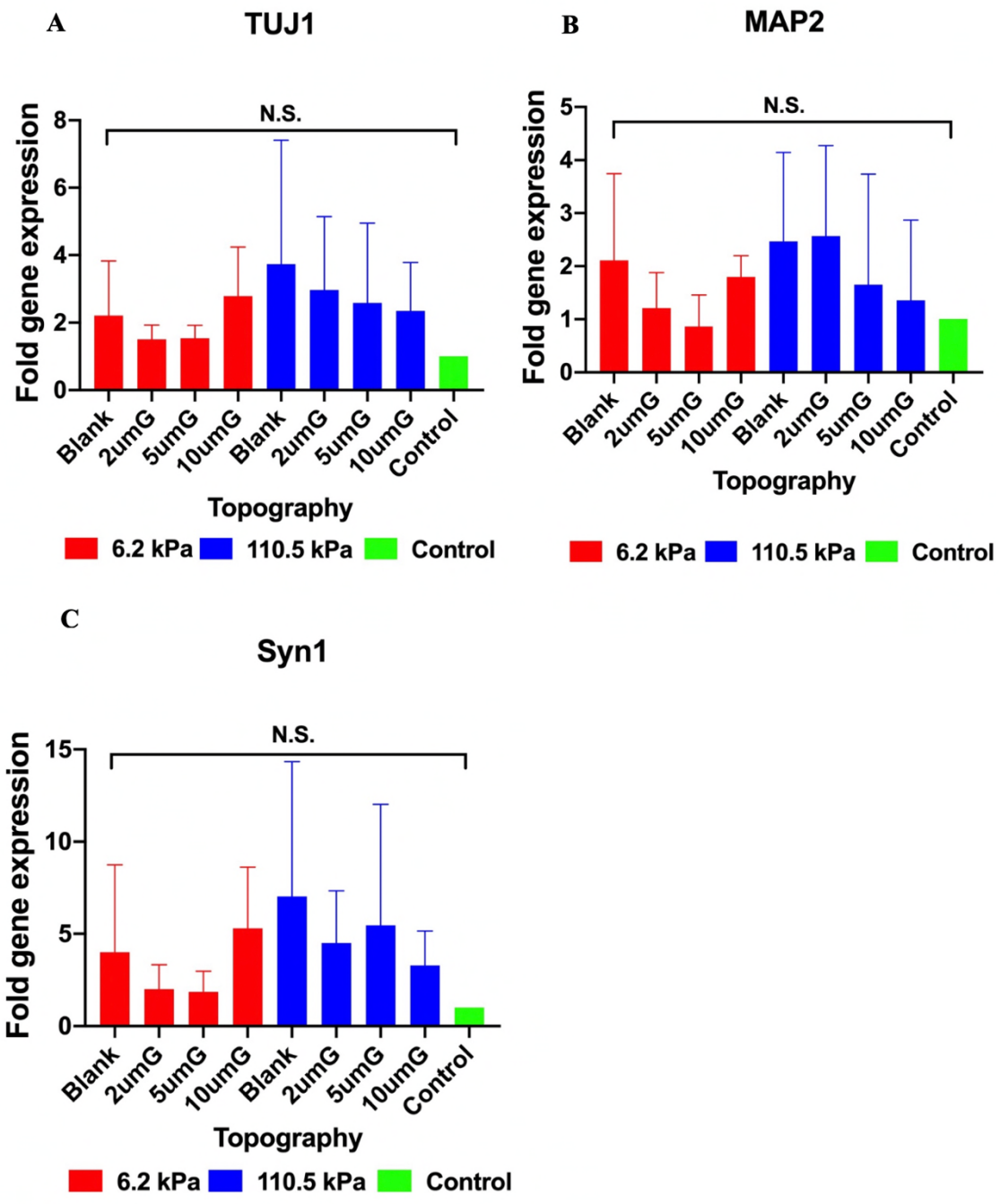

Figure 8. RT-qPCR quantification of gene expression of TUJ1 (A), MAP2 (B), and Syn1 (C). The gene expression level was expressed as the fold change of the gene normalized

to GAPDH of each of the samples and then normalized to the control on glass coverslips. WT hNPCs were seeded on the PAA-ACA gels with PLL+LAM coating. The PAA-ACA substrates were fabricated with unpatterned (Blank), 2 μm gratings (2 umG), 5 μm gratings (5 umG), and 10 μm gratings (10 umG) combined with the stiffness of 6.2 kPa and 110.5 kPa and differentiate for 21 days. Glass coverslips coated with PLL+LAM were used as control (Control). The level of gene expression was calculated using ΔΔCt method and fold gene expression is equal to $2^{\wedge-(\Delta\Delta Ct)}$. The data present the mean ± standard deviation values of three biological replicates and there was no statistical significance among each sample group.

3.4 Discussions

Topography and stiffness of substrates could individually and simultaneously affect cell behaviors, such as cell attachment, alignment, and differentiation[9, 12, 54]. However, the combined impacts of the topography and stiffness on neuronal differentiation and maturation of hNPCs have been rarely investigated. PAA-ACA hydrogels are excellent substrates for neural cell studies which have suitable biocompatibility and low toxicity[48]. Also, PAA-ACA gels can be easily fabricated with different topographies and stiffnesses. The stiffness can be controlled by changing the percentage of acrylamide and bisacrylamide[56]. The topographic patterns can be fabricated with prepared PET molds. The surface can also be modified with PLL and LAM, which could help to enhance the differentiation. Both WT and RTT hNPCs could respond to the PAA-ACA substrates with different topographies and stiffnesses. With the simple regulation of topographies and stiffnesses and cell response, PAA-ACA hydrogels provided a promising scaffold for further experiments of hNPCs.

According to our WT and RTT hNPCs behaviors on PAA-ACA substrates, the topographic patterns were able to guide the elongation of the cells. hNPCs extended in the direction parallel to the grating axis. Also, more cells could adhere to the gels with the

grating patterns compared to the unpatterned surfaces regardless of the stiffness. It seems the scaffold with gratings provided more cell alignment and attachment. From the immunofluorescence images, patter with narrow gratings could promote longer neurites. Softer substrates provided higher expression of the TUJ1 marker, which indicated the promotion of neuronal differentiation.

RT-qPCR is a quantitative method that is commonly used to analyze gene expression. For TUJ1 expression, studies have shown that neurons favor softer substrates while astrocytes prefer stiffer surfaces[12, 73, 74]. In our study, compared to the stiffer substrates (110.5 kPa), the softer surface (6.2 kPa) with various patterns all promoted more neuronal differentiation, which is consistent with others' studies. Also, Pan *et al*. demonstrated that the narrow width of the nanograting would have a higher neuronal differentiation expression [99]. In our softer sample group, 2 μm gratings promoted the most neuronal differentiation followed by 5 μm gratings. However, unpatterned substrates provided more neuronal differentiation than 10 μm grating substrates. Neurons seemed not to favor the combination of 10 μm gratings on softer substrates. In the stiffer sample group, 10 μm gratings provided the most neuronal differentiation, followed by 5 μm gratings and then 2 μm gratings. The tendency of the effect of topographic size was reversed. One possible hypothesis is that neuronal differentiation favor very soft substrates (less than 1 kPa)[12]. Therefore, when the stiffness was higher than 100 kPa, the topographic cue did not show a large difference, although the topographic grating still performed better than the unpatterned substrates. Moreover, 10 μm gratings on stiffer substrates provided more neuronal differentiation than 10 μm gratings on softer substrates. The interaction between topography and stiffness of the PAA-ACA gels would be one possible reason.

For MAP2 expression, the softer substrates with 2 and 5 μm gratings supported more neuronal maturation than all the stiffer substrates. For the more rigid substrates, the 10 μm gratings promote the most neuronal maturation, followed by 5 μm gratings and then 2 μm gratings. In contrast, 10 μm gratings promoted the least neuronal maturation for the

softer substrates, followed by 2 μm gratings and then 5 μm gratings. It may be because stiffness predominately affects cell differentiation and maturation. Li *et al.* stated the differentiation of rat bone marrow MSCs cells was mainly led by stiffness while topography or dimension plays a lesser role in regulating cell differentiation[93]. On the softer substrates, cells could all differentiate well and then be affected by topographic patterns. However, the rigid surface may not be favorable for neuronal cell differentiation, thus masking the regulative effect of topography.

While we observed consistent trends among the groups in each biological replicate, the large variation among the biological replica experiment may have affected the statistical analysis of the data. The variation observed among experiments could be due to variation in the RNA isolation process which may affect the quality and/or quantity of the RNA, and the variation potentially caused by the housekeeping gene. Panina *et al.* studied the housekeeping gene stability of the iPSCs reprogramming and reported substantial variations in housekeeping genes in the reprogramming process. Also, GAPDH was stated as one of the most stable genes, while ACTB was one of the least stable genes [100]. our previous study on hNPCs used GAPDH as the housekeeping gene. Therefore, GAPDH was first selected as the housekeeping gene. ACTB and HPRT1 are the two other commonly used genes. To check if different housekeeping gene might affect the qPCR, we tested samples with GAPDH, ACTB and HPRRT1. The average ± standard deviation values were 18.123 ± 0.846, 14.106 ± 0.585 and 21.896 ± 0.253 respectively. Since the ideal Ct value should not be lower than 16, ACTB would not be a suitable housekeeping gene for this experiment. With the lowest standard deviation, HPRT1 was suggested to be worth attempting for future analysis.

Besides the WT hNPCs, RTT cells also responded differently to the topography and stiffness. However, RTT cells proliferated and differentiated slower than WT hNPCs. It was necessary to find a balance seeding density for both WT and RTT hNPCs. Since neural cells can easily grow on top of each other, too high a density would lead to over

confluence. Too low seeding density would not support differentiation since neural cells prefer to grow together. After trying 7,500, 10,000, 20,000 and 25,000 cells/cm^2, the seeding density 20,000 cells/cm^2 was considered as an optimum option for both WT and RTT.

3.5 Conclusion

In conclusion, PAA-ACA substrates with various topographies and stiffnesses could regulate neuronal cell behaviors such as alignment, differentiation, and maturation. Both WT and RTT hNPCs responded to the PAA-ACA substrates coated with PLL+LAM. Also, PAA-ACA substrates could be fabricated with different topographies and stiffnesses and provide hNPCs attachment and differentiation for 21 days. Cells extended along with the grating's axis. Gratings could promote cell attachment and the neurite elongation

Moreover, topography and stiffness have a combined impact on neuronal differentiation and maturation, which should be considered prudently. The 2 μm gratings on softer PAA-ACA gels promoted the most neuronal differentiation and the 5 μm gratings on the softer surface supported the most neuronal maturation and degree of mature synapses. Soft substrates could overall support more neuronal differentiation, maturation and mature synapses compared to the stiff substrates.

Chapter 4 Effect of Topography and Biochemicals on Neuronal cells

4.1 Introduction

Both mechanical and biochemical modifications would affect cell behaviors such as cell attachment, proliferation, and differentiation. Due to their biocompatibility and low toxicity, PVA hydrogels are a great resource for cellular research. However, plain PVA hydrogels do not support cell adhesion and spreading because of their low affinity to protein[14]. Therefore, surface treatments are necessary for PVA hydrogels. With various biochemical modifications, such as extracellular matrix proteins and cell adhesion materials, cell attachment and differentiation could be stimulated and promoted. One example from Orlowska *et al.* showed that PC 12 cell lines could have better attachment and neurite outgrowth on Poly-L-lysine hydrobromide (PLL)/Laminin (LAM) and PLL/fibronectin coated substrates with the inducement of 100 ng/mL NGF[44]. In addition, fucoidan is a type of sulfated polysaccharide, which has been proved to enhance endothelial cell attachment and proliferation by our lab's previous study. The fucoidan conjugated PVA substrates could improve the endothelialization and hemocompatibility[63]. Therefore, PVA surface with fucoidan modification seems to be a candidate solution to promote neuronal differentiation.

Moreover, the topography would also have an influence. For instance, topographic PVA hydrogels could improve the attachment of endothelial cells[101]. Topography could also enhance cell alignment and elongation. However, some topographical patterns, such as grooves and ridges, constrain the neurite extension[45].

Therefore, we hypothesized that different topographies and biochemicals would regulate cell behaviors, such as adhesion, viability, and differentiation.

In this chapter, we evaluated the impact of topographies and biochemicals of PVA hydrogels. WT hNPCs and PC12 cell lines were seeded on PVA with different biochemicals. Then PC12 cell lines were differentiated on both unpatterned and patterned

PVA hydrogels, which were also modified with various biochemicals. The patterned PVA was fabricated using prepared patterned polydimethylsiloxane (PDMS) molds. The biochemical modifications were fucoidan, gelatin, fucoidan + LAM, and fucoidan + NGF. The percentage of differentiated cells and the neurite length were measured.

4.2 Method and Materials

4.2.1 PC12 Cell Line Maintenance and Differentiation

PC12 cell lines from American Type Culture Collection were cultured with Dulbecco′s Modified Eagle′s Medium (DMEM)-high glucose with 4500 mg/L glucose, L-glutamine, and sodium bicarbonate (D5796 Sigma Aldrich), 10% horse serum (LS26050070 Grand Island Biological Company), 10% Fetal Bovine Serum (FBS) (LS26140079 Grand Island Biological Company), and 1% penicillin-streptomycin 10,000 µg/ml (PS) (LS15140122 Grand Island Biological Company). The specific volume for each substance is shown below in Table 5.

Table 5. Composition in a volume of 50 ml maintenance media for PC12 cell lines.

Reagent	Maintenance Media	Final Concentration
DMEM - high glucose medium	39.5 ml	-
Horse serum	5 ml	10 %
Fetal Bovine Serum	5 ml	10 %
Penicillin streptomycin 10,000 µg/ml	0.5 ml	1 %

Once the cells reached 80% confluence, the supernatant culture media was aspirated. 3 ml fresh maintenance media was added back to each well of the 6-well plate or 7 ml for the 25 cm^2 flask. A 1000 µl pipette tip was used to gently scrape the cells from the plate surface from different directions. Then the cells were transferred to a 15 ml centrifuge tube and pipetted up and down quickly to loosen the cell chunks until there was no

conspicuous precipitate. Cells were counted by hemocytometer and seeded at 50,000 cell/ cm^2 on the 6-well plate or 25 cm^2 flask. The plate was coated with Collagen type IV (C5533 Sigma Aldrich) and incubated at 37 °C with 5% CO_2, 99% humidity. 50% of the maintenance was changed every other day.

Collagen type IV powder was first reconstituted in 0.25% acetic acid (695092 Sigma Aldrich) with a concentration of 1 mg/ml. The plates/flasks were coated with a concentration of 10µg/cm^2 at 37 °C for at least 6 hours or overnight at 4 °C. Excess fluid was removed, and the surface was allowed to dry in a 37 °C incubator. Before seeding the cells, the plates/flasks were washed with 1X PBS three times for 5 mins each time.

For differentiation, two kinds of differentiation media were used for PC 12 cell lines. One was composed of DMEM-high glucose medium, 1% horse serum, 1% 10,000 µg/ml PS and 4 µM retinoic acid (R2625 Sigma Aldrich) in dimethyl sulfoxide (DMSO) (D5879 Sigma Aldrich). The volume is shown below in Table 6.

Table 6. Composition in a volume of 50 ml differentiation media for PC12 cell lines with retinoic acid.

Reagent	Differentiation Media	Final Concentration
DMEM - high glucose medium	49 ml	-
Horse serum	0.5 ml	1 %
Penicillin streptomycin 10,000 µg/ml	0.5 ml	1 %
Retinoic acid (0.133 mM)	1.5 µl	4 µM

Another differentiation media was composed of DMEM-high glucose medium, 5% FBS, 1% 10,000 µg/ml PS, recombinant human beta-nerve growth factor (β-NGF) (450-01 PeproTech, Inc.) in deionized water with 0.1% bovine serum albumin (BSA) (A3294 Sigma Aldrich) and 1 µg/ml laminin mouse protein (LS23017015 Grand Island Biological Company). The amount of each substance is shown below in Table 7.

Table 7. Composition in a volume of 5 ml differentiation media for PC12 cell lines with NGF.

Reagent	Differentiation Media	Final Concentration
DMEM - high glucose medium	4450 µl	-
Fetal Bovine Serum	500 µl	5 %
Penicillin streptomycin 10,000 µg/ml	50 µl	1 %
β-Nerve growth factor (100 µg/ml)	1.5 µl	30 ng/ml
Natural Mouse Laminin	5 µl	1 µg/ml

4.2.2 Fabrication of Polyvinyl Alcohol (PVA) Hydrogel

4.2.2.1 Preparation of Crosslinking PVA

The fabrication method of poly (vinyl alcohol) (PVA) was according to our lab's previous publication[101]. A 10% (w/v) PVA solution was prepared with PVA powder (363081 Sigma Aldrich) dissolved in deionized water. The average molecular weight was from 85,000 to 124,000 and the solution was 87% to 89% hydrolyzed. The solution was first autoclaved for 20 min on fluid cycle and then placed on the stir plate allowing the mixture to homogenize for no longer than one week.

12 g of PVA solution was weighed in a beaker and 1 ml of 15% (w/v) sodium trimetaphosphate (STMP) (T5508 Sigma Aldrich) powder in deionized water was added. The STMP solution was prepared fresh and incubated in a 37 °C water bath allowing better dissolution. The PVA solution was mixed thoroughly for 5 min on the stir plate until no white-colour drops were visible. Then the speed of the stir plate was lowered to 150-200 rpm and 400 µl of 30% (w/v) sodium hydroxide (NaOH) (221465 Sigma Aldrich) in deionized water was added dropwise to increase the pH of the solution. Then the PVA

solution was mixed for another 5 min and transferred to a 50 ml centrifuge tube. The crosslinking PVA was centrifuged for at least 10 min at 2000 rpm.

4.2.2.2 Unpatterned PVA Films

For unpatterned PVA films, either 3g of the crosslinking PVA solution was poured into a 6 cm^2 petri-dish or 700 µl of the solution was added to each well for a 24-well plate. The petri-dishes or plates were covered with lids and placed in the wine cooler at 20 °C with 60% -70% humidity for 5 days ensuring the PVA was fully crosslinked. Then the lids were opened and left for another 3 to 5 days.

Once salt crystals were formed on the surface, the PVA films were demolded by washing with 10X PBS for three hours and 1X PBS for another three hours on the shaker. They were then washed with deionized water on the stir plate overnight. The excess edge part was cut, and it was ensured that the film was flat and fit into the 24-well plate. Then the films were dried in the 60 °C oven overnight to remove excess moisture.

The elastic modulus of PVA hydrogels were measured using Universal Mechanical Tester (UNMT-2MT, T1377 Center for Tribology, Inc.). The uniaxial tensile tests were reported in a previous publication[102]. Briefly, the dimensions such as width and thickness of the samples were measured. The grips were moved using the control panel and the hydrated PVA samples were placed in the middle of the grips. The tested were started with the force and the stroke were zeroed. The extension rate was 10 mm/min[63].

4.2.2.3 Patterned PVA Films

For patterned PVA films, a similar method was developed according to our lab's previous publication[101]. PDMS (SYLGARD™ 184 Dow Chemical Company) molds with 2 µm gratings, 10 µm gratings, and 1.8 µm convex lenses were fabricated on silicon templates. The 2 µm gratings refer to the topographic gratings with width of 2 µm, space of 2 µm and height of 2 µm and the 10 µm gratings refer to the topographic gratings with width of 10 µm, space of 10 µm and height of 10 µm. Also, the 1.8 µm convex lenses

refer to 1.8 μm diameter and 2 μm pitch convex microlens. The PDMS molds were treated with air plasma for 1 min, which is enough for cell culture applications. The plasma treatment was operated on fully dry samples. Then 700 μl of crosslinking PVA solution was cast on the patterned PDMS molds. The plate was centrifuged at 1500 rpm for 1 hour. A similar wash method was performed as mentioned above.

After the PVA hydrogels were dehydrated in the 60 °C oven overnight, the patterns were checked by the 3D measuring laser scanning microscope (LEXT™ OLS5100 Olympus).

4.2.3 The Modification of PVA Hydrogel Surface

PVA samples were activated with 100 mg/ml 1,1′-Carbonyldiimidazole (CDI) (115533 Sigma Aldrich) in DMSO (D5879 Sigma Aldrich). The plate was placed on the shaker for 1 hour at room temperature. The samples were briefly rinsed with 1X PBS three times to wash off the excess CDI. For fucoidan conjugation, PVA samples were immersed in 10 mg/ml aminated fucoidan (Maritech *Fucus vesiculosus* Extract, FVF2018531 Marinova, Australia) dissolved in PBS. The concentration of fucoidan was determined by Yao *et al* [63]. 500 μl fucoidan solution was added to each sample and incubated at 37 °C overnight. For gelatin modification, PVA samples were immersed in autoclaved 10 mg/ml gelatin (G9391 Sigma Aldrich) dissolved in deionized water. Similarly, 500 μl solution was added and incubated at 37 °C overnight. For PLL conjugation, after excess CDI was washed, PVA samples were sterilized under ultraviolet light for 20 min in the biosafety cabinet. Then the samples were immersed with 500 μl of 0.5 mg/ml PLL overnight at 4 °C.

The samples were washed with sterilized 1X PBS three times, each time for 3 mins and incubated with an antibiotic solution, which was composed of 1% Amphotericin B solution (30-003-CF Corning Incorporated), 10% 10,000 μg/ml PS and 1X PBS overnight in the biosafety cabinet. Then the samples were sterilized under ultraviolet light for 20

min in the biosafety cabinet. After the fluid was aspirated, autoclaved tube rings were inserted to immobilize the PVA samples to avoid floating. Another 500 µl antibiotic solution was added to each well and incubated for either 1 hr at room temperature or 30 min at 37 °C. The samples were washed five times, each time for 5 mins with 1X PBS before seeding the cells.

For the samples further conjugated with laminin, 500 µl of 20 µg/ml laminin diluted in 1X PBS was added on each sample and incubated for 1 hr at 37 °C. Samples were washed with sterilized 1X PBS one more time for 5 min before seeding cells.

For the samples further conjugated with NGF, 100 µg of NGF was first reconstituted with 900 µl sterilized deionized water and 100 µl of 0.1% BSA in 1X PSB. Then 100 µl of 100 µg/ml NGF was added on each sample and incubated for 1 hr at 37 °C. Samples were not washed before seeding cells.

4.2.4 Cell Seeding for Proliferation and Viability Analysis

PC 12 cell lines were seeded with maintenance media, shown above in Table 5. The seeding density was 20,000 cells/cm^2 and cells were maintained for 14 days in 37 °C incubator with 5% CO_2, 99% humidity.

4.2.5 Staining for Cell Viability Analysis

After culturing for 14 days, PC 12 cell lines were rinsed once with Dulbecco's phosphate-buffered saline (DPBS) (A1285801 Grand Island Biological Company). Then cells were incubated with 0.25 µl of 4 mM eBioscience™ Calcein AM Viability Dye (65-0853-39 Invitrogen™) and 1 µl of 2 µM Ethidium Homodimer-1 (EthD-1) (E1169 Invitrogen™) diluted with DPBS for each well. 500 µl of the solution was added to each sample and incubated for 30 min at room temperature. Then samples were washed with 1X PBS three times each for 1 min. Cells were analyzed with Zeiss fluorescence microscope right after the staining.

4.2.6 Cell Seeding for Differentiation Analysis

PC 12 cell lines were seeded directly with differentiation media with NGF and laminin, shown above in Table 7. The seeding density was 20,000 cells/cm^2 and cells were maintained for 3 days in a 37 °C incubator with 5% CO_2, 99% humidity.

4.2.7 Staining and Imaging for Cell Differentiation

After culturing for 3 days with differentiation media, the phase-contrast images were taken using Microscope Primovert (415510-1101-000 Carl Zeiss). Then the viability dye solution was prepared with 0.5 µl of 4 mM calcein-AM, 0.5 µl of PS and 49 µl of high glucose DMEM. 50 µl of dye solution was added to each well and the sample was incubated for 15 min at 37 °C. A Zeiss fluorescence microscope (Axio Observer Z1) was used for imaging and ImageJ was used for analysis.

4.3 Result

4.3.1 Characterization of Patterned PVA Hydrogels

The patterned PVA hydrogels were prepared with PDMS molds. Three dimensions were fabricated with 2 µm gratings, 10 µm gratings, and convex lenses. The surface characterization of the patterned PVA hydrogels and the cross-sectional view of the pattern are shown below in Figure 9. The mechanical property was measured by uniaxial tensile tests and the PVA fabricated with 10% PVA solution has an elastic modulus of 0.40 ± 0.62 MPa. This was consistent with the elastic modulus of PVA film of 0.54 ± 0.11 MPa, which was reported in our lab previous publication[102]. The representative 2 µm gratings pattern has topographic gratings with width of ~1.98 µm and height of ~1.96 µm and the 10 µm gratings has the topographic gratings with width of ~9.99 µm and height of ~9.99 µm. Also, the representative convex lenses pattern has the diameter of ~1.62 µm. The laser scanning microscopy images were taken by the 3D measuring laser scanning

microscope. The yellow arrow in the convex lens images (Figure 9 C and F) indicated the orientation of the cross section.

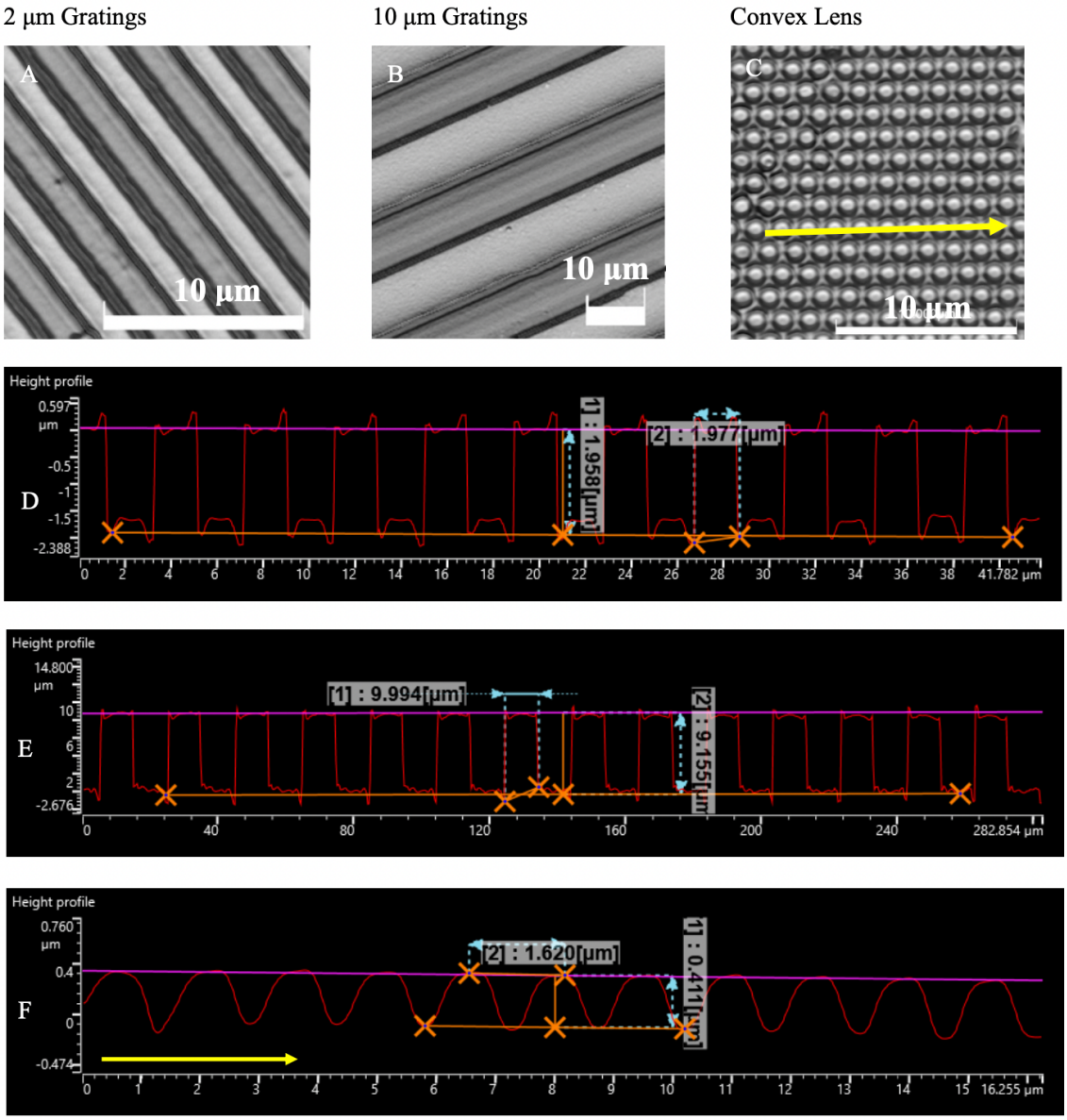

Figure 9. Surface characterization of patterned PVA hydrogels and the cross-sectional view of the patterns. The substrates were fabricated with 2 µm gratings (A), 10 µm

gratings (B), and 1.8 μm convex lenses (C). The laser scanning microscopy images were taken by the 3D measuring laser scanning microscope. (D) Cross-sectional view of the 2 μm gratings pattern. (E) Cross-sectional view of the 10 μm gratings pattern. (F) Cross-sectional view of the convex lenses pattern. The yellow arrow indicated the orientation of the cross section.

4.3.2 Effect of Different Biochemical Modification on hNPCs Adhesion

To evaluate the effect of various biochemical modifications of PVA hydrogels on cell adhesion and differentiation, The PVA surfaces were modified with CDI + LAM, CDI + PLL + LAM, and CDI + PLO + LAM (Figure 10).

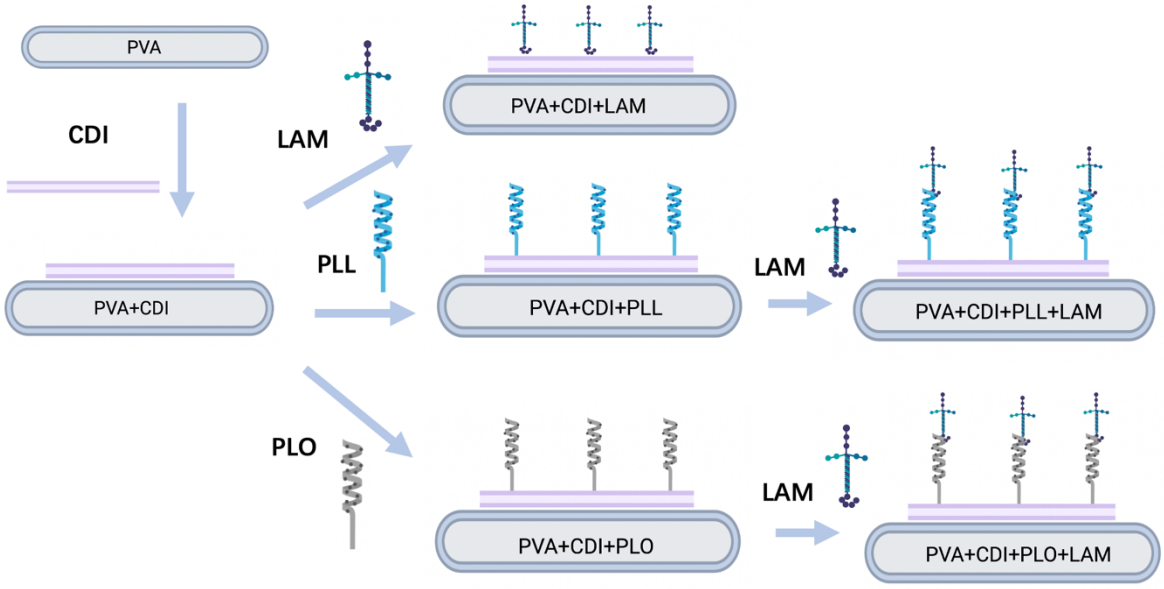

Figure 10. Schematic diagram of modified PVA preparation. The PVA surfaces were conjugated with CDI + LAM, CDI + PLL + LAM, and CDI + PLO + LAM.

Both WT and RTT hNPCs were cultured on the unpatterned PVA hydrogels and the seeding density was 50,000 cells/cm^2 (Figure 11). Cells were seeded with proliferation media and all the media were replaced with differentiation media after 24 hours. Glass

coverslips coated with LAM were used as a positive control to make sure cells were healthy (Figure 11 D and H). PVA hydrogels modified with CDI + LAM (Figure 11 A and E) could support the attachment of WT hNPCs after seeding while RTT cells rarely adhered to the PVA surface modified with CDI + LAM. Moreover, both WT and RTT hNPCs attached well and differentiated on the surface with CDI + PLL + LAM (Figure 11 B and F) modification. When PVA was conjugated with the CDI + PLO + LAM (Figure 11 C and G), WT hNPCs were attached to the surface and grew in small clumps. RTT hNPCs rarely attached and appeared as small circles. Also, with CDI+PLO+LAM modification, WT cells had few differentiations while no differentiation was seen in RTT cells.

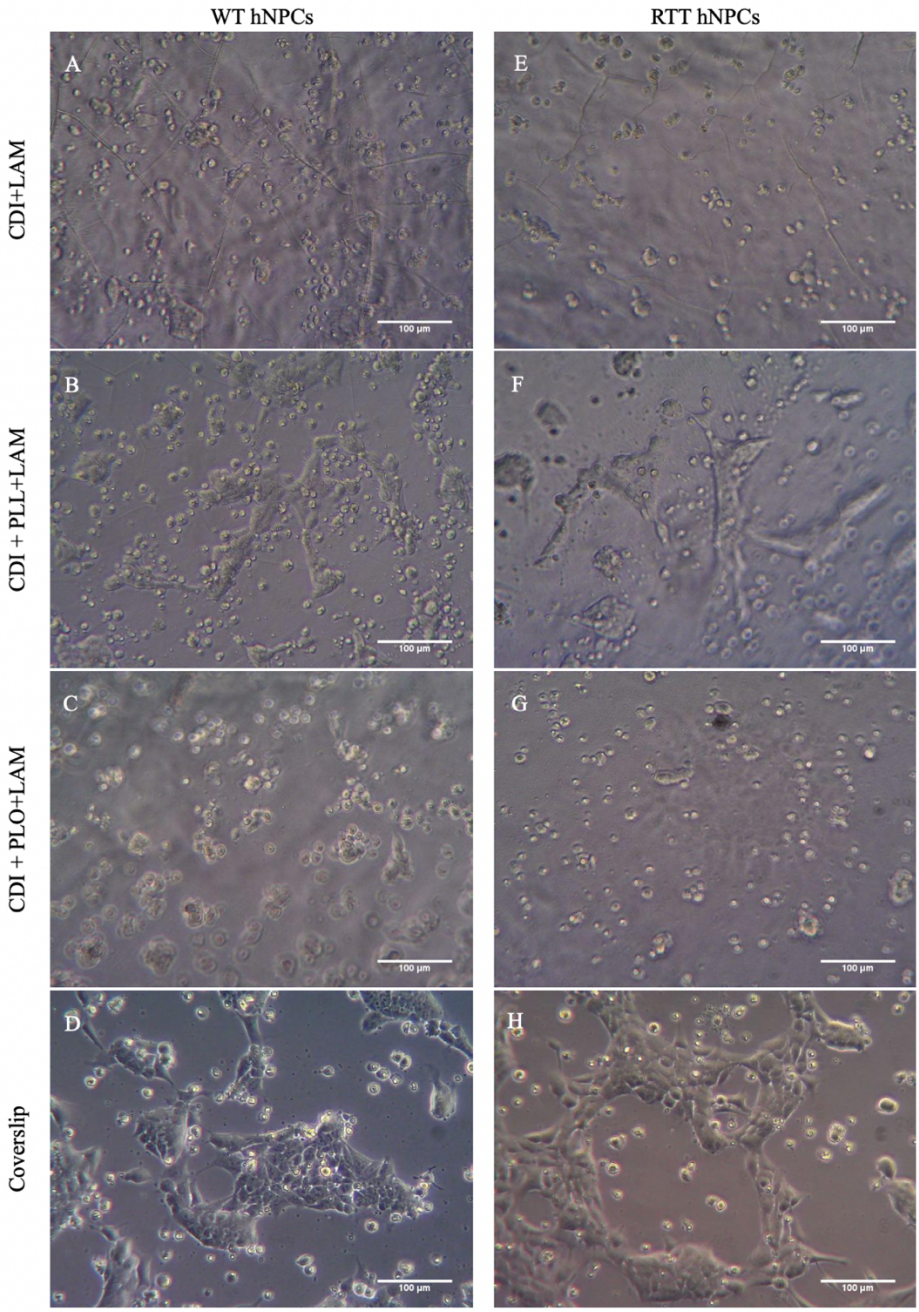

Figure 11. Representative phase-contrast images of WT and RTT hNPCs on unpatterned PVA hydrogels on Day 1 after the replacement of differentiation media. hNPCs were seeded on the PVA surfaces modified with CDI + LAM (A and E), CDI + PLL + LAM

(B and F) and CDI + PLO + LAM (C and G). Glass coverslips coated with laminin were used as a control (D and H). Cells were first seeded with proliferation media and ROCK inhibitor and then all media was changed to differentiation media after 24 hours. The seeding density was 50,000 cells/cm^2 and the scale bars in all images are 100 µm.

4.3.3 Effect of Different Biochemical Modifications on PC12 Adhesion and Viability

Since PC12 cells were easier to handle and the differentiation period was shorter than hNPCs, PC12 cells were used to detect the impact of different bioactive molecules of PVA substrates. The PVA surface modifications with CDI + fucoidan, CDI + gelatin, and CDI + PLL + LAM are shown below in Figure 12.

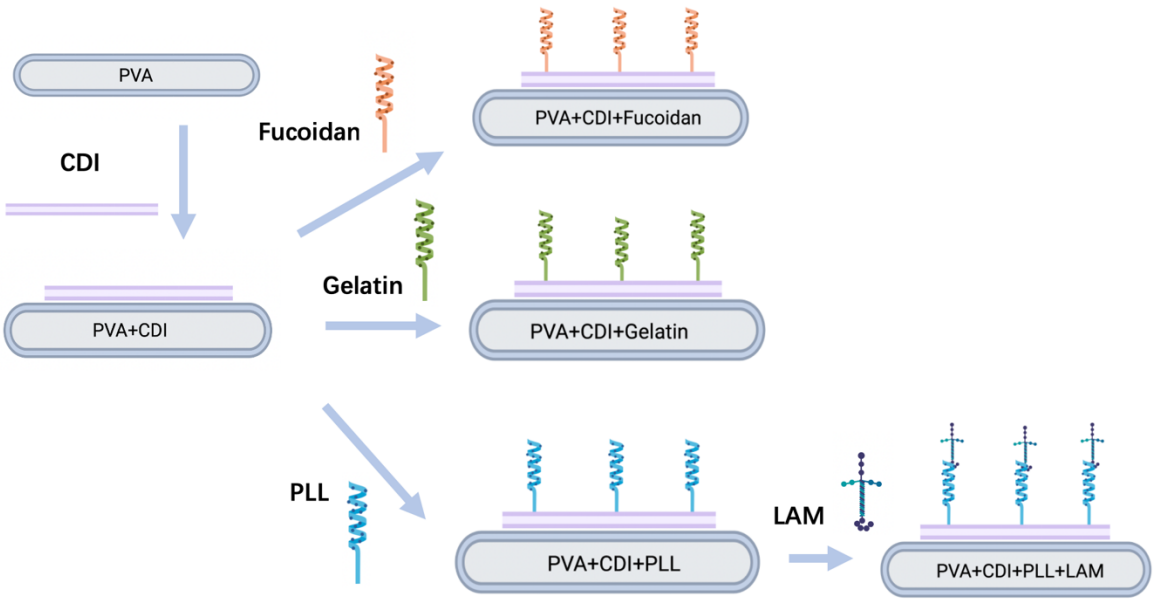

Figure 12. Schematic diagram of modified PVA preparation. The PVA surfaces were conjugated with CDI + fucoidan, CDI + gelatin, and CDI + PLL + LAM.

The cell adhesion and viability of PC 12 were tested on PVA substrates, which conjugated with CDI + fucoidan (Figure 13 A-C), CDI + gelatin (Figure 13 D-F), CDI + PLL + LAM (Figure 13 G-I), CDI + collagen type IV diluted in 0.01% acetic acid (Figure

13 J-L) and CDI + collagen type IV diluted in 0.05% acetic acid (Figure 13 M-O). Cells were cultured with proliferation media (shown in Table 5) for 14 days and stained against calcein-AM and EthD-1. Live cells were marked with calcein-AM and exhibited green fluorescence (Figure 13 A, D, G, J, M), and dead cells were marked with EthD-1 in red fluorescence (Figure 13 B, E, H, K, N). The merged channel shown in Figure 13 C, F, I, L and O. With the expression of live cells, PC12 could survive and adhere to all the modified surfaces.

PVA modified with CDI+PLL+LAM supported the most adhesion and cells showed the highest viability with minimal dead cells. The PVA surface modified with CDI + collagen type IV diluted in 0.05% acetic acid showed the lowest viability, which had the most EthD-1 positive cells. Also, cells seeded on the PVA hydrogels conjugated with CDI + fucoidan and CDI + gelatin presented similar viability.

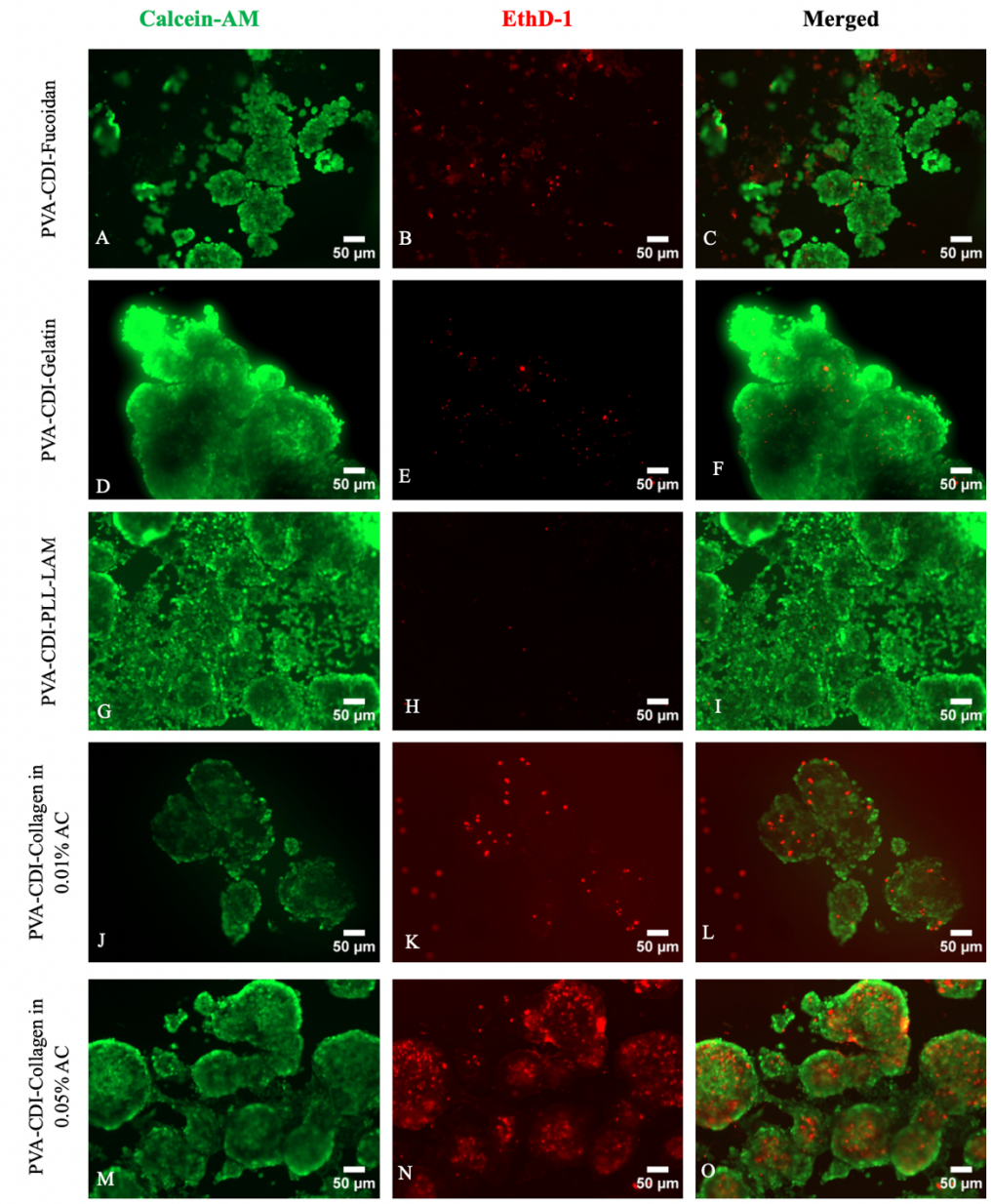

Figure 13. Representative fluorescence microscopy images of PC12 cell lines on unpatterned PVA hydrogels. PVA surfaces were conjugated with CDI + fucoidan (A-C), CDI + gelatin (D-F), CDI + PLL + LAM (G-I), CDI + collagen type IV diluted in 0.01% acetic acid (J-L) and CDI + collagen type IV diluted in 0.05% acetic acid (M-O). PC12

cell lines were seeded with maintenance media for 14 days and the seeding density was 20,000 cells/cm^2. Cells were stained with calcein-AM for live cell (green fluorescence) (Figure 13 A, D, G, J, M) and EthD-1 for dead cells (red fluorescence) (Figure 13 B, E, H, K, N). The merged channel shown in Figure 13 C, F, I, L and O. The scale bars in all images are 50 μm.

4.3.4 PC12 Differentiation Media with Different Biochemicals.

In order to induce differentiation, a serum-free medium or medium with reduced serum concentration would be needed. Media with different combinations of biochemicals were tested to examine which media would support cell adhesion and differentiation. PC12 cell lines were cultured with basal media and various differentiation media. The composition of each media is shown below in Table 8.

Table 8. Composition of PC12 media.

Media B (Basal media)	DMEM + 1% PS
Media D	DMEM + 1% PS + 30 ng/ml NGF
Media D-2	DMEM + 1% PS + 2% FBS + 30 ng/ml NGF
Media D-5	DMEM + 1% PS + 5% FBS + 30 ng/ml NGF
Media D-5 with LAM	DMEM + 1% PS + 5% FBS + 30 ng/ml NGF + 1 μg/ml LAM

PC 12 cell lines were seeded on unpatterned PVA hydrogels modified with CDI + fucoidan at the seeding density of 20,000 cells/cm^2. Cells were seeded with basal media and four kinds of differentiation media for three days (Figure 14). Media B (Figure 14A) could support cell adhesion, but no differentiation was induced. Media D (Figure 14 B) with added NGF could support more cell attachment but still no differentiation was induced. With the addition of 2% FBS, cells began to differentiate (Figure 14 C). Media D-5 supported more differentiation and neurite outgrowth as the percentage of FBS

increased to 5%. Media D-5 with LAM induced the most cell differentiation and neurite outgrowth. Also, the neurite length was longer when compared to other differentiation media. Media D-5 with LAM would be the optimum media for the following experiments.

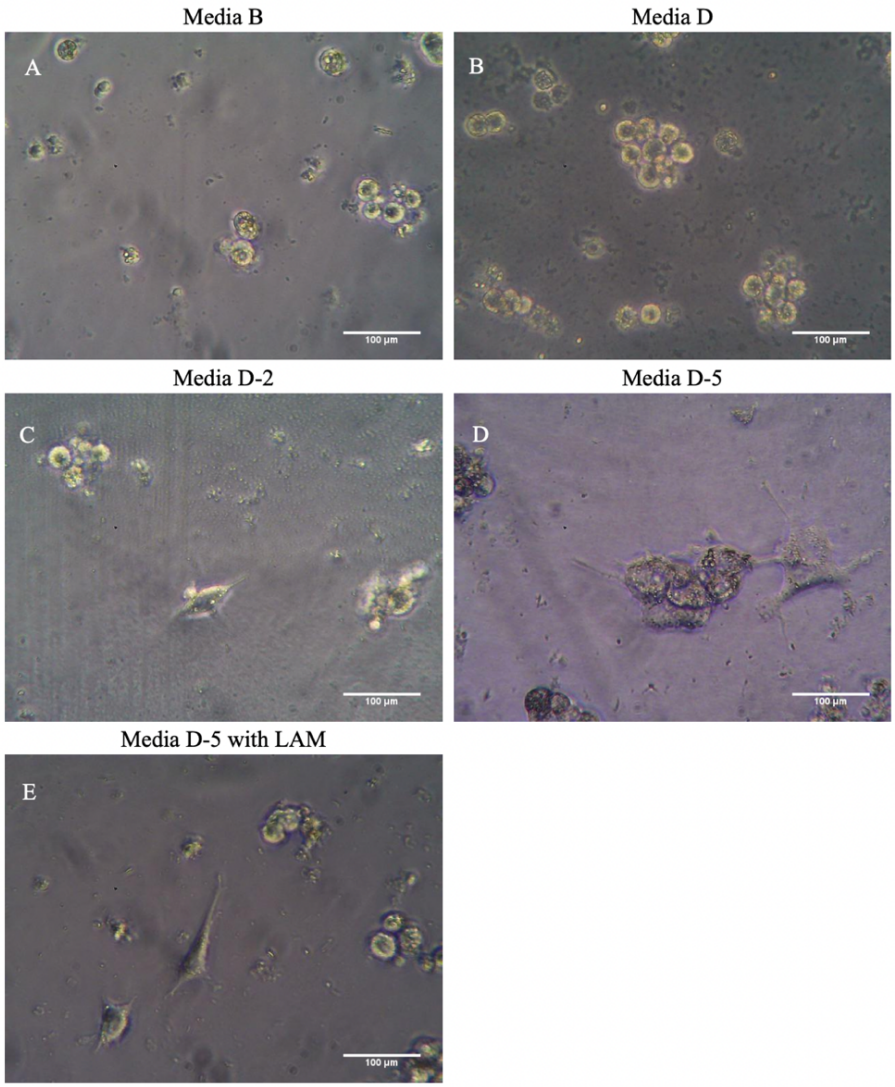

Figure 14. Representative phase-contrast images of PC12 cell lines on unpatterned PVA hydrogels with various compositions of media. The PVA surfaces were conjugated with CDI + Fucoidan and the seeding density was 20,000 cells/cm^2. (A) Media B contains

DMEM + 1% PS. (B) Media D contains DMEM + 1% PS + 30 ng/ml NGF. (C) Media D-2 contains DMEM + 1% PS + 2% FBS + 30 ng/ml NGF. (D) Media D-5 contains DMEM + 1% PS + 5% FBS + 30 ng/ml NGF. (E) Media D-5 with LAM contains DMEM + 1% PS + 5% FBS + 30 ng/ml NGF + 1 µg/ml LAM. PC12 cell lines were seeded directly with these media for three days and the scale bars in all images are 100 µm.

4.3.5 Effect of Topographical and Biochemical Modifications on PC12 differentiation

With the optimal differentiation media, PC12 cell lines were cultured on the PVA hydrogels with different topographies and biochemical modifications for three days. The PVA surfaces were first conjugated with CDI + fucoidan, CDI + gelatin, and CDI + fucoidan + LAM (Figure 15).

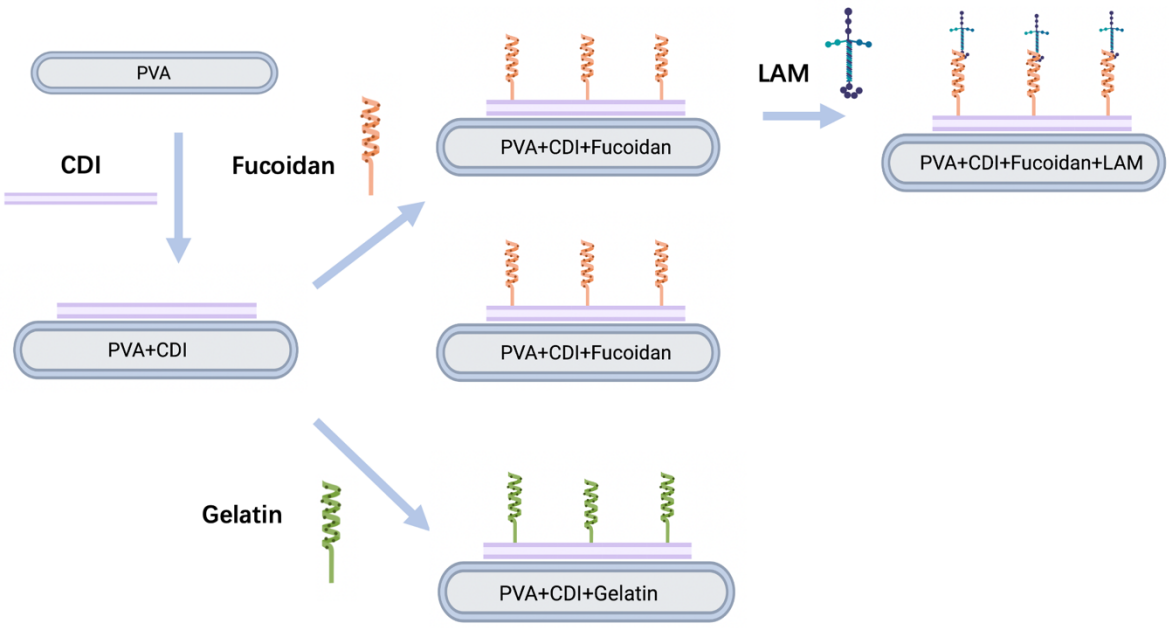

Figure 15. Schematic diagram of modified PVA preparation. The PVA surfaces were conjugated with CDI + fucoidan, CDI + gelatin, and CDI + fucoidan + LAM.

Then cells were seeded on the unpatterned PVA hydrogels (Figure 16 A, E, I) and PVA hydrogels with 2 µm gratings (Figure 16 B, F, J), 10 µm gratings (Figure 16 C, G,

K), and 1.8 μm convex lenses (Figure 16 D, H, L) at the seeding density of 20,000 cells/cm^2. Cells seeded on the unmodified PVA were shown in Figure 16 M. TCPS plates coated with collagen type IV diluted in 0.25% acetic acid were used as control and make sure the cells were healthy and able to differentiate (Figure 16 N). Since the phase-contrast images could not show the clear neurite, cells were stained with calcein-AM and exhibited green fluorescence after culturing for three days.

PC12 could differentiate on all the PVA surfaces with these modifications, while cells barely adhered to the unmodified PVA. PVA hydrogels conjugated with fucoidan could promote cell differentiation. Also, fucoidan + LAM showed better differentiation than fucoidan and gelatin modification. Moreover, the differentiation of PC12 cell lines was guided by the topographies on PVA substrates. The neurite extensions were aligned with the 2 μm and 10 μm grating's axis while cells spread randomly on the unpatterned PVA and 1.8 μm convex lenses topographies.

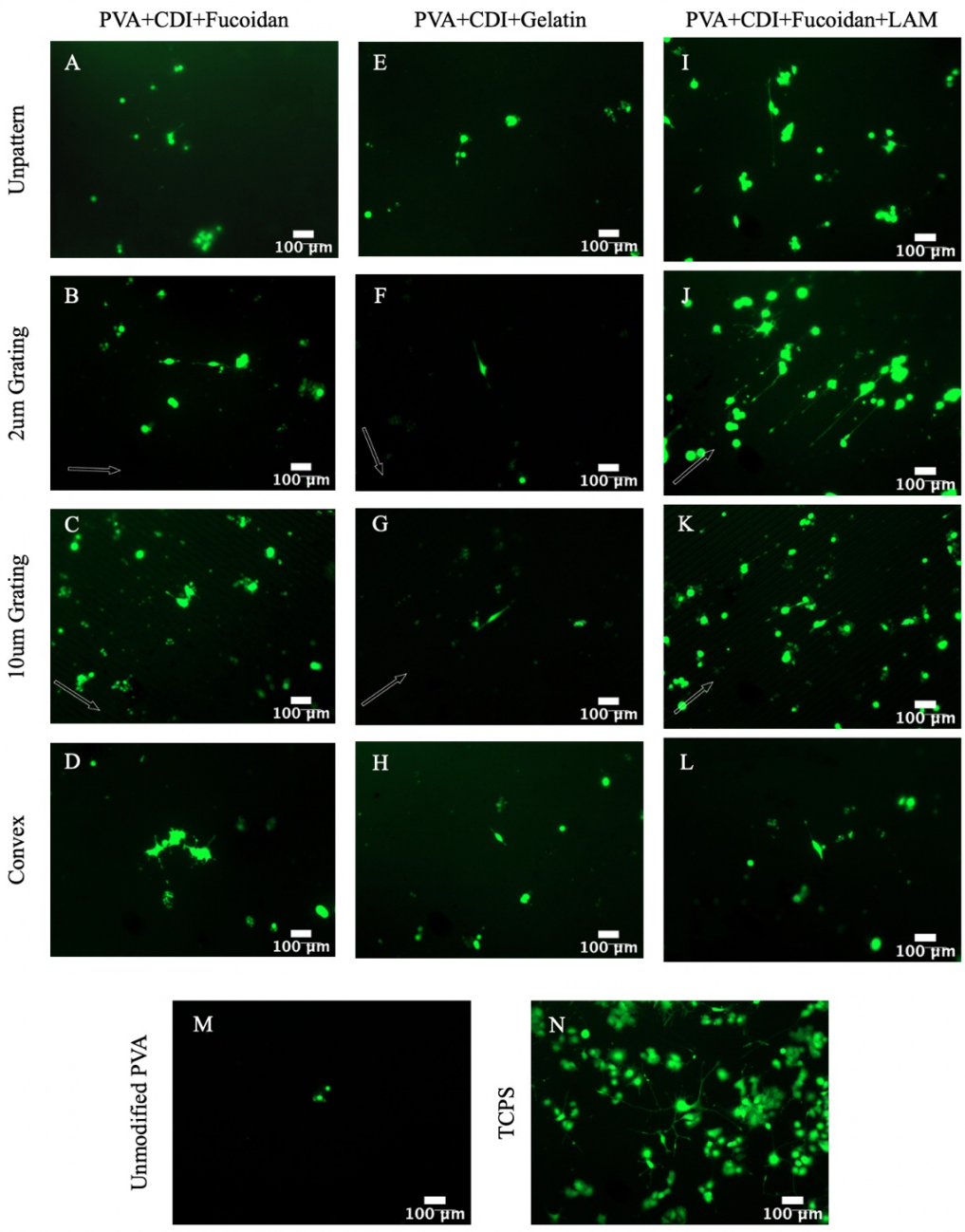

Figure 16. Representative fluorescence microscopy images of PC12 cell lines on PVA hydrogels with various topographical and biochemical modifications. Cells were cultured in media D-5 with LAM for three days and the seeding density was 20,000 cells/cm^2.

PVA surfaces were modified with CDI + fucoidan (A-D), CDI + gelatin (E-H) and CDI + fucoidan + LAM (I-L) on different topographies: unpatterned (A, E, I), 2 μm gratings (B, F, J), 10 μm gratings (C, G, K), and 1.8 μm convex lenses (D, H, L). (M) Unmodified PVA. (N) TCPS plate coated with collagen type IV diluted in 0.25% acetic acid. PC12 cell lines were stained with calcein-AM and exhibited green fluorescence after culturing for three days. The arrows with white outlines indicate the direction of gratings. The scale bars in all images are 100 μm.

The percentage of differentiated cells and the neurite length were shown in Figure 17. Similarly, PC12 cell lines were seeded on PVA substrates which were modified with CDI + fucoidan, CDI + gelatin and CDI + fucoidan + LAM combined with different topographies: unpatterned, 2 μm gratings, 10 μm gratings and 1.8 μm convex lenses. Cells were cultured in media D-5 with LAM for three days and the seeding density was 20,000 cells/cm^2.

Differentiated cells were considered to have neurite length that is 1.5 times longer than the cell length. About 200 cells were counted for each sample group and the ratio between differentiated cells and total cells was calculated (Figure 17 A). PVA surfaces modified with fucoidan + LAM promoted the most differentiation regardless of topography. Fucoidan modification induced more differentiation than gelatin modification, except for the unpatterned topography. In the fucoidan conjugation group, surfaces with topographical patterns had a higher percentage of differentiated cells than the unpatterned surface. The 2 μm gratings pattern promoted the most differentiation, followed by 10 μm gratings and 1.8 μm convex lenses. Cells seeded on the 2 μm gratings surface also presented the most differentiation in the gelatin modification group, while 1.8 μm convex lenses had the lowest percentage of differentiated cells. In the fucoidan + LAM conjugation group, the 2 μm gratings surface also supported the most differentiation. However, the other three topographies of unpatterned, 10 μm gratings and 1.8 μm convex

lenses had similar percentages. The unpatterned surfaces had a slightly higher differentiated cell number than the other two patterned substrates.

Overall, the 2 μm gratings pattern with fucoidan + LAM promoted the most differentiation while unpatterned PVA with fucoidan conjugation had the least differentiated cells. For topography, the 2 μm gratings pattern induced the most cell differentiation in all the biochemical modification groups. Also, among all biochemical modifications, fucoidan + LAM showed the most differentiated cells. The combination of topography and modification could further enhance neuronal differentiation.

The neurite length of each sample was measured and shown in Figure 17 B. The 2 μm gratings pattern on the fucoidan + LAM modification promoted the longest neurite length among all sample groups. In the fucoidan + LAM modification group, the average length on 2 μm gratings was 147.5 μm ± 49.7 μm, which was much longer than that of the unpatterned substrates ($p = 0.00005$) and 1.8 μm convex lenses ($p = 0.00001$). The 10 μm gratings pattern had the second-longest neurite length with an average length of 116.2 μm ± 47.2 μm, while 1.8 μm convex lenses had the shortest neurite length with an average length of 75.8 μm ± 31.6 μm.

The PVA surfaces that were modified with fucoidan had similar neurite lengths ($p > 0.999$) within different topographies. The 10 μm gratings pattern supported the longest neurite extension with an average length of 94.8 μm ± 37.4 μm.

Moreover, in the gelatin modification group, the 10 μm gratings pattern also induced the longest neurite length with an average length of 109.8 μm ± 30.2 μm, while unpatterned substrates showed the least neurite extension with an average length of 82.330 μm ± 46.5 μm.

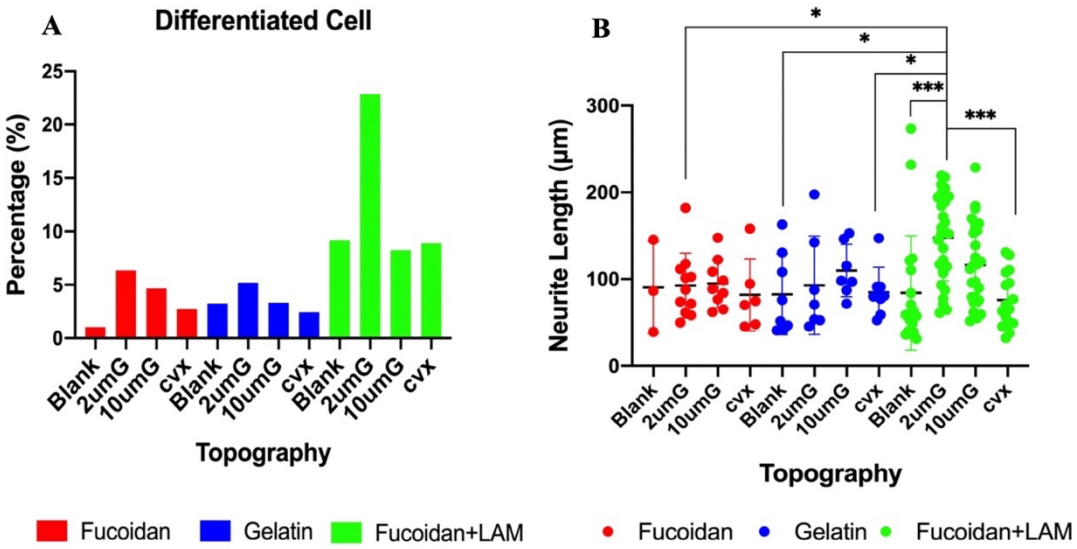

Figure 17. The percentage of differentiated cells (A) and the neurite length (B). PC12 cell lines were cultured in media D-5 with LAM for three days and the seeding density was 20,000 cells/cm^2. PVA surfaces were conjugated with CDI + fucoidan (red group), CDI + gelatin (blue group) and CDI + fucoidan + LAM (green group) combined with different topographies: unpatterned, 2 μm gratings, 10 μm gratings and 1.8 μm convex lenses. (B) The black line showed the mean value and the symbols * and *** denote $p < 0.05$ and $p < 0.001$.

4.3.6 Effect of PVA Substrates with NGF Modification on PC12 differentiation

To examine if NGF could be presented by binding onto the fucoidan groups immobilized on the PVA surface, the PVA substrates were conjugated with CDI + fucoidan, CDI + fucoidan + NGF, CDI + Gelatin, and CDI + gelatin + NGF (Figure 18).

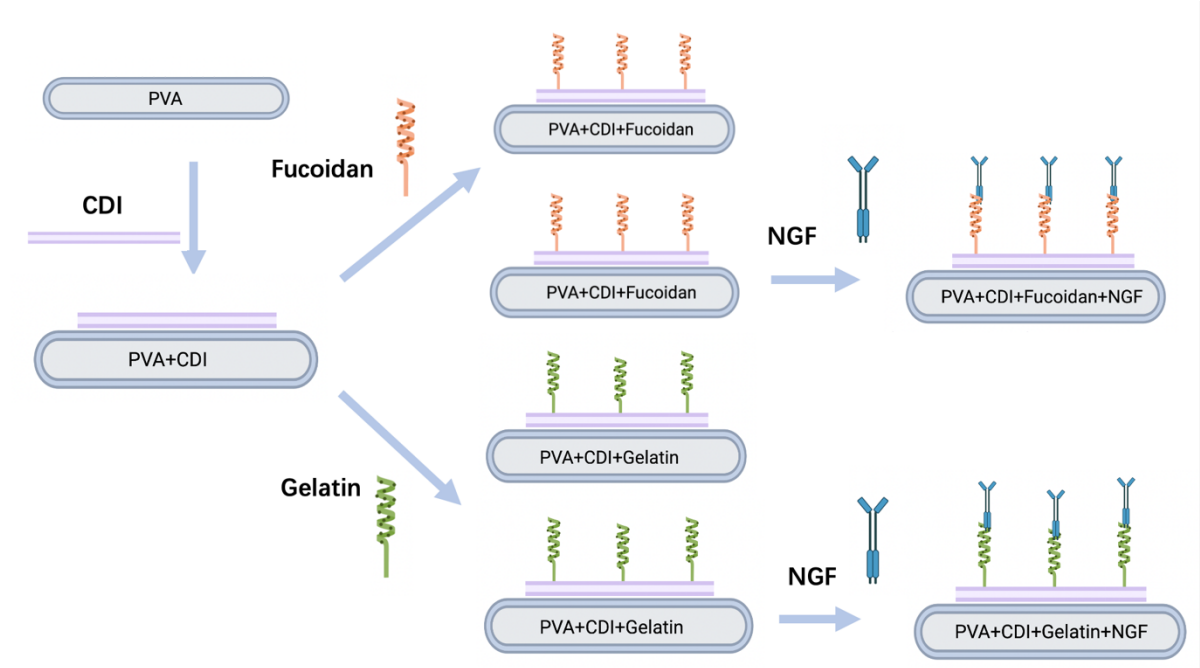

Figure 18. Schematic diagram of modified PVA preparation. The PVA surfaces were conjugated with CDI + fucoidan, CDI + fucoidan + NGF, CDI + Gelatin, and CDI + gelatin + NGF.

PC12 cell lines were cultured with media composed of DMEM, 1% PS and 5% FBS (Figure 19). Cells were seeded on both unpatterned PVA hydrogels (Figure 19 A-I) and PVA substrates with 2 μm gratings (Figure 19 E-H). Cells seeded on the unmodified PVA were used as a negative control (Figure 19 I) and the seeding density was 20,000 cells/cm^2. After culturing for three days, cells were stained with calcein-AM and exhibited green fluorescence.

PC12 could attach to the PVA surface modified with CDI + fucoidan (Figure 19 A and E) and CDI + gelatin (Figure 19 C and G), but they were unable to differentiate without NGF. PVA substrates conjugated with CDI + fucoidan + NGF (Figure 19 B and F) and CDI + gelatin + NGF (Figure 19 D and H) could induce cell differentiation on both unpatterned and 2 μm gratings PVA hydrogel. The modification of CDI + fucoidan + NGF on the 2 μm gratings pattern promoted more cell adhesion and differentiation when

compared to other modifications. Moreover, the neurite extension was aligned with the direction of the grating's axis.

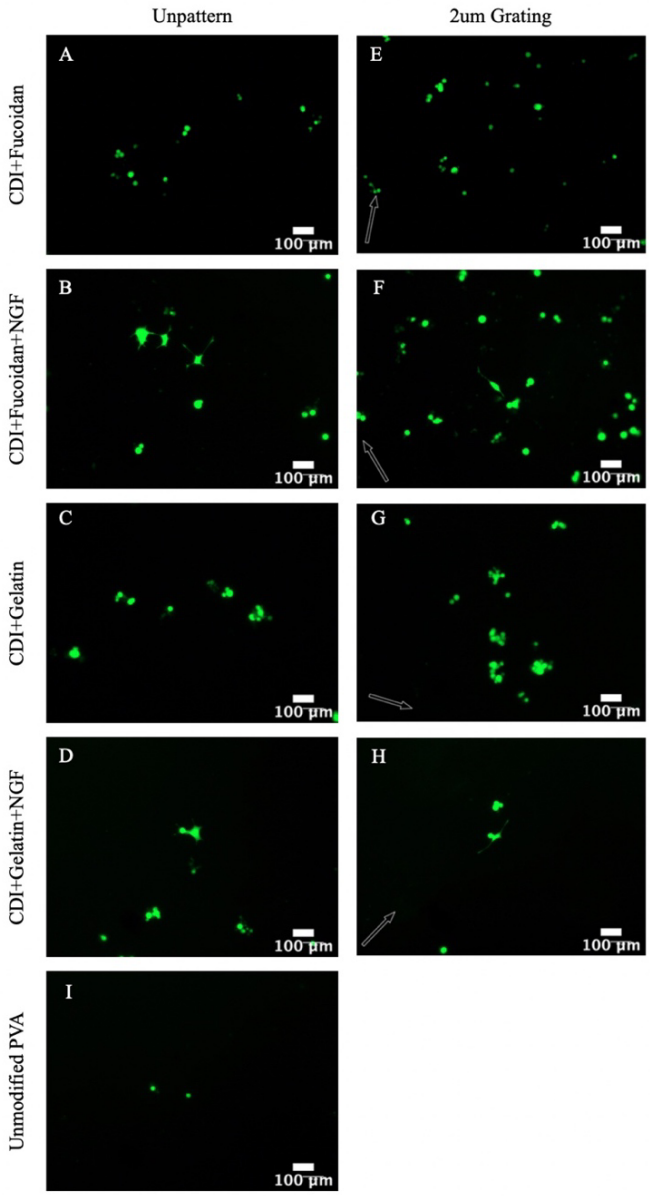

Figure 19. Representative fluorescence microscopy images of PC12 cell lines on PVA hydrogels to evaluate the NGF modification. Cells were cultured with media composed of DMEM, 1% PS and 5% FBS and seeded on both unpatterned A-I) and 2 μm gratings

(E-H) PVA substrates. The surfaces were modified with CDI + fucoidan (Figure 11 A and E), CDI + fucoidan + NGF (Figure 11 B and F), CDI + Gelatin (Figure 11 C and G), and CDI + gelatin + NGF (Figure 11 D and H). (I) Unmodified PVA. PC12 cell lines were stained with calcein-AM and exhibited green fluorescence after culturing for three days. The arrows with white outlines indicate the direction of gratings. The scale bars in all images are 100 μm.

Similarly, the percentage of differentiated cells is shown below in Figure 20. At least 100 cells were counted for each sample group. The percentage of differentiated cells referred to the ratio between differentiated cells and total cells. PVA substrates conjugated with fucoidan + NGF and gelatin + NGF could promote differentiation on both unpatterned and 2 μm gratings substrates. Also, for these two topographies, the biochemical modification of fucoidan + NGF showed a higher percentage of differentiated cells than gelatin + NGF. The topography of 2 μm gratings had more neurite outgrowth than the unpatterned one. Overall, the 2 μm gratings pattern on the fucoidan + NGF conjugation showed the highest percentage of differentiated cells, followed by the 2 μm gratings pattern on the gelatin + NGF modification.

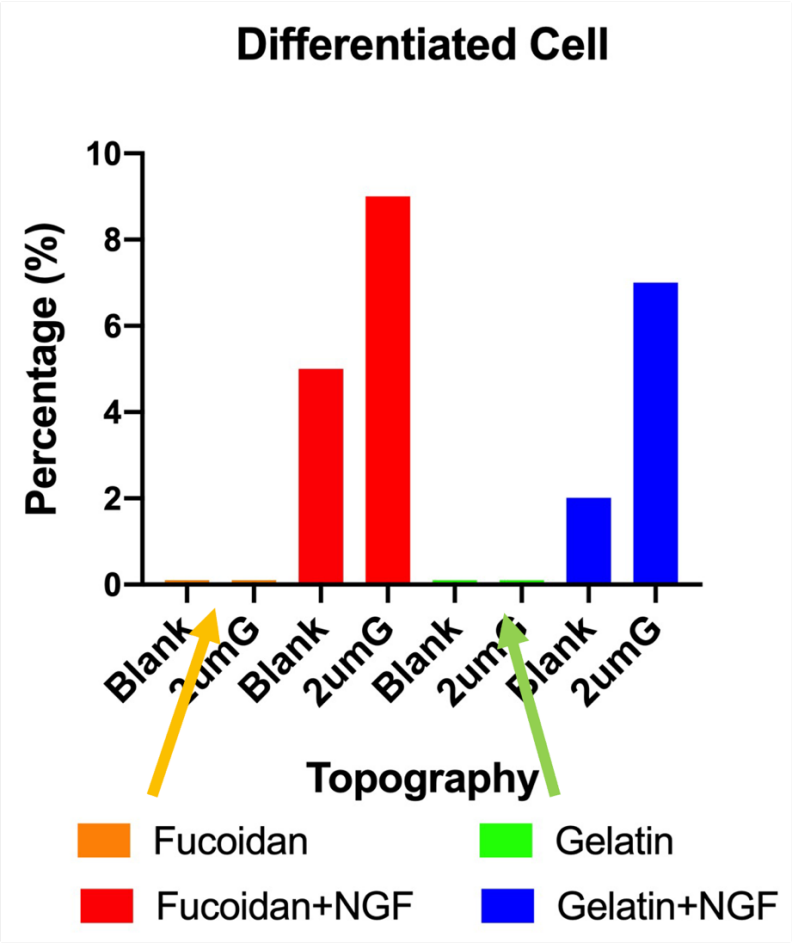

Figure 20. The percentage of differentiated cells. PC12 cell lines were culture in media composed of DMEM + 1% PS +5% FBS for three days and the seeding density was 20,000 cells/cm^2. PVA surfaces were conjugated with CDI + fucoidan (orange group), CDI + fucoidan + NGF (red group), CDI + gelatin (green group), and CDI + gelatin + NGF (blue group) combined with unpatterned and 2 μm gratings topographies.

4.4 Discussion

The topographical and biochemical properties of hydrogels could regulate cellular responses such as viability, proliferation, extension, and differentiation. PVA hydrogels have been used in tissue-mimicking, vascular implantation, and cell culture with suitable mechanical strength and low toxicity properties[58, 59]. PVA hydrogels with varying physical cues, such as topography would influence stem cell fate and direct the differentiation into target cell types[103]. Therefore, the combined effects of topographies and biochemicals warrant further investigation.

In this study, CDI was used to link various biochemicals to PVA. Conformational change of laminin is known to affect the bioactivity of laminin[104]. The failure of CDI + LAM in supporting hNPCs adhesion and differentiation may be attributed to the conformational change of laminin after direct binding to PVA with CDI. Furthermore, PLL with positively charged amino acid chains has been shown to encourage cell adhesion[105]. Since double coating of PLL + LAM could support cell adhesion and neurite outgrowth[44], PLL and PLO were added. PVA substrates conjugated with PLL + LAM could promote the attachment and differentiation of WT and RTT hNPCs, which is in accordance with others' findings. However, PLO + LAM induced minimal differentiation of WT hNPCs. A study from Pellett *et al.* showed PLO + LAM could support the differentiation of iPSC-derived neural stem cells. Also, Ge *et al.* stated PLO could promote more neuronal differentiation of NSPCs than PLL and fibronectin[78]. One possible reason is that the concentration of the PLO coating was too low. We directly used the purchased 0.1 mg/ml PLO solution, whereas the 0.5 mg/ml PLL was prepared from powder and then diluted to the desired concentration. Moreover, with a high seeding density of 50,000 cells/cm^2, the cells would be overly confluent, and a minimal amount of differentiation could be induced. Lowering the seeding density to 20,000 cells/cm^2 would help to promote differentiation.

Our group's previous study illustrated that PVA with fucoidan modification could promote endothelial cell attachment and proliferation[63]. Hence, the impacts of fucoidan on PC12 adhesion and neuronal differentiation were evaluated. Surface modifications such as fucoidan, gelatin, PLL + LAM, collagen type IV diluted in 0.01% and 0.05% acetic acid were coated on the PVA and could support cell adhesion and proliferation. The PC12 cell lines seeded on the PLL + LAM had the highest cell viability. Also, conjugation with fucoidan and gelatin showed better cell viability when compared to the modification with collagen type IV diluted in acetic acid.

By comparison of differentiation media, PC12 cell lines on PVA + CDI + fucoidan were unable to differentiate without the presence of serum. 30 ng/ml NGF was sufficient to support PC12 differentiation, although Orlowaska *et al.* suggested 100 ng/ml NGF could promote more differentiation[44]. In addition, laminin could enhance cell differentiation and neurite outgrowth[83]. The Media D-5 with LAM induced the most cell differentiation and neurite outgrowth as expected when compared to other media compositions.

The differentiation of PC12 could be supported by PVA hydrogels modified with fucoidan, gelatin, and fucoidan + LAM. The surface with fucoidan conjugation induced more neurite outgrowth than gelatin modification for all the patterned topographies, which proved the capability of fucoidan to support neuronal differentiation. Distler *et al.* demonstrated that alginate-gelatin-laminin hydrogels could facilitate neuronal differentiation and neuron migration of hiPSCs compared to alginate-gelatin hydrogels[106]. Our PVA surfaces modified with fucoidan + LAM had the highest percentage of the differentiated cells, which indicated fucoidan could positively exhibit LAM and further enhance differentiation.

Furthermore, topographic features could regulate cell migration, adhesion, and induce differentiation into specific lineages[107]. In this study, we analyzed the effect of topographic patterns: 2 μm gratings, 10 μm gratings, and 1.8 μm convex lenses on neurite

outgrowth and extension. In both fucoidan and gelatin modification groups, PVA hydrogels with grating patterns enhanced more PC12 differentiation than the unpatterned and convex lenses surface. The PC12 cells on the 2 μm gratings pattern had the highest percentage of differentiated cells. When examining neurite length, the gratings pattern also supported longer neurite elongation than the unpatterned and convex lenses surfaces. Comparing 2 μm and 10 μm gratings, PC12 cells on the 10 μm gratings pattern had the longest neurite extension. For the fucoidan + LAM conjugation group, the 2 μm gratings pattern not only induced the most differentiation, but PC12 cells on 2 μm gratings pattern also exhibited the longest neurite length. Although the 10 μm gratings pattern still promoted better neurite length than the unpatterned and convex lenses substrates, there were no significant differences in the percentage of differentiated cells on those patterns.

Since NGF has a heparin-binding site[108] and fucoidan and heparin are sulfated polysaccharide with similarities in structure[109], we hypothesized that NGF could bind to the fucoidan immobilized on PVA surface. The 2 μm gratings pattern on CDI + fucoidan + NGF modification showed the highest percentage of differentiated cells, which suggested the fucoidan could present NGF and further induce the neurite outgrowth.

4.5 Conclusion

In summary, PVA hydrogels with different topographies and biochemicals modulated cell adhesion, viability, and differentiation. Both WT and RTT hNPCs could adhere to the PVA surface modified with CDI + PLL + LAM. Also, PC12 cells lines show the best attachment and viability with CDI + PLL + LAM conjugation.

Serum was essential for inducing differentiation. In the differentiation media with LAM and NGF, PC12 could differentiate on CDI + fucoidan, CDI + gelatin, and CDI + fucoidan + LAM modified PVA substrates, combined with the unpatterned, 2 μm gratings, 10 μm gratings and 1.8 μm convex lenses topographies. The neurite extension was guided by the grating topographies. For biochemical modification, fucoidan could successfully

conjugate to the PVA substrates and improve neuronal differentiation. Laminin addition to fucoidan modified PVA hydrogels promoted neurite outgrowth and neurite length which proved the fucoidan could present laminin. In addition, when comparing the topographical effects, the 2 μm gratings pattern induced the most cell differentiation in all the biochemical modification groups and the longest neurite extension in fucoidan and gelatin modification group.

Cells cultured with media without NGF could still differentiate on the PVA substrates modified with CDI + fucoidan + NGF and CDI + gelatin and + NGF. Both fucoidan and gelatin could present NGF conjugation. Also, the 2 μm gratings pattern enhance more cell differentiation and longer neurite length than the unpatterned one.

Overall, the combination of topography and modification further improved neuronal differentiation. Fucoidan could be conjugated to the PVA substrates, and further presented LAM and NGF modification. The 2 μm gratings pattern with fucoidan + LAM promoted the most neurite outgrowth and neurite length in the differentiation media with LAM and NGF. The 2 μm gratings pattern with fucoidan + NGF induced the most neuronal differentiation in the differentiation media without LAM or NGF.

Chapter 5 Conclusions and Recommendations

5.1 General Conclusions

Mechanical and biochemical cues can enhance cellular response, such as attachment, alignment, and differentiation. These modifications like topography, stiffness, and biochemicals are promising to use in tissue engineering and further benefit the therapies of neurological diseases. The findings of this study showed that hydrogel substrates with topographical and stiffness modification regulated neuronal differentiation and maturation. The PAA-ACA gels could be fabricated with various topographies by prepared PET molds and different stiffness could be controlled by adjusting the ratio of acrylamide and bisacrylamide. WT and RTT hNPCs adhered to all the topographies and stiffnesses of the PAA-ACA substrates. Also, the topographical pattern promoted cell alignment and soft substrates could generally support more neuronal differentiation, maturation, and mature synapses than rigid substrates. The PAA-ACA gels with 2 μm gratings on the softer surface promoted the most neuronal differentiation and 5 μm gratings on the softer surface supported the most neuronal maturation and synaptic maturation.

Moreover, the combination of topography and biochemicals can improve cell adhesion, viability, and differentiation. Both hNPCs and PC12 cell lines adhered and responded to the PVA hydrogels with different surface modifications. PVA surface modified with fucoidan, gelatin, and PLL + LAM could support cell survival and attachment. Also, the topographical and biochemical modification could enhance cell differentiation. The grating topographies guided the neurite extension and improved neurite alignment. Fucoidan could present the LAM and NGF binding and further promote neurite outgrowth and elongation. However, cells were unable to adhere or differentiate in the absence of serum.

Overall, with the enhancement of cell attachment, viability, and neuronal differentiation, mechanical and biochemical cues could provide promising modifications of hydrogels for cell studies.

5.2 Future Recommendations

According to the results of this thesis, several recommendations could be proposed. Since the neuronal differentiation and maturation are regulated by both topography and stiffness, more topographical patterns, such as grating sizes lower than 2 μm or one size between 5 μm and 10 μm gratings could be added for a comprehensive test. Also, softer substrate, with E close to 1 kPa or E range from 1 to 10 kPa would be a good idea to add for comparison since neuronal differentiation favors the substrates with lower rigidity. Another important factor is the housekeeping gene in the RT-qPCR test. The purity of the RNA sample may contribute to the variation. Also, a more stable housekeeping gene should be tested to reduce batch to batch variation, thus providing more consistent data for statistical analysis. Moreover, since RTT hNPCs could respond to the PAA-ACA substrates with different topographies and stiffnesses, further investigation of the neuronal differentiation and maturation could be conducted with a similar method of WT hNPCs.

In addition, topographical and biochemical modification could benefit cell adhesion, viability, and differentiation. PVA with suitable modification, such as a higher concentration of PLO or topographic pattern, could support hNPCs culturing. Also, the grating topography is a promising modification, whereas the convex lenses pattern seems not to promote neurite outgrowth and elongation. Topography with narrower grating pattern, which with a smaller grating width, spacing and height would be a suggested direction to evaluate. Moreover, the results in chapter 4.3.5 are required more biological replicates. Also, the results in chapter 4.3.6 showed the neurite length analysis of the 2 μm gratings pattern on CDI + fucoidan + NGF immobilization from one biological

replicate. The lack of biological replicas and the insufficient cell count may contribute to the large variation observed. More biological replicates are suggested to be added. More topographies such as nanoscale gratings pattern are also worth attempting to evaluate the effect of NGF conjugation on PVA substrates.

Letter of Copyright Permission

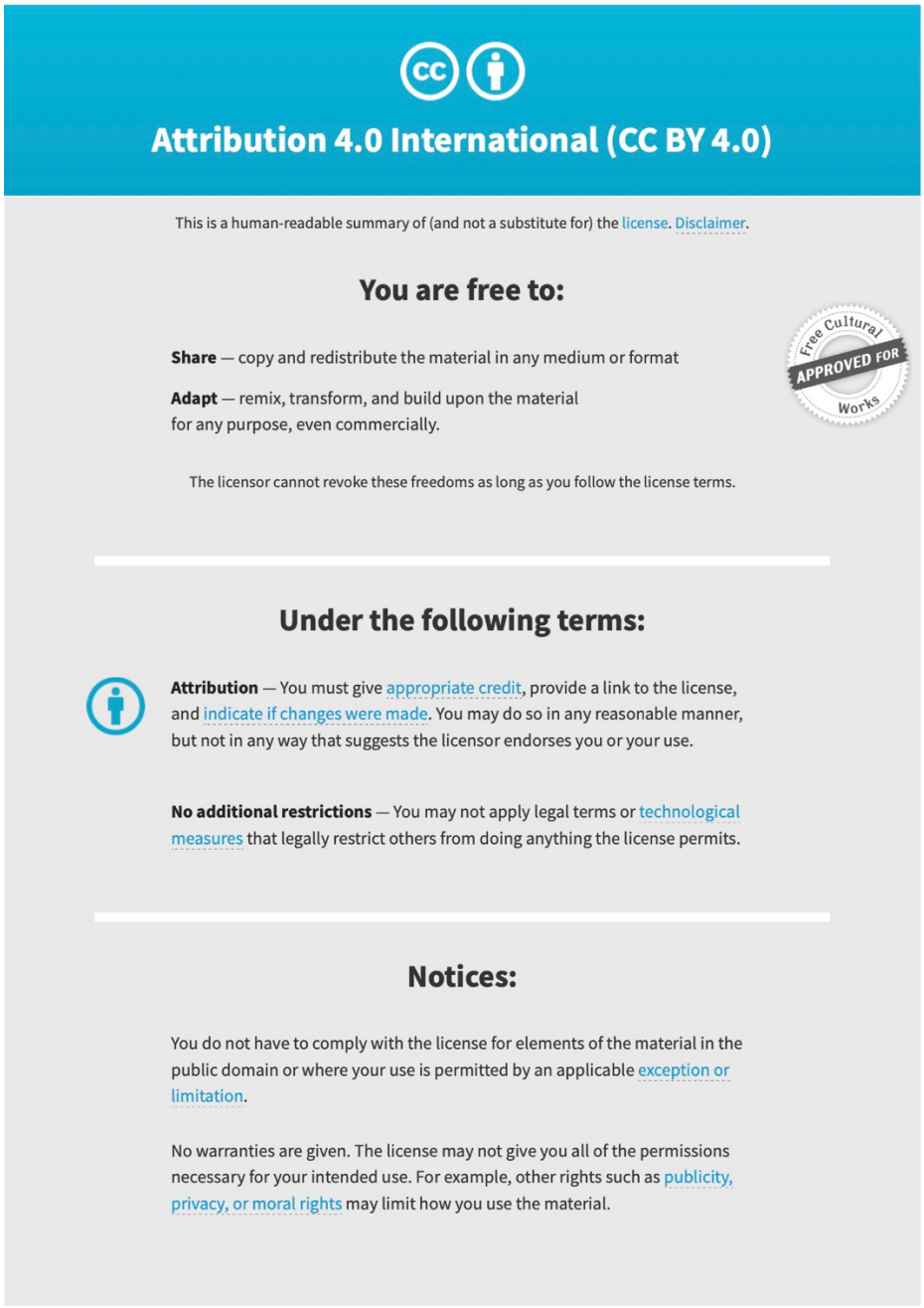

Attribution 4.0 International (CC BY 4.0)

This is a human-readable summary of (and not a substitute for) the license. Disclaimer.

You are free to:

Share — copy and redistribute the material in any medium or format

Adapt — remix, transform, and build upon the material for any purpose, even commercially.

The licensor cannot revoke these freedoms as long as you follow the license terms.

Under the following terms:

Attribution — You must give appropriate credit, provide a link to the license, and indicate if changes were made. You may do so in any reasonable manner, but not in any way that suggests the licensor endorses you or your use.

No additional restrictions — You may not apply legal terms or technological measures that legally restrict others from doing anything the license permits.

Notices:

You do not have to comply with the license for elements of the material in the public domain or where your use is permitted by an applicable exception or limitation.

No warranties are given. The license may not give you all of the permissions necessary for your intended use. For example, other rights such as publicity, privacy, or moral rights may limit how you use the material.

References

(1) Gitler, A. D.; Dhillon, P.; Shorter, J. Neurodegenerative disease: models, mechanisms, and a new hope. *Disease Models & Mechanisms* **2017**, *10* (5), 499-502. DOI: 10.1242/dmm.030205 (acccessed 1/20/2022).

(2) Bonnamain, V.; Neveu, I.; Naveilhan, P. Neural stem/progenitor cells as a promising candidate for regenerative therapy of the central nervous system. *Front Cell Neurosci* **2012**, *6*, 17-17. DOI: 10.3389/fncel.2012.00017 PubMed.

(3) Tang, Y. W.; Yu, P.; Cheng, L. Current progress in the derivation and therapeutic application of neural stem cells. *Cell Death Dis* **2017**, *8*. DOI: ARTN e3108

10.1038/cddis.2017.504.

(4) Lee, V. M.; Louis, S. A.; Reynolds, B. A. Neural Stem Cells: Identification, Function, Culture, and Isolation. STEMCELL Technologies Inc: 2015.

(5) Martinez-Cerdeno, V.; Noctor, S. C. Neural Progenitor Cell Terminology. *Front Neuroanat* **2018**, *12*. DOI: ARTN 104

10.3389/fnana.2018.00104.

(6) Kim, S. U.; Lee, H. J.; Kim, Y. B. Neural stem cell-based treatment for neurodegenerative diseases. *Neuropathology* **2013**, *33* (5), 491-504. DOI: 10.1111/neup.12020.

(7) De Gioia, R.; Biella, F.; Citterio, G.; Rizzo, F.; Abati, E.; Nizzardo, M.; Bresolin, N.; Comi, G. P.; Corti, S. Neural Stem Cell Transplantation for Neurodegenerative Diseases. *Int J Mol Sci* **2020**, *21* (9). DOI: ARTN 3103

10.3390/ijms21093103.

(8) Cui, L. N.; Yao, Y.; Yim, E. K. F. The effects of surface topography modification on hydrogel properties. *Apl Bioeng* **2021**, *5* (3). DOI: Artn 031509

10.1063/5.0046076.

(9) Qi, L.; Li, N.; Huang, R.; Song, Q.; Wang, L.; Zhang, Q.; Su, R. G.; Kong, T.; Tang, M. L.; Cheng, G. S. The Effects of Topographical Patterns and Sizes on Neural Stem Cell Behavior. *Plos One* **2013**, *8* (3). DOI: ARTN e59022

10.1371/journal.pone.0059022.

(10) Kraning-Rush, C. M.; Reinhart-King, C. A. Controlling matrix stiffness and topography for the study of tumor cell migration. *Cell Adhes Migr* **2012**, *6* (3), 274-279. DOI: 10.4161/cam.21076.

(11) Stukel, J. M.; Willits, R. K. Mechanotransduction of Neural Cells Through Cell-Substrate Interactions. *Tissue Eng Part B-Re* **2016**, *22* (3), 173-182. DOI: 10.1089/ten.teb.2015.0380.

(12) Leipzig, N. D.; Shoichet, M. S. The effect of substrate stiffness on adult neural stem cell behavior. *Biomaterials* **2009**, *30* (36), 6867-6878. DOI: 10.1016/j.biomaterials.2009.09.002.

(13) Kozaniti, F. K.; Deligianni, D. D.; Georgiou, M. D.; Portan, D. V. The Role of Substrate Topography and Stiffness on MSC Cells Functions: Key Material Properties for Biomimetic Bone Tissue Engineering. *Biomimetics* **2022**, *7* (1), 7.

(14) Huang, C. Y.; Hu, K. H.; Wei, Z. H. Comparison of cell behavior on pva/pva-gelatin electrospun nanofibers with random and aligned configuration. *Sci Rep-Uk* **2016**, *6*. DOI: ARTN 37960

10.1038/srep37960.

(15) Kular, J. K.; Basu, S.; Sharma, R. I. The extracellular matrix: Structure, composition, age-related differences, tools for analysis and applications for tissue engineering. *J Tissue Eng* **2014**, *5*, 2041731414557112. DOI: 10.1177/2041731414557112.

(16) Stangor, C. a. W., J. . 4.4 Putting It All Together: The Nervous System and the Endocrine System. In *Introduction to Psychology – 1st Canadian Edition*, BCcampus, 2010.

(17) Ladran, I.; Tran, N.; Topol, A.; Brennand, K. J. Neural stem and progenitor cells in health and disease. *Wires Syst Biol Med* **2013**, *5* (6), 701-715. DOI: 10.1002/wsbm.1239. Rietze, R. L.; Reynolds, B. A. Neural stem cell isolation and characterization. *Method Enzymol* **2006**, *419*, 3-23. DOI: 10.1016/S0076-6879(06)19001-1.

(18) Fukusumi, H.; Shofuda, T.; Bamba, Y.; Yamamoto, A.; Kanematsu, D.; Handa, Y.; Okita, K.; Nakamura, M.; Yamanaka, S.; Okano, H.; et al. Establishment of Human Neural Progenitor Cells from Human Induced Pluripotent Stem Cells with Diverse Tissue Origins. *Stem Cells Int* **2016**, *2016*. DOI: Artn 7235757

10.1155/2016/7235757.

(19) Ye, L.; Swingen, C.; Zhang, J. Induced pluripotent stem cells and their potential for basic and clinical sciences. *Curr Cardiol Rev* **2013**, *9* (1), 63-72. DOI: 10.2174/157340313805076278 PubMed.

(20) Hong, Y. J.; Do, J. T. Neural Lineage Differentiation From Pluripotent Stem Cells to Mimic Human Brain Tissues. *Front Bioeng Biotech* **2019**, *7*. DOI: ARTN 400

10.3389/fbioe.2019.00400.

(21) Zhu, Y. Q.; Li, X.; Janairo, R. R. R.; Kwong, G.; Tsou, A. C. D.; Chu, J. S.; Wang, A. J.; Yu, J.; Wang, D.; Li, S. Matrix stiffness modulates the differentiation of neural crest stem cells in vivo. *J Cell Physiol* **2019**, *234* (5), 7569-7578. DOI: 10.1002/jcp.27518.

(22) Takahashi, K.; Tanabe, K.; Ohnuki, M.; Narita, M.; Ichisaka, T.; Tomoda, K.; Yamanaka, S. Induction of pluripotent stem cells from adult human fibroblasts by defined factors. *Cell* **2007**, *131* (5), 861-872. DOI: 10.1016/j.cell.2007.11.019.

(23) Paavilainen, T.; Pelkonen, A.; Makinen, M. E. L.; Peltola, M.; Huhtala, H.; Fayuk, D.; Narkilahti, S. Effect of prolonged differentiation on functional maturation of human pluripotent stem cell-derived neuronal cultures. *Stem Cell Res* **2018**, *27*, 151-161. DOI: 10.1016/j.scr.2018.01.018.

(24) Chiodo, A. E.; Sitrin, R. G.; Bauman, K. A. Sleep disordered breathing in spinal cord injury: A systematic review. *J Spinal Cord Med* **2016**, *39* (4), 374-382. DOI: 10.1080/10790268.2015.1126449.

(25) Dumont, R. J.; Okonkwo, D. O.; Verma, R. S.; Hurlbert, R. J.; Boulos, P. T.; Ellegala, D. B.; Dumont, A. S. Acute spinal cord injury, part I: Pathophysiologic mechanisms. *Clin Neuropharmacol* **2001**, *24* (5), 254-264. DOI: Doi 10.1097/00002826-200109000-00002.

(26) Moini, J.; Piran, P. Chapter 1 - Histophysiology. In *Functional and Clinical Neuroanatomy*, Moini, J., Piran, P. Eds.; Academic Press, 2020; pp 1-49.

(27) Walker, T.; Huang, J.; Young, K. Neural Stem and Progenitor Cells in Nervous System Function and Therapy. *Stem Cells Int* **2016**, *2016*. DOI: Artn 1890568

10.1155/2016/1890568.

(28) Cole, A. E.; Murray, S. S.; Xiao, J. H. Bone Morphogenetic Protein 4 Signalling in Neural Stem and Progenitor Cells during Development and after Injury. *Stem Cells Int* **2016**, *2016*. DOI: Artn 9260592

10.1155/2016/9260592.

(29) Mothe, A. J.; Zahir, T.; Santaguida, C.; Cook, D.; Tator, C. H. Neural Stem/Progenitor Cells from the Adult Human Spinal Cord Are Multipotent and Self-Renewing and Differentiate after Transplantation. *Plos One* **2011**, *6* (11). DOI: ARTN e27079

10.1371/journal.pone.0027079.

(30) Amir, R. E.; Van den Veyver, I. B.; Wan, M.; Tran, C. Q.; Francke, U.; Zoghbi, H. Y. Rett syndrome is caused by mutations in X-linked MECP2, encoding methyl-CpG-binding protein 2. *Nat Genet* **1999**, *23* (2), 185-188. DOI: Doi 10.1038/13810.

(31) Schanen, C.; Francke, U. A severely affected male born into a Rett syndrome kindred supports X-linked inheritance and allows extension of the exclusion map. *Am J Hum Genet* **1998**, *63* (1), 267-269. DOI: Doi 10.1086/301932.

(32) Kim, K. Y.; Hysolli, E.; Park, I. H. Neuronal maturation defect in induced pluripotent stem cells from patients with Rett syndrome. *P Natl Acad Sci USA* **2011**, *108* (34), 14169-14174. DOI: 10.1073/pnas.1018979108.

(33) Shovlin, S.; Tropea, D. Transcriptome level analysis in Rett syndrome using human samples from different tissues. *Orphanet J Rare Dis* **2018**, *13*. DOI: ARTN 113

10.1186/s13023-018-0857-8.

(34) Andoh-Noda, T.; Akamatsu, W.; Miyake, K.; Matsumoto, T.; Yamaguchi, R.; Sanosaka, T.; Okada, Y.; Kobayashi, T.; Ohyama, M.; Nakashima, K.; et al. Differentiation of multipotent neural stem cells derived from Rett syndrome patients is biased toward the astrocytic lineage. *Mol Brain* **2015**, *8*. DOI: ARTN 31

10.1186/s13041-015-0121-2.

(35) Chahrour, M.; Zoghbi, H. Y. The story of Rett syndrome: From clinic to neurobiology. *Neuron* **2007**, *56* (3), 422-437. DOI: 10.1016/j.neuron.2007.10.001.

(36) Nguyen, A. T.; Mattiassi, S.; Loeblein, M.; Chin, E.; Ma, D.; Coquet, P.; Viasnoff, V.; Teo, E. H. T.; Goh, E. L.; Yim, E. K. F. Human Rett-derived neuronal progenitor cells in 3D graphene scaffold as an in vitro platform to study the effect of electrical stimulation on neuronal differentiation. *Biomed Mater* **2018**, *13* (3). DOI: ARTN 034111

10.1088/1748-605X/aaaf2b.

(37) Das, K. P.; Freudenrich, T. M.; Mundy, W. R. Assessment of PC12 cell differentiation and neurite growth: a comparison of morphological and neurochemical measures. *Neurotoxicol Teratol* **2004**, *26* (3), 397-406. DOI: 10.1016/j.ntt.2004.02.006.

(38) Vaudry, D.; Stork, P. J.; Lazarovici, P.; Eiden, L. E. Signaling pathways for PC12 cell differentiation: making the right connections. *Science* **2002**, *296* (5573), 1648-1649. DOI: 10.1126/science.1071552.

(39) Wiatrak, B.; Kubis-Kubiak, A.; Piwowar, A.; Barg, E. PC12 Cell Line: Cell Types, Coating of Culture Vessels, Differentiation and Other Culture Conditions. *Cells-Basel* **2020**, *9* (4). DOI: ARTN 958

10.3390/cells9040958.

(40) Hu, R. D.; Cao, Q. Y.; Sun, Z. Q.; Chen, J. Y.; Zheng, Q.; Xiao, F. A novel method of neural differentiation of PC12 cells by using Opti-MEM as a basic induction medium. *Int J Mol Med* **2018**, *41* (1), 195-201. DOI: 10.3892/ijmm.2017.3195.

(41) Greene, L. A.; Tischler, A. S. Establishment of a Noradrenergic Clonal Line of Rat Adrenal Pheochromocytoma Cells Which Respond to Nerve Growth-Factor. *P Natl Acad Sci USA* **1976**, *73* (7), 2424-2428. DOI: DOI 10.1073/pnas.73.7.2424.

(42) Sierra-Fonseca, J. A.; Najera, O.; Martinez-Jurado, J.; Walker, E. M.; Varela-Ramirez, A.; Khan, A. M.; Miranda, M.; Lamango, N. S.; Roychowdhury, S. Nerve growth factor induces neurite outgrowth of PC12 cells by promoting G beta gamma-microtubule interaction. *Bmc Neurosci* **2014**, *15*. DOI: ARTN 132

10.1186/s12868-014-0132-4.

(43) Ferrari, A.; Faraci, P.; Cecchini, M.; Beltram, F. The effect of alternative neuronal differentiation pathways on PC12 cell adhesion and neurite alignment to nanogratings. *Biomaterials* **2010**, *31* (9), 2565-2573. DOI: 10.1016/j.biomaterials.2009.12.010.

(44) Orlowska, A.; Perera, P. T.; Al Kobaisi, M.; Dias, A.; Nguyen, H. K. D.; Ghanaati, S.; Baulin, V.; Crawford, R. J.; Ivanova, E. P. The Effect of Coatings and Nerve Growth Factor on Attachment and Differentiation of Pheochromocytoma Cells. *Materials* **2018**, *11* (1). DOI: ARTN 60

10.3390/ma11010060.

(45) Foley, J. D.; Grunwald, E. W.; Nealey, P. F.; Murphy, C. J. Cooperative modulation of neuritogenesis by PC12 cells by topography and nerve growth factor. *Biomaterials* **2005**, *26* (17), 3639-3644. DOI: 10.1016/j.biomaterials.2004.09.048.

(46) Wu, Y. B.; Xiang, Y.; Fang, J. H.; Li, X. K.; Lin, Z. W.; Dai, G. L.; Yin, J.; Wei, P.; Zhang, D. M. The influence of the stiffness of GelMA substrate on the outgrowth of PC12 cells. *Bioscience Rep* **2019**, *39*. DOI: Artn Bsr20181748

10.1042/Bsr20181748.

(47) Caliari, S. R.; Burdick, J. A. A practical guide to hydrogels for cell culture. *Nat Methods* **2016**, *13* (5), 405-414. DOI: DOI 10.1038/nmeth.3839.

(48) Chai, Q. Y.; Jiao, Y.; Yu, X. J. Hydrogels for Biomedical Applications: Their Characteristics and the Mechanisms behind Them. *Gels-Basel* **2017**, *3* (1). DOI: ARTN 6

10.3390/gels3010006.

(49) Gyles, D. A.; Castro, L. D.; Silva, J. O. C.; Ribeiro-Costa, R. M. A review of the designs and prominent biomedical advances of natural and synthetic hydrogel formulations. *Eur Polym J* **2017**, *88*, 373-392. DOI: 10.1016/j.eurpolymj.2017.01.027.

(50) Fan, D.; Staufer, U.; Accardo, A. Engineered 3D Polymer and Hydrogel Microenvironments for Cell Culture Applications. *Bioengineering-Basel* **2019**, *6* (4). DOI: ARTN 113

10.3390/bioengineering6040113.

(51) Bahram, M. *An Introduction to Hydrogels and Some Recent Applications*; IntechOpen, 2016.

(52) Liu, Y.; Hsu, S. H. Synthesis and Biomedical Applications of Self-healing Hydrogels. *Front Chem* **2018**, *6*. DOI: ARTN 449

10.3389/fchem.2018.00449.

(53) Yip, A. K.; Iwasaki, K.; Ursekar, C.; Machiyama, H.; Saxena, M.; Chen, H. L.; Harada, I.; Chiam, K. H.; Sawada, Y. Cellular Response to Substrate Rigidity Is Governed by Either Stress or Strain. *Biophys J* **2013**, *104* (1), 19-29. DOI: 10.1016/j.bpj.2012.11.3805.

(54) Al-Haque, S.; Miklas, J. W.; Feric, N.; Chiu, L. L. Y.; Chen, W. L. K.; Simmons, C. A.; Radisic, M. Hydrogel Substrate Stiffness and Topography Interact to Induce Contact Guidance in Cardiac Fibroblasts. *Macromol Biosci* **2012**, *12* (10), 1342-1353. DOI: 10.1002/mabi.201200042.

(55) Engler, A. J.; Sen, S.; Sweeney, H. L.; Discher, D. E. Matrix elasticity directs stem cell lineage specification. *Cell* **2006**, *126* (4), 677-689. DOI: 10.1016/j.cell.2006.06.044.

(56) Wang, T.; Qu, G. W.; Wang, C.; Cheng, Y. Z.; Shang, J.; Zheng, J.; Feng, Z. Q.; Chen, Q.; He, N. Y. Importance of Polyacrylamide Hydrogel Diverse Chains and Cross-Linking Density for Cell Proliferation, Aging, and Death. *Langmuir* **2019**, *35* (43), 13999-14006. DOI: 10.1021/acs.langmuir.9b02799.

(57) Pelham, R. J.; Wang, Y. L. Cell locomotion and focal adhesions are regulated by substrate flexibility. *P Natl Acad Sci USA* **1997**, *94* (25), 13661-13665. DOI: DOI 10.1073/pnas.94.25.13661.

(58) Jiang, S.; Liu, S.; Feng, W. PVA hydrogel properties for biomedical application. *J Mech Behav Biomed Mater* **2011**, *4* (7), 1228-1233. DOI: 10.1016/j.jmbbm.2011.04.005.

(59) Ma, S. J.; Wang, S. W.; Li, Q.; Leng, Y. T.; Wang, L. H.; Hu, G. H. A Novel Method for Preparing Poly(vinyl alcohol) Hydrogels: Preparation, Characterization, and Application. *Ind Eng Chem Res* **2017**, *56* (28), 7971-7976. DOI: 10.1021/acs.iecr.7b01812.

(60) Hassan, C. M.; Peppas, N. A. Structure and morphology of freeze/thawed PVA hydrogels. *Macromolecules* **2000**, *33* (7), 2472-2479. DOI: DOI 10.1021/ma9907587.

(61) Vrana, N. E.; Liu, Y. R.; McGuinness, G. B.; Cahill, P. A. Characterization of poly(vinyl alcohol)/chitosan hydrogels as vascular tissue engineering scaffolds. *Macromol Symp* **2008**, *269*, 106-110. DOI: 10.1002/masy.200850913.

(62) Chaouat, M.; Le Visage, C.; Baille, W. E.; Escoubet, B.; Chaubet, F.; Mateescu, M. A.; Letourneur, D. A Novel Cross-linked Poly(vinyl alcohol) (PVA) for Vascular Grafts. *Adv Funct Mater* **2008**, *18* (19), 2855-2861. DOI: 10.1002/adfm.200701261.

(63) Yao, Y.; Zaw, A. M.; Anderson, D. E. J.; Hinds, M. T.; Yim, E. K. F. Fucoidan functionalization on poly(vinyl alcohol) hydrogels for improved endothelialization and hemocompatibility. *Biomaterials* **2020**, *249*. DOI: ARTN 120011

10.1016/j.biomaterials.2020.120011.

(64) Yim, E. K. F.; Pang, S. W.; Leong, K. W. Synthetic nanostructures inducing differentiation of human mesenchymal stem cells into neuronal lineage. *Exp Cell Res* **2007**, *313* (9), 1820-1829. DOI: 10.1016/j.yexcr.2007.02.031.

(65) Moe, A. A. K.; Suryana, M.; Marcy, G.; Lim, S. K.; Ankam, S.; Goh, J. Z. W.; Jin, J.; Teo, B. K. K.; Law, J. B. K.; Low, H. Y.; et al. Microarray with Micro- and Nano-topographies Enables Identification of the Optimal Topography for Directing the Differentiation of Primary Murine Neural Progenitor Cells. *Small* **2012**, *8* (19), 3050-3061. DOI: 10.1002/smll.201200490.

(66) Norman, J.; Desai, T. Methods for fabrication of nanoscale topography for tissue engineering scaffolds. *Ann Biomed Eng* **2006**, *34* (1), 89-101. DOI: 10.1007/s10439-005-9005-4.

(67) Ko, J.; Mohtaram, N. K.; Ahmed, F.; Montgomery, A.; Carlson, M.; Lee, P. C. D.; Willerth, S. M.; Jun, M. B. G. Fabrication of poly (epsilon-caprolactone) microfiber scaffolds with varying topography and mechanical properties for stem cell-based tissue engineering applications. *J Biomat Sci-Polym E* **2014**, *25* (1), 1-17. DOI: 10.1080/09205063.2013.830913.

(68) Chua, J. S.; Chng, C. P.; Moe, A. A. K.; Tann, J. Y.; Goh, E. L. K.; Chiam, K. H.; Yim, E. K. F. Extending neurites sense the depth of the underlying topography during neuronal differentiation and contact guidance. *Biomaterials* **2014**, *35* (27), 7750-7761. DOI: 10.1016/j.biomaterials.2014.06.008.

(69) Collinsworth, A. M.; Zhang, S.; Kraus, W. E.; Truskey, G. A. Apparent elastic modulus and hysteresis of skeletal muscle cells throughout differentiation. *Am J Physiol-Cell Ph* **2002**, *283* (4), C1219-C1227. DOI: 10.1152/ajpcell.00502.2001.

(70) Discher, D. E.; Janmey, P.; Wang, Y. L. Tissue cells feel and respond to the stiffness of their substrate. *Science* **2005**, *310* (5751), 1139-1143. DOI: 10.1126/science.1116995.

(71) Park, J. S.; Chu, J. S.; Tsou, A. D.; Diop, R.; Tang, Z. Y.; Wang, A. J.; Li, S. The effect of matrix stiffness on the differentiation of mesenchymal stem cells in response to TGF-beta. *Biomaterials* **2011**, *32* (16), 3921-3930. DOI: 10.1016/j.biomaterials.2011.02.019.

(72) Saha, K.; Keung, A. J.; Irwin, E. F.; Li, Y.; Little, L.; Schaffer, D. V.; Healy, K. E. Substrate Modulus Directs Neural Stem Cell Behavior. *Biophys J* **2008**, *95* (9), 4426-4438. DOI: 10.1529/biophysj.108.132217.

(73) Flanagan, L. A.; Ju, Y. E.; Marg, B.; Osterfield, M.; Janmey, P. A. Neurite branching on deformable substrates. *Neuroreport* **2002**, *13* (18), 2411-2415. DOI: 10.1097/00001756-200212200-00007.

(74) Georges, P. C.; Miller, W. J.; Meaney, D. F.; Sawyer, E. S.; Janmey, P. A. Matrices with compliance comparable to that of brain tissue select neuronal over glial growth in mixed cortical cultures. *Biophys J* **2006**, *90* (8), 3012-3018. DOI: 10.1529/biophysj.105.073114.

(75) Stukel, J. M.; Willits, R. K. The interplay of peptide affinity and scaffold stiffness on neuronal differentiation of neural stem cells. *Biomed Mater* **2018**, *13* (2). DOI: ARTN 024102

10.1088/1748-605X/aa9a4b.

(76) Khan, S.; Newaz, G. A comprehensive review of surface modification for neural cell adhesion and patterning. *J Biomed Mater Res A* **2010**, *93a* (3), 1209-1224. DOI: 10.1002/jbm.a.32698.

(77) Yavin, E.; Yavin, Z. Attachment and Culture of Dissociated Cells from Rat Embryo Cerebral Hemispheres on Polylysine-Coated Surface. *J Cell Biol* **1974**, *62* (2), 540-546. DOI: DOI 10.1083/jcb.62.2.540.

(78) Sydor, J. R.; Nock, S. Protein expression profiling arrays: tools for the multiplexed high-throughput analysis of proteins. *Proteome Science* **2003**, *1* (1), 3. DOI: 10.1186/1477-5956-1-3.

(79) Kusindarta, D. L. *The Role of Extracellular Matrix in Tissue Regeneration*; IntechOpen, 2018.

(80) Csapo, R.; Gumpenberger, M.; Wessner, B. Skeletal Muscle Extracellular Matrix - What Do We Know About Its Composition, Regulation, and Physiological Roles? A Narrative Review. *Front Physiol* **2020**, *11*. DOI: ARTN 253

10.3389/fphys.2020.00253.

(81) Bosman, F. T.; Stamenkovic, I. Functional structure and composition of the extracellular matrix. *J Pathol* **2003**, *200* (4), 423-428. DOI: 10.1002/path.1437.

(82) Yue, B. Biology of the extracellular matrix: an overview. *J Glaucoma* **2014**, *23* (8 Suppl 1), S20-S23. DOI: 10.1097/IJG.0000000000000108 PubMed.

(83) Tanzer, M. L. Current concepts of extracellular matrix. *J Orthop Sci* **2006**, *11* (3), 326-331. DOI: 10.1007/s00776-006-1012-2.

(84) Engler, A. J.; Sen, S.; Sweeney, H. L.; Discher, D. E. Matrix elasticity directs stem cell lineage specification. *Cell* **2006**, *126* (4), 677-689. DOI: 10.1016/j.cell.2006.06.044.

(85) Lin, H. Y.; Tsai, C. C.; Chen, L. L.; Chiou, S. H.; Wang, Y. J.; Hung, S. C. Fibronectin and laminin promote differentiation of human mesenchymal stem cells into insulin producing cells through activating Akt and ERK. *J Biomed Sci* **2010**, *17*. DOI: Artn 56

10.1186/1423-0127-17-56.

(86) Ge, H. F.; Tan, L.; Wu, P. F.; Yin, Y.; Liu, X.; Meng, H.; Cui, G. Y.; Wu, N.; Lin, J. K.; Hu, R.; et al. Poly-L-ornithine promotes preferred differentiation of neural stem/progenitor cells via ERK signalling pathway. *Sci Rep-Uk* **2015**, *5*. DOI: ARTN 15535

10.1038/srep15535.

(87) Aloe, L.; Rocco, M. L.; Bianchi, P.; Manni, L. Nerve growth factor: from the early discoveries to the potential clinical use. *J Transl Med* **2012**, *10*. DOI: Artn 239

10.1186/1479-5876-10-239.

(88) Sharma, S. V.; Bell, D. W.; Settleman, J.; Haber, D. A. Epidermal growth factor receptor mutations in lung cancer. *Nat Rev Cancer* **2007**, *7* (3), 169-181. DOI: 10.1038/nrc2088 From NLM.

(89) Nguyen, T. H.; Kim, S. H.; Decker, C. G.; Wong, D. Y.; Loo, J. A.; Maynard, H. D. A heparin-mimicking polymer conjugate stabilizes basic fibroblast growth factor. *Nat Chem* **2013**, *5* (3), 221-227. DOI: 10.1038/Nchem.1573.

(90) Abdelhakim, M.; Lin, X. X.; Ogawa, R. The Japanese Experience with Basic Fibroblast Growth Factor in Cutaneous Wound Management and Scar Prevention: A Systematic Review of Clinical and Biological Aspects. *Dermatology Ther* **2020**, *10* (4), 569-587. DOI: 10.1007/s13555-020-00407-6.

(91) Liu, Y. X.; Song, Z. H.; Zhao, Y.; Qin, H.; Cai, J.; Zhang, H.; Yu, T. X.; Jiang, S. M.; Wang, G. W.; Ding, M. X.; et al. A novel chemical-defined medium with bFGF and N2B27 supplements supports undifferentiated growth in human embryonic stem cells. *Biochem Bioph Res Co* **2006**, *346* (1), 131-139. DOI: 10.1016/j.bbrc.2006.05.086.

(92) Choi, K. C.; Yoo, D. S.; Cho, K. S.; Huh, P. W.; Kim, D. S.; Park, C. K. Effect of Single Growth Factor and Growth Factor Combinations on Differentiation of Neural Stem Cells. *J Korean Neurosurg S* **2008**, *44* (6), 375-381. DOI: 10.3340/jkns.2008.44.6.375.

(93) Li, Z.; Gong, Y. W.; Sun, S. J.; Du, Y.; Lu, D. Y.; Liu, X. F.; Long, M. Differential regulation of stiffness, topography, and dimension of substrates in rat

mesenchymal stem cells. *Biomaterials* **2013**, *34* (31), 7616-7625. DOI: 10.1016/j.biomaterials.2013.06.059.

(94) Chin, E. W. M.; Marcy, G.; Yoon, S. I.; Ma, D. L.; Rosales, F. J.; Augustine, G. J.; Goh, E. L. K. Choline Ameliorates Disease Phenotypes in Human iPSC Models of Rett Syndrome. *Neuromol Med* **2016**, *18* (3), 364-377. DOI: 10.1007/s12017-016-8421-y.

(95) Yip, A. K.; Iwasaki, K.; Ursekar, C.; Machiyama, H.; Saxena, M.; Chen, H.; Harada, I.; Chiam, K. H.; Sawada, Y. Cellular response to substrate rigidity is governed by either stress or strain. *Biophys J* **2013**, *104* (1), 19-29. DOI: 10.1016/j.bpj.2012.11.3805 From NLM.

(96) Mattiassi, S. Biophysical cues to enhance neuronal differentiation. University of Waterloo, 2021.

(97) Yip, A. K.; Nguyen, A. T.; Rizwan, M.; Wong, S. T.; Chiam, K. H.; Yim, E. K. F. Anisotropic traction stresses and focal adhesion polarization mediates topography-induced cell elongation. *Biomaterials* **2018**, *181*, 103-112. DOI: 10.1016/j.biomaterials.2018.07.057.

(98) Gómez, R. L.; Sendín, L. N. Relative Expression Analysis of Target Genes by Using Reverse Transcription-Quantitative PCR. In *Cereal Genomics: Methods and Protocols*, Vaschetto, L. M. Ed.; Springer US, 2020; pp 51-63.

(99) Pan, F.; Zhang, M.; Wu, G. M.; Lai, Y. K.; Greber, B.; Scholer, H. R.; Chi, L. F. Topographic effect on human induced pluripotent stem cells differentiation towards neuronal lineage. *Biomaterials* **2013**, *34* (33), 8131-8139. DOI: 10.1016/j.biomaterials.2013.07.025.

(100) Panina, Y.; Germond, A.; Masui, S.; Watanabe, T. M. Validation of Common Housekeeping Genes as Reference for qPCR Gene Expression Analysis During iPS Reprogramming Process. *Sci Rep-Uk* **2018**, *8*. DOI: ARTN 8716

10.1038/s41598-018-26707-8.

(101) Cutiongco, M. F. A.; Goh, S. H.; Aid-Launais, R.; Le Visage, C.; Low, H. Y.; Yim, E. K. F. Planar and tubular patterning of micro and nano-topographies on poly(vinyl alcohol) hydrogel for improved endothelial cell responses. *Biomaterials* **2016**, *84*, 184-195. DOI: 10.1016/j.biomaterials.2016.01.036.

(102) Ino, J. M.; Sju, E.; Ollivier, V.; Yim, E. K. F.; Letourneur, D.; Le Visage, C. Evaluation of hemocompatibility and endothelialization of hybrid poly(vinyl alcohol) (PVA)/gelatin polymer films. *J Biomed Mater Res B* **2013**, *101* (8), 1549-1559. DOI: 10.1002/jbm.b.32977.

(103) Metavarayuth, K.; Sitasuwan, P.; Zhao, X.; Lin, Y.; Wang, Q. Influence of Surface Topographical Cues on the Differentiation of Mesenchymal Stem Cells in Vitro. *Acs Biomater Sci Eng* **2016**, *2* (2), 142-151. DOI: 10.1021/acsbiomaterials.5b00377.

(104) DiGiacomo, V.; Meruelo, D. Looking into laminin receptor: critical discussion regarding the non-integrin 37/67-kDa laminin receptor/RPSA protein. *Biol Rev* **2016**, *91* (2), 288-310. DOI: 10.1111/brv.12170.

(105) Lam, M. T.; Longaker, M. T. Comparison of several attachment methods for human iPS, embryonic and adipose-derived stem cells for tissue engineering. *J Tissue Eng Regen M* **2012**, *6*, s80-s86. DOI: 10.1002/term.1499.

(106) Distler, T.; Lauria, I.; Detsch, R.; Sauter, C. M.; Bendt, F.; Kapr, J.; Rutten, S.; Boccaccini, A. R.; Fritsche, E. Neuronal Differentiation from Induced Pluripotent Stem Cell-Derived Neurospheres by the Application of Oxidized Alginate-Gelatin-Laminin Hydrogels. *Biomedicines* **2021**, *9* (3). DOI: ARTN 261

10.3390/biomedicines9030261.

(107) Huang, J. Y.; Chen, Y. W.; Tang, C. Q.; Fei, Y.; Wu, H. Y.; Ruan, D. F.; Paul, M. E.; Chen, X.; Yin, Z.; Heng, B. C.; et al. The relationship between substrate topography and stem cell differentiation in the musculoskeletal system. *Cell Mol Life Sci* **2019**, *76* (3), 505-521. DOI: 10.1007/s00018-018-2945-2.

(108) Song, H. X.; Wu, T.; Yang, X. T.; Li, Y. Z.; Ye, Y.; Li, B.; Liu, T.; Liu, S. H.; Li, J. H. Surface Modification with NGF-Loaded Chitosan/Heparin Nanoparticles for Improving Biocompatibility of Cardiovascular Stent. *Stem Cells Int* **2021**, *2021*. DOI: Artn 9941143

10.1155/2021/9941143.

(109) Colliec-Jouault, S.; Bavington, C.; Delbarre-Ladrat, C. Heparin-like entities from marine organisms. *Handb Exp Pharmacol* **2012**, (207), 423-449. DOI: 10.1007/978-3-642-23056-1_19.